Online ISSN: 2249-4596
Print ISSN: 0975-5861
DOI: 10.17406/GJRE

Global Journal of Researches in Engineering: A

Mechanical & Mechanics Engineering

Highlights

- Hydrogen for Mobility
- Zero Carbon Transportation System
- Power Harvesting in Drones
- Dynamic Analysis of Planetary Systems

Discovering Thoughts, Inventing Future

VOLUME 24 ISSUE 1 VERSION 1.0

Global Journal of Researches in Engineering: A
Mechanical and Mechanics Engineering

Global Journal of Researches in Engineering: A
Mechanical and Mechanics Engineering

Volume 24 Issue 1 (Ver. 1.0)

Open Association of Research Society

Incorporation No.: 0423089
License No.: 42125/022010/1186
Registration No.: 430374
Import-Export Code: 1109007027
Employer Identification Number (EIN):
USA Tax ID: 98-0673427

Global Journals Inc.

*(A Delaware USA Incorporation with "Good Standing"; **Reg. Number: 0423089**)*

Sponsors: *Open Association of Research Society*
Open Scientific Standards

Publisher's Headquarters office

Global Journals® Headquarters
945th Concord Streets,
Framingham Massachusetts Pin: 01701,
United States of America
USA Toll Free: +001-888-839-7392
USA Toll Free Fax: +001-888-839-7392

Offset Typesetting

Global Journals Incorporated
2nd, Lansdowne, Lansdowne Rd., Croydon-Surrey,
Pin: CR9 2ER, United Kingdom

Packaging & Continental Dispatching

Global Journals Pvt Ltd
E-3130 Sudama Nagar, Near Gopur Square,
Indore, M.P., Pin:452009, India

Find a correspondence nodal officer near you

To find nodal officer of your country, please email us at *local@globaljournals.org*

eContacts

Press Inquiries: *press@globaljournals.org*
Investor Inquiries: *investors@globaljournals.org*
Technical Support: *technology@globaljournals.org*
Media & Releases: *media@globaljournals.org*

Pricing (Excluding Air Parcel Charges):

Yearly Subscription (Personal & Institutional)
250 USD (B/W) & 350 USD (Color)

Editorial Board

Global Journal of Research in Engineering

Dr. Omid Gohardani

Ph.D. Senior Aerospace/Mechanical/ Aeronautical, Engineering professional M.Sc. Mechanical Engineering, M.Sc. Aeronautical Engineering B.Sc. Vehicle Engineering Orange County, California, US

Dr. Paolo Veronesi

Ph.D., Materials Engineering, Institute of Electronics, Italy President of the master Degree in Materials Engineering Dept. of Engineering, Italy

Contents of the Issue

Global Journal of Researches in Engineering: A
Mechanical and Mechanics Engineering
Volume 24 Issue 1 Version 1.0 Year 2024
Type: Double Blind Peer Reviewed International Research Journal
Publisher: Global Journals
Online ISSN: 2249-4596 & Print ISSN: 0975-5861

Hydrogen for Mobility: A Pathway to a Zero Carbon Transportation System

By Marc Abbott

Abstract- Eliminating hydrocarbon transportation must be a fundamental goal for society if we are to negate Climate Change and its consequences. No source of CO2 emissions comes close to that of hydrocarbon fueled internal combustion engines and if we are to transition to a zero-carbon energy system, a viable alternative to hydrocarbon fuels must be found. Lithium-Ion powered vehicles or EV's present society with a paradox, they emit zero emissions however the life cycle of Lithium-Ion batteries is a source of environmental concern through mining, deforestation of carbon sinks, the immense electrification requirements for battery production, recycling, and recharging.

This communication proposes Hydrogen for Mobility as the future fuel for a pathway to a Zero Carbon Transportation System through utilizing both the existing internal combustion engine (ICE) and most existing transportation infrastructure, at the same time being cost effective, efficient and zero emitting. An overview of technologies will be discussed along with their Technology Readiness, benefits, and issues. This discussion expands on the concepts discussed in 'Mobile Modular Hydrogen Power Generation – a Zero Carbon Energy System'. https://doi.org/10.5296/ijgs.v7i1.xxxx

Keywords: *hydrogen, biofuel, fuel cell, electric, mobility, engine, vehicle, emissions.*

GJRE-A Classification: *LCC Code: TL1-845*

HYDROGENFORMOBILITYAPATHWAYTOAZEROCARBONTRANSPORTATIONSYSTEM

Strictly as per the compliance and regulations of:

Hydrogen for Mobility: A Pathway to a Zero Carbon Transportation System

Marc Abbott

Abstract- Eliminating hydrocarbon transportation must be a fundamental goal for society if we are to negate Climate Change and its consequences. No source of CO_2 emissions comes close to that of hydrocarbon fueled internal combustion engines and if we are to transition to a zero-carbon energy system, a viable alternative to hydrocarbon fuels must be found. Lithium-Ion powered vehicles or EV's present society with a paradox, they emit zero emissions however the life cycle of Lithium-Ion batteries is a source of environmental concern through mining, deforestation of carbon sinks, the immense electrification requirements for battery production, recycling, and recharging.

This communication proposes Hydrogen for Mobility as the future fuel for a pathway to a Zero Carbon Transportation System through utilizing both the existing internal combustion engine (ICE) and most existing transportation infrastructure, at the same time being cost effective, efficient and zero emitting. An overview of technologies will be discussed along with their Technology Readiness, benefits, and issues. This discussion expands on the concepts discussed in 'Mobile Modular Hydrogen Power Generation – a Zero Carbon Energy System'. https://doi.org/10.5296/ijgs.v7i1.xxxx

Keywords: hydrogen, biofuel, fuel cell, electric, mobility, engine, vehicle, emissions.

I. Introduction

a) Transporting Humanity: The Internal Combustion Engine (ICE)

The internal combustion engine has powered vehicle transportation on an enormous scale for the last century from people finding freedom to travel 24/7 using passenger cars to freight transported by trucks. The internal combustion engine has played a fundamental part in developing this transportation system and modern society as we know it today.

As of 2016 the estimated global vehicle transport fleet stood at 1.416 billion (Michaux, 2021a), by 2022 global transportation contributed to approximately 20% of global CO_2 emissions or 7.97 Gigatons, road or vehicle transportation contributed to 12% of global CO_2 emissions (Statista, 2023). By 2050 global passenger demand alone is expected to double (OCED, 2023) with urban passenger (vehicle, bus, train) CO_2 emissions increasing by 39% to 3012 million tons per annum (OCED, 2023a). Given the growth forecasts our 2015 Paris agreement commitments and transition to net zero by 2050 are simply not achievable without fundamental change in our consumption of hydrocarbons or change in demand for global mobility.

b) What problems need to be solved?

To achieve a Zero Carbon Transportation system will require many problems to be solved, with some likely still unknown.

Vehicle transport is low cost, efficient and accessible on a global scale; for example, at the end of 2021 there were approximately 250 million passenger cars in the European Union (Eurostat, 2023), with access to 113,642 services stations (Fuels Europe, 2022) giving a staggering accessibility ratio of 1 service station for every 2200 passenger cars, undoubtably we take this ease of access for granted, and this gives rise to two problems that will take decades to solve:

1. How do you replace the existing vehicle transportation system on a like for like basis? That is to say that any alternative system must be at a minimum as efficient, accessible, and low cost as the existing system.
2. Practically transition from hydrocarbons to an equivalent zero carbon fuel bearing in mind hydrocarbons have powered society through generating electricity on a global scale, produced plastics, medicines and even DVDs. Couple this with the employment and economic benefits of the last century and you have what I call 'The Hydrocarbon Complex'' This complex will be extremely difficult to replicate or replace from a fuel or energy perspective let alone from a self-preservation point of view.

This short communication will address these problems by discussing why hydrogen should be the zero carbon alternative to hydrocarbon fuels for vehicle transportation and through 'Repurposing' how we can utilize almost all our existing transportation infrastructure and the internal combustion engine to support hydrogen as the zero emission vehicle ZEV standard (emit less than 1g of CO2 per kWh per km) fuel of the future with minimal life cycle environmental impact. (European Commission, 2023)

**Note 1,2,3

Author: Future Energy Innovations. Hamden Valley Drive, Richmond, Texas, USA. e-mail: Marc.Abbott@Gmail.com

II. Analysis of the Solution

a) Mobility is Needed 24/7/365

Mobility is not only needed 24/7/365 but demanded and, in many ways, taken as a given. The COVID pandemic accelerated demand for mobility through the growth in home deliveries, drive through convenience services and mobility services like Uber and Lyft. In 2022 Uber drivers completed 7.6 billion trips surpassing its previous peak of 6.9 billion trips in 2019 (Business of Apps, 2023) coupled with population growth which by 2050 will grow to 9.8 billion from 7.6 billion an increase of 29% (United Nations, 2023) and it reinforces inevitable growth of people and freight transportation and with it increased demand for hydrocarbons. Now more than ever we need to start transitioning to hydrogen as the zero emissions fuel for future mobility. To put into perspective the urgency needed one gallon of gasoline contains 5.5 pounds of carbon by weight and emits 20 pounds of CO_2 when combusted (Fuel Economy Gov, 2021). By comparison hydrogen chemically contains no carbon and will meet ZEV European standards when used in internal combustion engines.

Aside from emerging electrolysis and engine technologies that will enable hydrogen as the future fuel for mobility it also creates circularity through continuously repurposing and recycling not only existing vehicle engines but also existing hydrocarbon fueling infrastructure. Why mine Lithium and Cobalt and other metals for EV batteries with their associated environmental impacts: deforestation, water pollution, etc. (Washington Post, 2018) when we can create a circular zero carbon hydrogen mobility ecosystem?

b) The Alternatives: Biofuel, Electric and Fuel Cell Vehicles?

In the vehicle and engine technology race there are three main alternatives to hydrogen: biofuels, electric, and fuel cell vehicles. I now discuss these including their benefits, issues, technology readiness, and environmental impacts summarized.

i. *Biofuel Vehicles*

Biofuels are fuels composed of or produced from biological raw materials such as Ethanol (bio-alcohol), Palm Oil, Fatty Acid Methyl Ester (FAME) and Hydrotreated Vegetable Oil (HVO), these raw materials are almost always used as a bio-blend to standard gasoline or diesel, with the exception being pure ethanol fuels. Biofuels are classified as Low Carbon Fuels (US Energy Information Administration, 2022) and not Zero Carbon Fuels, with existing concerns including environmental and social (food and agriculture for fuels), engine compatibility and low fuel economy. Vehicles that use bio-blends above E15 namely E20, E25 and E85 are commonly referred to as flex-fuel vehicles and require specially coated fuel lines and engine components due to corrosion issues. E85 fuel efficiency is 27% less than that of regular gasoline (which contains up to 10% ethanol) and requires more frequent engine oil changes due to fuel dilution. (The Drive, 2023) The highest ethanol blend E100 is only available in Brazil and cannot be used in standard flex fuel engines since they are designed to work with a maximum of E85, an additional major drawback of E100 is its unavailability at retail fuel stations in the USA. (Protech Fuel, 2023) Given this there is still a case for biofuels as a low carbon fuel alternative but realistically only a transition fuel. The most often overlooked drawback with alternative energy sources including fuels is the energy penalty and on average energy outputs from ethanol production is less than the respective fossil fuel energy inputs. (Pimentel, D., Patzek, T.W., 2005)

It is inescapable that gasoline and diesel are needed for ethanol blending and when you consider the production energy penalty, biofuels become less attractive as a future fuel solution and will never achieve zero carbon emissions.

ii. *Electric Vehicles (EV's)*

Electric vehicles or EV's as they are commonly referred to have come to the fore as the zero emission solution primarily for passenger cars and to a lesser extent heavy duty vehicles and motorcycles. Demand for EV's is surging as can be noted by Tesla's recent production record of 1,845,985 EV units in 2023 (CNBC, 2023). However, perception versus reality in the EV ecosystem that they are zero emission vehicles is questionable especially when we consider the full lifecycle of an EV.

EV's use either NMC (Nickel Manganese Cobalt) or LFP (Lithium Iron Phosphate) batteries as their power source with LFP batteries now preferred as they can accommodate 2.5 times the discharge cycles of a NMC battery (ZeCar, 2023). Aside known negative environmental impacts of mining minerals such Cobalt and Nickel and associated labor exploitation practices (Earth Org, 2022) EV's have a higher environmental footprint than combustion vehicles when they are first produced at the factory (ZeCar, 2022) for example "it takes the all-electric Volvo XC40 to drive 146,000km until it breaks even the carbon footprint of the gasoline XC40 (assuming grid charging)". (ZeCar, 2022a) The counter argument is that EV's will be charged using wind or solar power only, but that is wishful thinking as daily wind and solar only account for a maximum of 13.7% of US electricity generation (EIA, 2022) and assumes favorable weather conditions.

EV battery recycling is a growing area of concern from an environmental perspective. Not only do you have to consider the metallurgical recycling processes but also the disposal processes for electrolytes and their additives. The two main recycling processes Pyrometallurgical and Hydrometallurgy both emit carbon as part of the process (5.81 kg CO_2 -eq/kwh) for the former given the high temperature smelting required through using hydrocarbons and (2.86 kg CO_2 -eq/kwh) for the latter. (Floodlight, 2023) Although Hydrometallurgy is less energy intense it produces significant toxic gases and wastewater adding to environmental concerns.

Direct Physical recycling is a promising technology, albeit there are still carbon emissions associated with the process (3.65 kg CO_2 -eq/kwh) but much less secondary waste, however it is still in its infancy as the technology is not mature. (Floodlight, 2023a)

Both NMC and LFP batteries contain electrolyte additives to stabilize the cathodes, organic compounds such as 1,3,2-dioxathiolane 2,2-dioxide in NMC electrolytes (Nature, 2022) and Fluoroethylene Carbonate in LFP electrolytes (JACS, 2018) are toxic substances and extremely harmful to humans and the environment. (ECHA, 2023 & 2023a)

The EV revolution is well underway but to claim zero emissions is simply not true. Considering the questionable sustainability and ethics in battery production and end of life environmental concerns it is reasonable to state that EV's do not provide a pathway to a zero emissions transportation system.

iii. *Hydrogen Fuel Cell Vehicles*

Fuel Cell Vehicles (FCV's) are electric vehicles powered by hydrogen fuel cells instead of batteries (batteries are still used albeit on a smaller scale to capture energy from the regenerative braking system, to be used when extra power is required). Hydrogen fuel cells convert hydrogen into electricity using a Proton/ Polymer Electrolyte Membrane (PEM) and Platinum catalyst at the anode which is then used to power the vehicles electric motor. Figure 1.0 illustrates how a typical PEM Hydrogen Fuel Cell works (Fuel Economy, 2023).

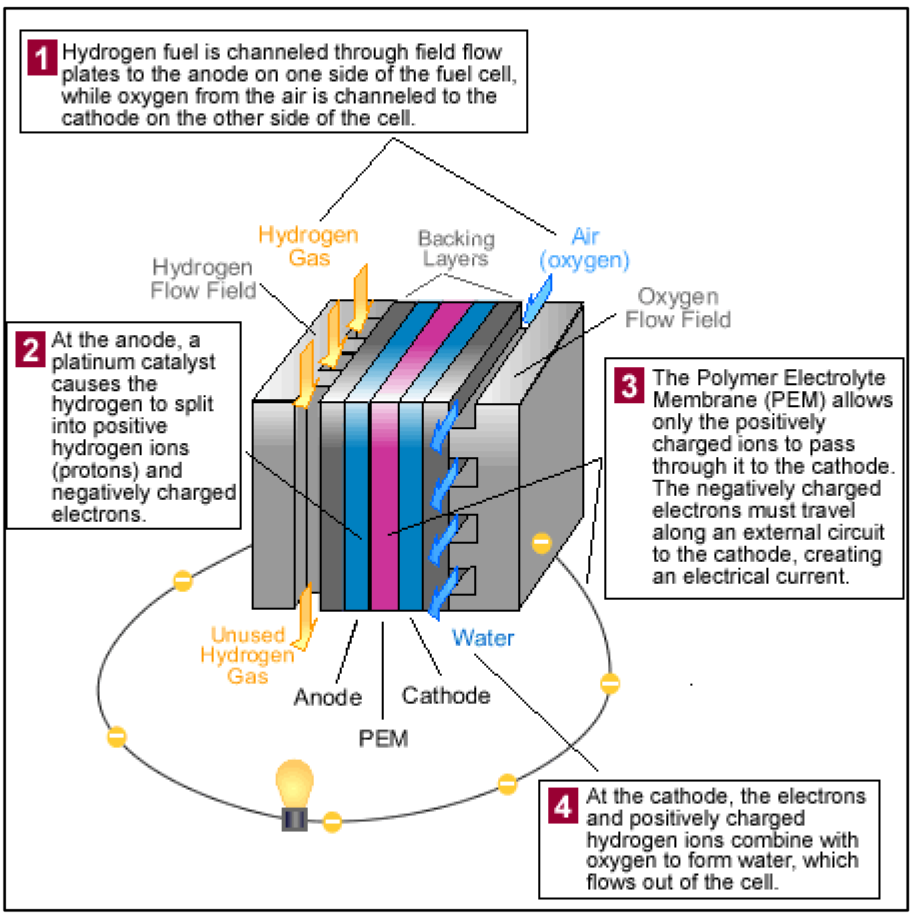

Figure 1.0: Typical PEM Hydrogen Fuel Cell

At the major vehicle component level there is very little difference between a fuel cell vehicle and electric vehicle with only the power sources and the hydrogen fuel tank the major differences. Figure 1.1 illustrates a Fuel Cell Vehicle vs. Electric Vehicle (AFDC, 2023 and 2023a).

Global Journal of Research in Engineering (A) XXIV Issue I Version I Year 2024

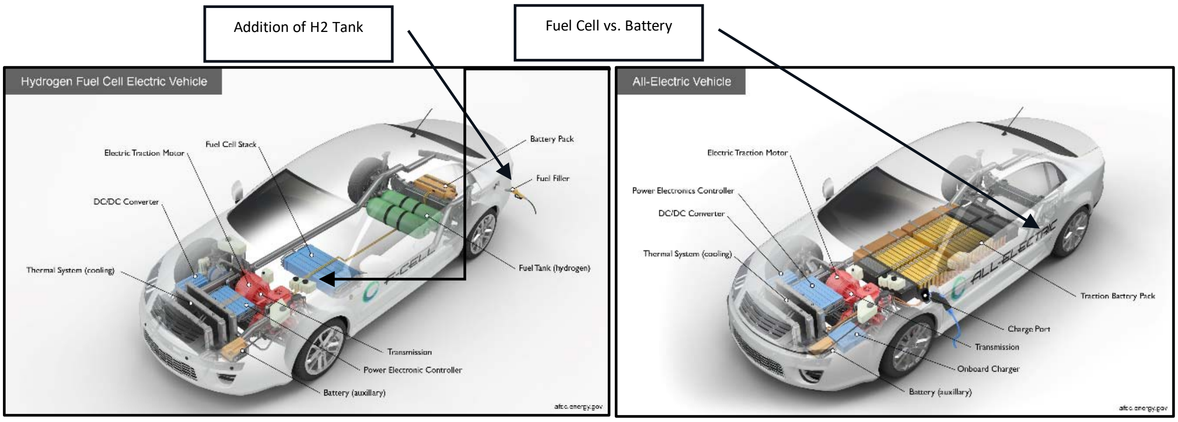

Figure 1.1: Hydrogen Fuel Cell Vehicle comparison vs. Electric Vehicle

The benefit of FCV's is the use of hydrogen as fuel instead of large battery cells such as those in EV's, however it is critical that green hydrogen is used to ensure fewer carbon emissions, or the emissions argument is weak. Other benefits include less time to refuel with hydrogen versus EV recharging and a lower vehicle weight. A Tesla battery on average weighs 1190lbs (The Motor Digest, 2023) this extra weight negatively impacts stopping distance and inflicts additional damage to road infrastructure (Streets NM, 2016).

The downside of FCV's and likely the reason for slow adaption are numerous but three main challenges stand out, low voltage produced by the fuel cell, the cost of platinum for use as a catalyst and the absence of hydrogen fueling infrastructure. A typical fuel cell produces less than 1.16volts (Fuel Economy, 2023a) not near enough to drive an electric motor, therefore fuel cells are stacked together to achieve the desired voltage for example the Toyota Mirai has 330 fuel cells stacked together to power the 310-volt electric motor (Toyota, 2023). The fuel cell anode Platinum catalyst is a costly precious metal making fuel cell stacks prohibitively expensive. The biggest issue though is the absence of hydrogen fueling infrastructure, California leads the way in hydrogen infrastructure investment with the remainder of the US as of December 2023 having one hydrogen refueling station in Hawaii with others on the east coast under construction (GLP Autogas, 2024). The issue of available hydrogen infrastructure applies equally to the proposed hydrogen fueled internal combustion engine; however, a novel solution is proposed that significantly reduces cost and timeline for deployment.

c) The Hydrogen Fueled Internal Combustion Engine (H2 for ICE)

The public perception of the internal combustion engine (ICE) one could argue is flawed and by that, I mean that it is seen by the public as simply a gasoline or diesel engine for vehicles and nothing more, you can therefore reasonably conclude that the drive to abolish the internal combustion engine by governments (CNET, 2023) is based on this perception. Fundamentally this is false, the internal combustion engine is nothing more than a heat engine that converts heat to mechanical work. Heat generation is through combustion of fuel with oxygen, usually air. Gasoline and diesel dominate as the preferred fuel for the internal combustion engine, however using hydrogen as a fuel is physically no different than using diesel or gasoline, at the same time hydrogen achieves the European ZEV standards. A zero carbon transportation system can only be achieved using hydrogen as a fuel while preserving our future demand for global population mobility.

Development of the internal combustion engine has historically always focused on gasoline or diesel as the primary source of fuel, however recent industry developments have focused on re-purposing the existing internal combustion engine to use hydrogen with on road trials expected mid-2024. The technology package for ICE conversion to hydrogen consists of three main activities, engine modification, vehicle integration, calibration and testing, all discussed below:

i. *Internal Combustion Engine Modifications Required for Hydrogen Fuel*

Maximizing reuse of existing components is critical as it reduces cost and ensures the simplest solution. Taking this into consideration repurposing the existing internal combustion engine involves, at the highest level, three fundamental tasks where original component removal or replacement is needed. There are many lesser sub-tasks that could be discussed, and these are also dependent on the type of engine being converted, but for the purposes of this discussion the focus is on three engine modifications:

1. *Removal of Exhaust Gas Recirculation (EGR):* The primary function of the EGR system is to reduce nitrogen oxide emissions. This is achieved through routing a percentage of oxygen deficient exhaust gases back to the engine intake to limit peak combustion temperatures and thus limiting NOx production. Whether the EGR needs to be removed

or can be disabled will be determined through on road testing.

2. *Intake Manifold Modification:* Existing intake manifolds need to be modified for hydrogen fuel. Modification will likely be through adoption of a dedicated hydrogen manifold spacer that includes provision for hydrogen injection and pressure sensing along with ports to direct flow to the intake valves. A consequence of this modification and a vehicle integration task to be addressed is increased engine width.
3. *Boosting: Installation of a Super Turbo:* The function of a Super Turbo is to allow increased performance and efficiency across the engine's range of duty cycles. The Super Turbo is a mechanically driven turbocharger that enables bi-directional power transfer and speed ratio control between the turbocharger and the engine. It is an on-demand boost system that responds to the engine's command for air flow. (SuperTurbo Technologies, 2020) The Super Turbo enables the hydrogen engine to achieve the European ZEV standards while maintaining diesel or gasoline ICE power, efficiency and on road performance.

Figure 1.2 Innovative High Speed Traction Drive (SuperTurbo Technologies, 2020) illustrates a Super Turbo installed in a typical Internal Combustion Engine.

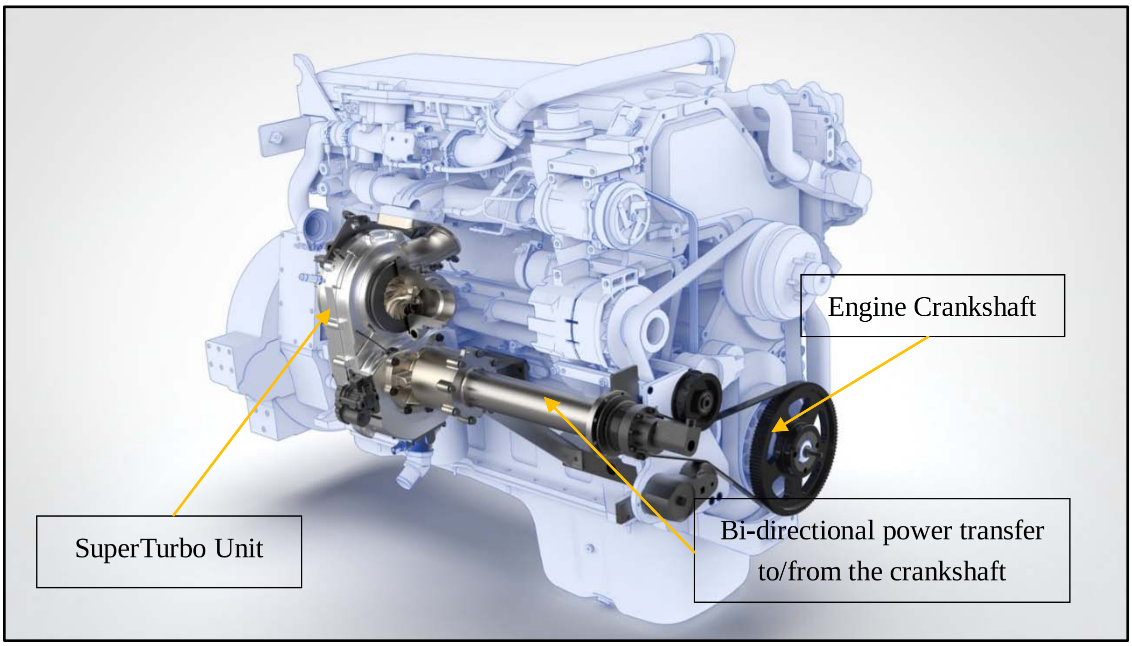

Figure 1.2: Innovative High Speed Traction Device (Super Turbo)

In addition to engine and vehicle integration modifications, appropriate calibration and testing is required. Vehicle integration addresses activities such as modifying the engine bay to accommodate added engine width, addition of hydrogen storage tanks and upgrading of the engine control systems (ECU) to combust hydrogen fuel efficiently. Calibration focuses primarily on steady state engine operation, hydrogen combustion performance and qualification of emissions to meet European ZEV standards. Testing will initially be conducted using specialized engine test benches and vehicle dynamometers to confirm all calibrations meet standards, then on-road durability testing before operational deployment in late 2024.

Figure 1.3 illustrates a hydrogen vehicle integration package using a Cummins base engine (Cummins, 2022).

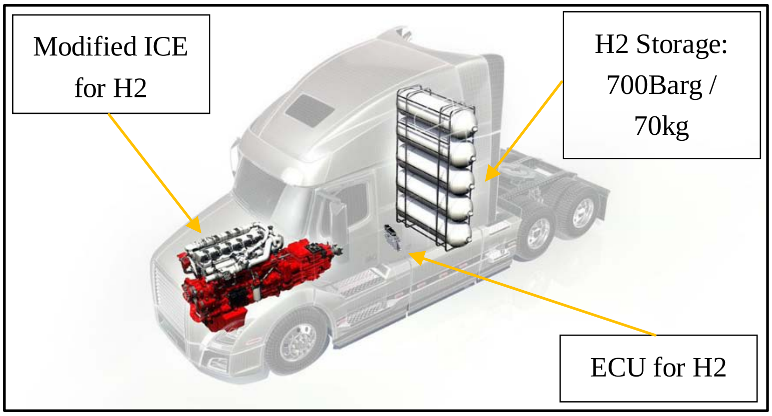

Figure 1.3: Hydrogen Vehicle Integration Package

ii. *Hydrogen Vehicle Use Cases*

Hydrogen fuelled internal combustion engines are currently being developed for Heavy Duty vehicles (any vehicle exceeding 26,000lbs) along with government research funding now being available for development of H_2 in ICE for the rail sector (US DOE, 2024). In the longer term when infrastructure starts to develop there is no reason that medium and light duty trucks along with passenger cars cannot transition to hydrogen fuelled internal combustion engines.

d) *The Hydrogen Refuelling Platform*

We already have global retail or service stations in place designed and optimized over decades for not only fuel but everyday items such as groceries, would it not therefore seem logical to repurpose this existing infrastructure for hydrogen? What would need to be done to the existing infrastructure to achieve this? Let's discuss the two technology platforms needed to repurpose existing infrastructure for hydrogen fuel on a global scale.

i. *Hydrogen Forecourt Production Technology*

The end goal is a zero carbon transportation system therefore, all sources of CO_2 emissions need to be eliminated, whether being in supply, production, or demand. Forecourt production technology objectives are to eliminate supply and production CO_2 emissions, there are two key activities:

1. *On site production of green hydrogen:* The proposal is to use the same in-situ modular AEM Electrolysis concept as discussed in 'Mobile Modular Hydrogen Power Generation – a Zero Carbon Energy System' (https://doi.org/10.5296/ijgs.v7i1.xxxx) to generate on-site green hydrogen with the electrolyzer capacity sized to expected daily demand. No other method of hydrogen production is considered.
2. *Reduced Cost and Environmental Impact:* Producing on-site hydrogen eliminates distribution via compressed gas trucking reducing significantly overall supply costs but more importantly eliminating all CO_2 emissions from trucking. A standalone renewable energy source would need to be installed should the grid not be 100% green.

ii. *Hydrogen Retail Technology Platform*

Retail sales of hydrogen have evolved very slowly and only to a small extent in California. To scale for a global market a hydrogen retail technology platform needs to focus on safety, quality, and customer experience with high utilization, there are three key activities:

1. *Retail safety:* Safe scaling of hydrogen fueling infrastructure requires focus on developing safety activities and standards that differ significantly from gasoline and diesel. Baseline safety standards are in place but need refining and developed further for highly utilized service stations in densely populated areas.
2. *Hydrogen quality sensor:* Off-spec hydrogen will damage internal combustion engines and can cause spurious emissions. Quality sensors to detect CO and water will need refining for high utilization.
3. Hydrogen dispenser design: Current dispensers are designed for dispensing on a small scale and require upgrading to accommodate high volume dispensing and further mistake and error proofing before mass adaption by the public.

iii. *Comparing Future Fuel Vehicles*

Table 1.0 compares the differences of biofuel, electric and fuel cell vehicles versus hydrogen for internal combustion engine (H2 for ICE).

Table 1.0: Comparison of Biofuels, Electric and Fuel Cell Vehicles vs. (H2 for ICE)

	Biofuel Vehicle	Electric Vehicle	Fuel Cell Vehicle	H2 for ICE
Technology Readiness	9 – System proven and operational	9 – System proven and operational	9 – System proven and in service at small scale	7 – Prototype demonstrated; road trials planned
Benefit 1	Fuel sourced from partly renewable sources	High on road performance	Zero on road emissions	Zero emission lifecycle
Benefit 2	Low carbon fuel classification	Zero on road emissions	Supported by several states including California	Circularity and ability to repurpose existing engines and vehicles
Benefit 3	Practicable interim solution	Access to EV charging solutions growing rapidly	Hydrogen fuelling infrastructure attracting investment	Equal performance versus gasoline engine
Benefit 4		Starting to be price competitive with mass adaption	Hydrogen safety concerns already mitigated	Existing infrastructure can be used with modifications
Issue 1	Needs blended with gasoline and diesel	Environmental impact of battery materials including recycling	Needs fuel cells to be stacked to achieve required voltage for the electric motor	Hydrogen fuelling infrastructure needs to expand rapidly
Issue 2	Social concerns. 'Food for fuels'	Fossil fuel charging is the norm not the exception	Platinum catalyst makes vehicle costly	AEM electrolysis technology needs fully proved at scale
Issue 3	Lower fuel efficiency at higher blends E85 for example	Heavier vehicle negatively impacts infrastructure	Low power vehicle needs battery to boost under certain conditions	Low public awareness and still concerns with using hydrogen
Issue 4	Needs specific flex fuel vehicles to be successful	High milage needed for emissions to break even with ICE vehicles	Hydrogen fuelling infrastructure needs to expand rapidly	Scarcity of parts for hydrogen engine modifications

III. Discussion

Our modern transportation system has taken over a century to establish and often taken for granted is the scale it has achieved, the convenience provided through service or retail stations where you can purchase gasoline to groceries and quite simply how humanity could not function without this network that exists today. As already discussed, there are approximately 113,000 service stations in Europe, why not repurpose these to accommodate hydrogen as the zero-carbon fuel of the future?

Biofuel, electric and fuel cell vehicles present alternative solutions to reducing carbon emissions, some achieve this better than others, but none achieve hydrogen's lifecycle of zero carbon emissions.

Biofuels with their reliance on hydrocarbons for blending and the need for flex fuel vehicles are not the solution and electric vehicles are surely just an interim fix as we cannot ignore the environmental and societal impacts of mineral mining and the sources of electricity for re-charging. The USA as an example, generates most of its electricity from hydrocarbon fueled power stations, EV charging using renewable power is the exception rather than the norm. Fuel cell vehicles are an anomaly somewhere in between EV and H2 for ICE, but with no game-changing benefits for the user, coupled with the need for expensive precious metals as a catalyst and their longevity as a solution is questionable.

Hydrogen is the most abundant element in the universe and up until now there has been no reason to develop it as a source of fuel, but this needs to change. Hydrocarbon resources are finite, and we underestimate the transition from them to an efficient, globally accessible, and cost-effective alternative such as hydrogen at our peril. Using hydrogen as a pathway to a zero carbon transportation system comes with many challenges but they are not all conceptual we have engineered exceptionally efficient internal combustion engines, to not capitalize on them is a waste of technological progress, modifying them for hydrogen fuel is well within our technical capabilities. The infrastructure is in place but repurposing this is more a challenge to our 'Group Think' on energy transition solutions than a technical hurdle. Producing green hydrogen using AEM water electrolysis will be the production solution, scaling the electrolyzer output to the huge volumes needed for global transportation will be the final challenge.

Lastly, I leave you with a very elegant graph that leaves no doubt the positive impact using hydrogen as fuel has on CO_2 emissions. Figure 1.4 illustrates the relationship between CO_2 emissions versus using hydrogen (Power Magazine, 2021).

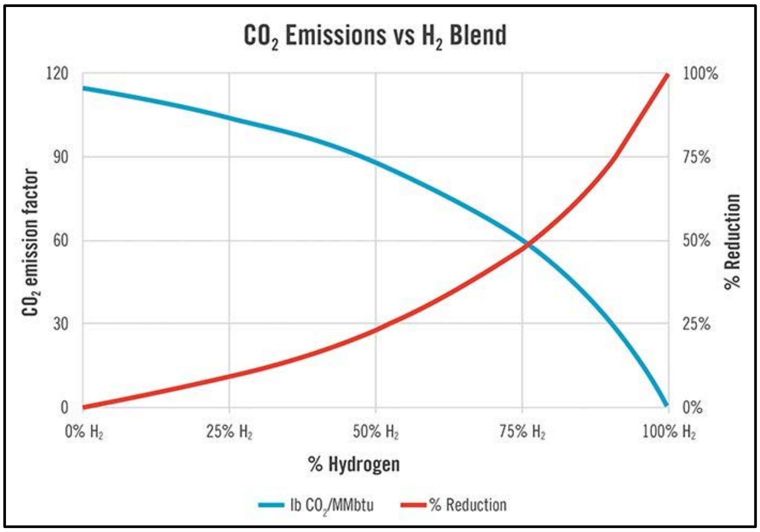

Figure 1.4: CO2 Emissions versus H2 Blend

References Références Referencias

1. Michaux, S. (2021a). Assessment of the Extra Capacity Required of Alternative Energy Electrical Power Systems to Completely Replace Fossil Fuels. *Geological Survey of Finland*, p266.
2. Statista: Global Data and Intelligence, 2023 https://www.statista.com/topics/7476/transportation-emissions-worldwide/#topicOverview
3. OCED (Organization for Economic Co-operation and Development) Library, 2023 https://www.oecd-ilibrary.org/sites/9789282108000-5-en/index.html?itemId=/content/component/9789282108000-5-en
4. OCED (Organization for Economic Co-operation and Development) Library, 2023a https://doi.org/10.1787/888933442489
5. Eurostat, 2023 https://ec.europa.eu/eurostat/statistics-explained/index.php?title=Passenger_cars_in_the_EU
6. Fuels Europe, 2022 https://www.fuelseurope.eu/uploads/files/modules/documents/file/1663230286_ioJP58jl02UbyFRDDIjlzMIlIEhEFPiv1mPSAtU9.pdf
7. European Commission, 2023 https://climate.ec.europa.eu/eu-action/transport/road-transport-reducing-co2-emissions-vehicles/reducing-co2-emissions-heavy-duty-vehicles_en
8. Business of Apps, 2023 https://www.businessofapps.com/data/uber-statistics/
9. United Nations, 2023 https://www.un.org/en/desa/world-population-projected-reach-98-billion-2050-and-112-billion-2100
10. Fuel Economy Gov, 2021 https://www.fueleconomy.gov/feg/contentincludes/co2_inc.htm
11. Washington Post, 2018 https://www.washingtonpost.com/news/in-sight/wp/2018/02/28/the-cost-of-cobalt/
12. US Energy Information Administration, 2022 https://www.eia.gov/energyexplained/biofuels/
13. The Drive, 2023 https://www.thedrive.com/cars-101/36563/what-is-flex-fuel
14. Protec Fuel, 2023 https://protecfuel.com/e15-e85-e100/
15. Pimentel, D., Patzek, T.W. (2005) Ethanol Production Using Corn, Switchgrass, and Wood; Biodiesel Production Using Soybean and Sunflower. *Nat Resour Res* **14**, 65–76. https://doi.org/10.1007/s11053-005-4679-8
16. CNBC, 2023 https://www.cnbc.com/2024/01/02/tesla-tsla-q4-2023-vehicle-delivery-and-production-numbers.html
17. ZeCar, 2023 https://zecar.com/resources/what-are-lfp-nmc-nca-batteries-in-electric-cars
18. Earth Organization, 2022 https://earth.org/cobalt-mining/
19. ZeCar, 2022a https://zecar.com/resources/electric-car-mythbusters-ownership-impact-part-3
20. ZeCar, 2022b https://zecar.com/resources/electric-car-mythbusters-ownership-impact-part-3
21. EIA (Energy Information Administration), 2022 https://www.eia.gov/tools/faqs/faq.php?id=427&t=3
22. Floodlight, 2023 https://floodlightinvest.com/recycling-of-lithium-batteries-and-ghg-emissions/
23. Floodlight, 2023a https://floodlightinvest.com/recycling-of-lithium-batteries-and-ghg-emissions/
24. Nature, 2022 https://www.nature.com/articles/s41598-022-22018-1
25. JACS (Journal of the American Chemical Society), 2018 https://pubs.acs.org/doi/10.1021/jacs.8b03408
26. ECHA (European Chemicals Agency), 2023 https://www.echa.europa.eu/substance-information/-/substanceinfo/100.122.762
27. ECHA (European Chemicals Agency), 2023 https://echa.europa.eu/substance-information/-/substanceinfo/100.000.757

28. Fuel Economy, 2023 https://www.fueleconomy.gov/feg/fcv_PEM.shtml
29. AFDC (Alternative Fuels Data Centre), 2023 https://afdc.energy.gov/vehicles/how-do-fuel-cell-electric-cars-work
30. AFDC (Alternative Fuels Data Centre), 2023a https://afdc.energy.gov/vehicles/how-do-all-electric-cars-work
31. The Motor Digest, 2023 How Much Do Tesla Batteries Weigh? - The Motor Digest.
32. Street NM, 2016 Chart of the Day: Vehicle Weight vs Road Damage Levels - Streets.mn
33. Fuel Economy, 2023a https://www.fueleconomy.gov/feg/fcv_PEM.shtml
34. Toyota UK, 2023 https://media.toyota.co.uk/wp-content/uploads/sites/5/pdf/210426M-NG-Mirai-Tech-Spec.pdf
35. GLP Autogas, 2024 Hydrogen Stations USA. Map and List Updated (glpautogas.info)
36. CNET (Computer Network), 2023 https://www.cnet.com/roadshow/news/states-banning-new-gas-powered-cars/
37. SuperTurbo Technologies, 2020 https://www.superturbo.net/wp-content/uploads/2022/03/STT-Hydrogen-EPT-3.17.22.pdf
38. Cummins Inc, 2022 https://www.cummins.com/news/2022/06/13/hydrogen-engine-insights-truck-and-bus-manufacturers
39. US DOE (Department of Energy), 2024 https://eere-exchange.energy.gov/Default.aspx?Search=propulsion%20technologies&SearchType=
40. Power Magazine, 2021 https://www.powermag.com/environmental-and-permitting-considerations-for-decarbonizing-with-hydrogen/

Notes

Note 1: For the purposes of this discussion when referring to hydrogen, I mean green hydrogen produced via renewable energy and AEM water electrolysis.

Note 2: The number in an ethanol blend, for example 10 in E10 represents the maximum percentage of ethanol the blend contains; E10 contains up to a maximum of 10% ethanol.

Note 3: The terms zero carbon and zero emission are used interchangeably in this document but refer to the same outcome, the same is applicable to retail or service station.

Note 4: I have worked in the energy industry for over twenty-five years in many countries and currently lead the deployment of new energy technologies for a large global technology company with a focus on water electrolysis and carbon capture development. Aside from the references listed I have first-hand experience and knowledge of the advances in AEM electrolysis, materials-based storage and fuel and lubricants technology including vehicle testing. Please feel free to contact me for further information or discussion.

This page is intentionally left blank

Global Journal of Researches in Engineering: A
Mechanical and Mechanics Engineering
Volume 24 Issue 1 Version 1.0 Year 2024
Type: Double Blind Peer Reviewed International Research Journal
Publisher: Global Journals
Online ISSN: 2249-4596 & Print ISSN: 0975-5861

The Main Methodological Postulate of Pyrometry and the Need for its Revision

By Alexandr Frunze

Abstract- The analysis of the methodological principles on which pyrometry is based is carried out. Special attention is paid to the main methodological postulate and its consequences. The roots of its formation are considered. It is shown that the large methodological errors characteristic of pyrometry are a direct consequence of the system of priorities arising from this postulate. A new basic methodological postulate of pyrometry is formulated, it is shown that the development of the ideas contained in it will reduce the number of methodological errors by an order of magnitude or more, and the necessary and sufficient conditions for this reduction are formulated.

Keywords: pyrometry, methodological principles, radiation laws, spectral emissivity, temperature dependence of emissivity, reference means for spectral emissivity.

GJRE-A Classification: LCC Code: TJ1-1570

THEMAINMETHODOLOGICALPOSTULATEOFPYROMETRYANDTHENEEDFORITSREVISION

The Main Methodological Postulate of Pyrometry and the Need for its Revision

Alexandr Frunze

Abstract- The analysis of the methodological principles on which pyrometry is based is carried out. Special attention is paid to the main methodological postulate and its consequences. The roots of its formation are considered. It is shown that the large methodological errors characteristic of pyrometry are a direct consequence of the system of priorities arising from this postulate. A new basic methodological postulate of pyrometry is formulated, it is shown that the development of the ideas contained in it will reduce the number of methodological errors by an order of magnitude or more, and the necessary and sufficient conditions for this reduction are formulated.

Keywords: pyrometry, methodological principles, radiation laws, spectral emissivity, temperature dependence of emissivity, reference means for spectral emissivity.

I. Introduction

The rapid development of microelectronics and microprocessor technology in the last quarter of the 20th century made it possible to bring instrument engineering to a qualitatively higher level. In many industries, the instrumental errors of measuring instruments have decreased to fractions of a percent. Pyrometers are no exception here.

But at the same time, as is known, any of the pyrometry methods has inherent methodical errors[1], the magnitude of which can reach 10 ... 15%, i.e. an order of magnitude or more exceeding the instrumental ones. There are still no ways to *guarantee* their reduction to the level of 1-2%. And the most significant thing is that over the past half century, it has not been possible to reduce the magnitude of these methodological errors in relation to any material whose non-contact temperature measurement may be in demand. And the reason for this, of course, is not at all due to dishonesty or low qualifications of researchers.

II. On the Need to Analyze the Methodology of Pyrometry

The author of this work argues that the problems of pyrometry are methodological in nature. Their solution requires analysis and possible revision of the methodological principles of pyrometry. The work [1] is devoted to this analysis.

Author: e-mail: alex.fru@mail.ru

For applied science, methodology is understood as a system (complex, interconnected set) of postulates and principles of research activity, which a scientist relies on in the course of obtaining and developing knowledge within a given specific scientific discipline or several scientific disciplines ([2]).

Obviously, there are methodological postulates, principles and approaches common to all branches of technical sciences (the obligation of mathematical calculations or modeling, the correspondence of calculated data to experimental data, etc.), and there are also particular, specific ones that apply only to individual industries or to one specific industry. It is quite obvious that it is not methodological principles and postulates common to all branches of technical sciences that slow down the development of pyrometry, because even in related fields (for example, in contact methods of temperature control) there are no problems of large methodical errors. Therefore, the source of irreducible methodical errors should be sought in specific methodological postulates and principles of pyrometry.

However, the methodological postulates and principles specific to pyrometry have not yet been clearly formulated. The reason is that most specialists in this field have not yet realized that the problems of incessant huge methodical errors are methodical in nature. The desire to formulate methodological principles and postulates that determine the course of development of a particular industry arises only after realizing the futility of trying to solve the problem within the framework of existing knowledge. Half a century of stomping in place on the issue of reducing methodical errors from a 10...20 percent level to units or fractions of a percent just suggests that there is a need to revise the methodological postulates and principles of pyrometry.

III. Methodological Principles and Approaches in Pyrometry

The principles and approaches most characteristic of modern pyrometry are listed below ([1]):

1. Regular resumption of attempts to find the temperature of the measured object only by its radiation, based only on Planck's or Wien's laws, without taking into account its radiative properties.

[1] The errors of the method

Global Journal of Research in Engineering (A) XXIV Issue I Version I Year 2024

2. Consideration of the emissivity [2] as a minor, secondary, and even interfering factor, both in theoretical constructions and in the practical implementation of pyrometry methods.
3. The use of only those reference means during verification[3] and calibration that perfectly implement the laws of radiation ("absolutely black bodies", BB).
4. The lack of reference means and measuring instruments of spectral emissivity.
5. The almost universal disregard of the dependence of the spectral emissivity characteristic of most objects on the temperature of the object and on the state of its surface (roughness, the presence of liquids, oil films, etc.).
6. Reduction (both in theoretical calculations and in practice) of the complex influence of emissivity to a one–dimensional effect described by a simple numerical coefficient, with complete disregard for the fact that emissivity is not a coefficient, but a function of at least two variables.
7. The use of various adjustment organs in almost all modern pyrometers, which make it possible to adjust the measurement results in any direction within a fairly wide range.
8. The lack of developed algorithms for determining the actual temperature of an object by its pseudo-temperature (brightness, partial radiation, radiation or spectral ratio), taking into account the temperature dependence of the emissivity characteristic of most objects.

As for paragraphs 3, 4 and 7, they are obvious. The statement of paragraph 2 also becomes obvious when analyzing almost all books published over the past 50 years, the authors of which try to cover pyrometry as a whole, rather than highlight certain selected issues. In these books, the laws of Planck, Wien, Stefan-Boltzmann, Rayleigh-Jeans, Kirchhoff, Lambert are usually described in detail first, and only after that the concept of emissivity is introduced, characterizing the difference between the radiation of real objects and the radiation of the BB.

According to claim 1, measurements in polarized light can be noted [3], the use of multiband spectral-ratio pyrometers with narrow spectral bands [4], the use of spectrometers [5], etc.

As a confirmation of what was said in paragraphs 5, 6 and 8, the following can be cited.

In the known relations present in almost all books on pyrometry, linking the actual temperature of an object T_d with its brightness or radiation temperature, the emissivity appears in the form of constants ε_λ, ε_s:

$$\frac{1}{T_d} = \frac{1}{T_b} + \frac{\lambda}{c_2}\ln\varepsilon_\lambda \tag{1}$$

where T_d is the actual temperature, K; T_b is the brightness temperature measured by the pyrometer, K; $c_2 = 1.4380\cdot10^{-2}$m·K; λ is the operating wavelength of the monochromatic brightness pyrometer, m; ε_λ is the radiation coefficient of the object at the wavelength λ.

$$T_д = T_r / \sqrt[4]{\varepsilon_s} \tag{2}$$

where T_d is the actual temperature, K; T_r is the radiation temperature measured by the pyrometer, K; ε_s is the integral radiation coefficient.

However, if we take into account that ε_λ and ε_s are not constants, but functions of wavelength λ and temperature T_d, and instead of *constants* substitute *functions* $\varepsilon(\lambda, T_d)$ in (1) and $\varepsilon_s(T_d)$ in (2), then simple calculation relations (1) and (2) turn into equations unsolvable in analytical form. There are no algorithms for solving these equations in general.

IV. The Main Methodological Postulate of Pyrometry

The analysis of the above methodological principles and approaches characteristic of modern pyrometry allows us to identify something common to all of them without exception. This is the *implicitly postulated priority of radiation laws in this industry over all other laws and patterns* used to determine the temperature of heated bodies by their radiation. It is she who is today the main methodological postulate specific to pyrometry, which hinders its development.

This methodological postulate has a historical origin, since the laws of radiation were formulated back in the XIX century, and there is still no theory that would link the radiative characteristics of a substance with its physico-chemical constants, and at the same time would not diverge from experimental data *in the entire spectral range.*

Of particular importance is the fact that this priority is postulated implicitly, by stealth. None of the researchers claims that finding the *exact* temperature of an object by its radiation without knowing its radiative properties is possible. But in practice, all modern research in pyrometry is aimed precisely at finding the temperature of heated objects without knowing their radiative characteristics. After all, if this succeeds, it will be possible to forget about the dreary measurements of the emissivity, depending on both the state of the object's surface and its temperature. From this point of view, the game is worth the candle, since there are still no devices for measuring emissivity, and experimental installations that allow this to be done are large, expensive, low-mobility, measurements on them require

[2] Further, everywhere by the emissivity of an object we will understand its spectral $\varepsilon(\lambda)$ or temperature-spectral $\varepsilon(\lambda,T)$ emissivity

[3] In Russia, verification is the confirmation by one of the accredited state metrological centers of the declared metrological characteristics of the device being verified

high qualifications and a lot of time. Therefore, the prospect of learning how to measure temperature by radiation without knowing the radiative properties looks very tempting.

The most likely solution to this problem seems to be using spectrometers, so today most research is conducted in this area [5]. However, the possibility of such a solution *for any predetermined material* is not yet obvious.

If we return to the pyrometers, then the following should be noted. The above-mentioned emissivity characterizes the difference between the radiation of a real object and the radiation of an BB. If the differences are small, then the measurement error with a pyrometer calibrated according to the BB is also small. But for many objects that have to be measured with pyrometers, the differences in their radiation spectrum are quite large from the spectrum of the radiation of the BB.

An BB-calibrated pyrometer, by definition, cannot correctly measure the temperature of an object that does not emit as an BB. The error that occurs during such measurements is the main methodical error, it is determined not by the quality of calibration, but by the problem of the measurement method (i.e., the need to measure an object that emits differently from the sample from which the pyrometer was calibrated). How can such an error be reduced or eliminated altogether?

In today's practice, pyrometers are equipped with regulators, with the help of which a certain coefficient can be entered into them, usually taking a value from 0.1 to 0.99...1. This coefficient is usually called the “blackness coefficient”, “degree of blackness” or “radiation coefficient”. Using this coefficient, the operator can change the measurement result. It is assumed that he knows the “correct” value of this coefficient, and by setting it, he will correct the pyrometer readings and eliminate the mentioned methodical error.

To understand the negative consequences of this approach, you need to ask yourself – where do these coefficients come from? In the best case, measurements once made under these conditions are usually quite rough, with a small number of samples, without fully taking into account all factors affecting the result, without estimating the error. But more often – from literary sources compiled according to the same measurement results, performed by unknown people, unknown when, and with the same disadvantages.

The main thing here is that with this approach, *the correction value is not calculated, but determined experimentally by selecting the radiation coefficient for the value at which the pyrometer will show the correct result (or one that is considered correct for one reason or another)* [4]. Let's add to this that manufacturers do not provide information about what the algorithm for correcting the measurement results of the radiation coefficient entered into this pyrometer is. The latter completely excludes the possibility of correctly accounting for the effect on the pyrometer measurement result of the difference between the radiation spectrum of the measuring object and the frequency response spectrum, the dependence of this difference on the temperature of the object itself, and on the spectral range of the pyrometer, and on the width of the range, and on the state of the surface of the object, and a number of other parameters. As a result, fitting to the expected result remains the only way to correct. In production practice, this leads to the fact that the technologist does not know which of the radiation coefficients to choose from the abundance available in various sources. As a result, the selection is made “by eye” so that the measurement result corresponds to the expected one. This is where users have measurement errors with pyrometers up to 10-20%.

That is, the user is trying to eliminate the methodical error, but the method used today to exclude it does *not guarantee* its reduction. With a successful combination of circumstances, it can decrease to the level of 1-2%, and if unsuccessful, it can remain at the same level of 10-20%. And at the same time, the instrumental errors of modern pyrometers often do not exceed 0.2... 0.5%. That is, the improvement of pyrometers in terms of further reducing the instrumental error at this stage is meaningless, because it does not lead to an increase in measurement accuracy. *Improving the accuracy of measurements in pyrometry has run into a barrier of methodical errors.* How to overcome it?

[4] This is a problem that many still do not realize. Correction by experimentally selected coefficients causes very serious complaints from the point of view of metrology. This can be explained using such a simple example. Let's assume that we measure small voltage values in a printed circuit assembly with a DC microvoltmeter. As is known, when the copper probe of the device comes into contact with the Kovar pin of the chip, a fairly significant contact potential difference occurs, about 30 mV at room temperature. It is quite obvious that if, instead of subtracting this potential difference from the measurement result (adjusted, moreover, taking into account the temperature of the output of the chip), we smoothly “tweak” the gain of the microvoltmeter to the value that, according to someone once made estimates, gives the correct value of the measured value, then not only about the unity of measurements in radio engineering, but also their accuracy can be forgotten. *It is unacceptable to exclude errors by the method of “fitting an experimentally selected coefficient to the correct result”,* without relying on the measurement of the influencing quantity and on knowledge of its dependencies on certain environmental parameters.

Global Journal of Research in Engineering (A) XXIV Issue I Version I Year 2024 13

V. The Need to Isolate the Planck Component from the Total Radiation of the Object

To overcome this barrier, it is necessary to realize what happens when measuring when we neglect the influence of the radiative properties of the measured object. Let's turn to Fig. 1. Here are the Spectral Radiance (SR) of transformer steel when heated to 1127°C in a nitrogen-hydrogen atmosphere (1) and high-alumina firebrick heated in air to the same temperature (2). The results are obtained based on the data given in [4]. Here, for comparison, the SR of the source of ideal Planck radiation – BB (3) at the same 1127°C is given. Obviously, the isolation of the Planck component[5] 3 from dependencies 1 and 2 is an operation completely unobvious, none of the radiation temperature measuring devices is designed to solve this problem.

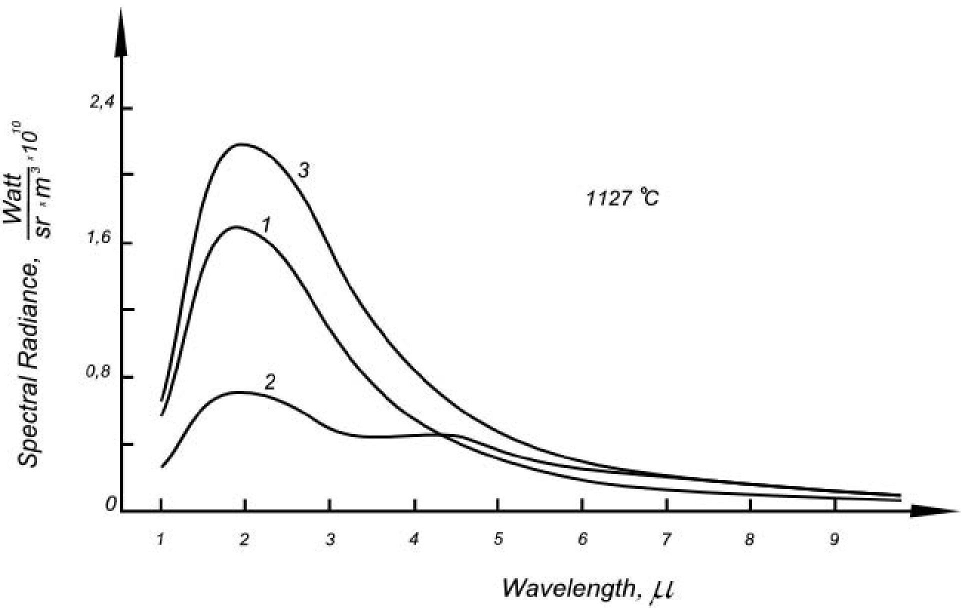

Figure 1: Spectral Radiance (SR) of transformer steel when heated to 1127°C in a nitrogen-hydrogen atmosphere (1), high-alumina firebrick heated in air to the same temperature (2) and BB at 1127°C (3)

The need to isolate the Planck component from the complete SR of an object arose at the dawn of the development of practical pyrometry. This turned out to be necessary because pyrometers are universally calibrated by BB, and after such calibration they can correctly measure the temperature of only those objects that emit as BB – "black" and "gray". When measuring other objects, it is that part of their radiation that distinguishes it from the radiation of the BB, and introduces an additional error, which we call methodical. Therefore, in order to exclude it, one way or another, its banking component must be isolated from the entire radiation of the object. Or somehow exclude the influence of non-Plank component.

VI. Spectral Emissivity and its Role in Eliminating Methodical Errors

The spectral emissivity can be defined as the result of the functional division of the SR of a real object into the SR of an BB (hereinafter, functional division is understood to be the division of the ordinate of the function-divisible by the ordinate of the divisor function for the same abscissa for the set of all possible abscissae).

Figure 2 shows the dependences on the wavelength of the spectral emissivity of transformer steel (1) and high alumina firebrick (2), corresponding to a temperature of 1127°C [4]. As noted, we call these *functions* spectral emissivity in order to distinguish them from the *coefficients*[6] *introduced into energy pyrometers* and still called by inertia by many users of pyrometers and authors of articles on pyrometry "emissivity". Let's add that the spectral emissivity is also a function of the temperature of the object.

[5] Here and further, under the Planck component (Planck curve), we will understand the CR BB.

[6] In this paper, the author calls this coefficient the "radiation coefficient", not emissivity.

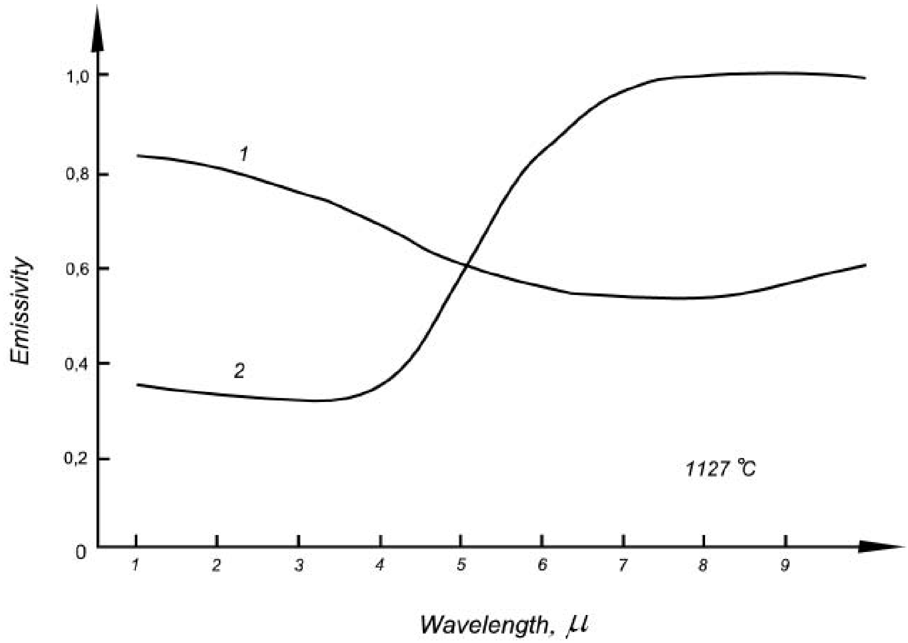

Figure 2: Spectral emissivity of transformer steel when heated to 1127°C in a nitrogen-hydrogen atmosphere (1), and high-alumina firebrick heated in air to the same temperature (2)

Thus, the spectral emissivity is a function that contains the difference between the SR of a real object and the SR of an BB having an equal temperature with the object. Its non-accounting (or incorrect accounting) does not make it possible to correctly convert the SR of the measured object into a Planck curve of equal temperature with the object, according to which this temperature can be measured without any systematic errors using an BB-calibrated pyrometer.

One of the ways of such a separation of the Planck component from the total radiation spectrum is the functional division of the SR of a real object into its real spectral emissivity. However, this is possible only if we have at our disposal almost complete spectral dependences of the SR and emissivity, i.e. lying in the wavelength range where the values of the Planck curves for these objects exceed 0.5-1% of their maxima. This is typical for spectral pyrometry, which is at the initial stage of its development. But pyrometers are not spectrometers, and such a functional division is impossible for them. Nevertheless, knowledge of the spectral emissivity is also necessary for classical energy pyrometers[7] and pyrometers of spectral ratio (at least in the range of spectral sensitivity of these measuring instruments). However, it should be used in the allocation of the Planck component in a slightly different way. Here is one of the options for such a selection.

First, the full view of the object's SR is calculated for all measured temperatures (for example, with a given step within the entire measurement range). To do this, for each of the temperatures, its spectral emissivity is functionally multiplied by its Planck function. Next, using the obtained SR, a set of pseudo–temperatures (brightness, or radiation, or spectral ratio - depending on which type of devices the correction is performed) is calculated. This calculation can be performed using calibration[8] functions. Then a table is formed in which the actual temperature is assigned to each of the obtained pseudo–temperatures - the one whose Planck curve was used to calculate this pseudo-temperature. And at the last stage, the actual temperature of the measured object is determined based on the result of the pyrometer measurement using the above-mentioned recalculation table ([6]). When using the real spectral emissivity in this algorithm, methodical errors are excluded, and the error is determined only by the instrumental errors of the pyrometer used.

In fact, in this case, we modify the scale determining function (inverse of the calibration function) of the pyrometer so that it takes into account the difference between the SR of the measured object and the SR of the BB. Which is essentially equivalent to separating the Planck component from the total flux of its radiation.

Once again, I would like to draw readers attention to an important statement – if we want to measure temperature with a pyrometer without

[7] Energy pyrometers are understood to be all pyrometers having only one radiation receiver, which determine the temperature by the magnitude of the signal from the receiver, i.e. by the magnitude of the energy flow that came to it

[8] The calibration function is, in this case, the dependence of the voltage at the output of the receiver signal amplifier (for an energy pyrometer) or the spectral ratio (for a pyrometer of the spectral ratio) on the temperature of the BB

methodical errors, we must somehow isolate the aforementioned Planck component from all the radiation that came to the pyrometer. Its measurement with an BB-calibrated pyrometer will give the desired result. Or, one way or another, exclude the influence of a non-Planck component, which will lead to the same measurement result.

And how do we allocate the Planck component today? Few people have thought about this – the extraction operation, which is the result of a complex mathematical calculation, has been replaced by correction using coefficients [9] introduced into pyrometers, most often determined experimentally. The task of isolating the Planck component in today's pyrometry has been simplified to the limit – the radiation flux that came to the energy pyrometer is actually simply divided by the radiation coefficient introduced into it. A complex functional transformation is ultimately reduced to division by a constant taken from tables, which very often have a very distant relation to the measured object. Hence the methodical errors, which are absolutely independent of the pyrometer's own instrumental error.

Naturally, classical pyrometers are not spectrometers, they do not measure the SR with some kind of normalizing coefficient, but its integral value in the form of a signal at the output of their radiation receiver. Therefore, the functional division mentioned above is not a task for them. If we are talking about energy pyrometers, then correction by the radiation coefficient is all they can do. But then the procedure for isolating the Planck component should somehow "migrate" at least to the calculation of the radiation coefficient. Such a calculation of the radiation coefficient, taking into account the spectral emissivity $\varepsilon(\lambda, T)$, is described below (see (4)). However, it has certain limitations, which will be described later. Therefore, the task of comprehensively eliminating the influence of temperature-spectral emissivity on the pyrometer measurement result is still relevant. Taking into account all the above, it will be formulated and specified in the last subsection of this article.

It is safe to say that devices for remote temperature measurement will continue to be calibrated according to BB in the future. Consequently, the task of isolating the Planck component from the full SR, according to which these devices will measure temperature, will also remain. And its solution is impossible without knowledge of the spectral emissivity. And the more precisely it is determined (as well as the more accurately the calibration of the measuring instrument used is carried out), the more accurately the temperature of the measured object will be determined. In a different way, using some averaged coefficients introduced into pyrometers, it will not be possible to get rid of methodical errors.

[9] For very narrow-band pyrometers and for full-radiation pyrometers, correction in accordance with (1) and (2) is quite acceptable, but with certain reservations: firstly, it is still necessary to know the temperature-spectral emissivity of the object, and secondly, the radiation coefficients depend on temperature, sometimes strongly, and for the choice of their exact values require knowledge of the very temperature of the object for which they are needed to measure. The latter greatly limits the correction according to (1) and (2) for accurate measurements.

VII. About the New Basic Methodological Postulate of Pyrometry

All of this means the need to rethink the basic methodological postulate mentioned above, which is specific to pyrometry, which consists in the fact that to determine the temperature of an object by its radiation, it is enough to know and use only the laws of radiation, ignoring accumulated or still missing knowledge about the radiative properties of specific objects. It should be replaced by a postulate proclaiming that *the exclusion of methodical errors in non-contact measurement of its temperature is impossible without knowledge of the real* (not generalized or averaged!) *the spectral emissivity of a particular measured object, and its correct accounting.* Attempts to deceive nature and continue to ignore the need to accumulate knowledge about the radiative properties of objects will leave unchanged methodical errors that have hindered the development of pyrometry for more than half a century.

However, this is not all. Since until now there has not been a theory that adequately connects the spectral emissivity with the physico-chemical constants of the object's material, it will be necessary to obtain the necessary information about the spectral emissivity experimentally. At the same time, it should be noted that at the moment there are no specialized measuring instruments for spectral emissivity on the market. Nevertheless, in the works of the author ([7, 8] the technical possibility of creating such measuring instruments is demonstrated, two such devices are described, one of which is protected by a patent of the Russian Federation.

The author also argues the need to have a verification scheme for such devices, as well as a currently missing standard of emissivity, which will stand at the top of this verification scheme ([9, 10]).

VIII. About what else is Needed

However, knowledge of the spectral emissivity is only a necessary condition for reducing or completely eliminating large methodical errors inherent in pyrometry methods. It is not sufficient for this reduction, since algorithms and methods for minimizing/eliminating these errors with full consideration of temperature-spectral emissivity are either insufficiently developed or absent. Therefore, it is necessary to solve the following scientific problems.

1. As is known, when measuring of "non-gray" objects with spectral-ratio pyrometers, they have a methodical error, the mechanism of which is discussed in detail in [11]. The ratio (3) is known, which allows (knowing the spectral emissivity) to compensate for this methodical error:

$$\frac{1}{T_d} - \frac{1}{T_{sp.rel}} = \ln\frac{\varepsilon_{\lambda_1}}{\varepsilon_{\lambda_2}} \frac{1}{c_2} \frac{1}{\frac{1}{\lambda_1} - \frac{1}{\lambda_2}} \qquad (3)$$

where T_d is the actual temperature, K; $T_{sp.rel}$ is the temperature of the spectral ratio measured by the pyrometer, K; $c_2 = 1.4380 \cdot 10^{-2}$ m· K; λ_1 and λ_2 are the operating wavelengths of the narrowband pyrometer of the spectral ratio, m; ε_{λ_1} and ε_{λ_2} are the emission coefficients at wavelengths λ_1 and λ_2.

However, this ratio is valid only for pyrometers with narrow (no more than 10…20nm) spectral bands.

At the same time, the vast majority of spectral-ratio pyrometers produced today are broadband, the width of the spectral bands of their sensitivity is tens or even hundreds of nanometers. As a result, ratio (3) is essentially inapplicable for the absolute majority of pyrometers used in practice, and has more theoretical than practical value. Therefore, a universal method is needed to correct the methodical error that occurs when measuring the temperature of "non-gray" objects with any pyrometers of spectral ratio. This method is developed and described in [6, 12]. They present an algorithm for machine calculation of the temperature of the spectral ratio of "non-gray" objects using a calibration function, and an experimental study of the method is carried out. However, the proposed method (as well as in the ratio (3)) does not take into account the temperature dependence of the spectral emissivity. Therefore, the method needs to be improved, taking into account this dependence.

Thus, the problem can be formulated as follows: the above-mentioned universal method for correcting pyrometers of the spectral ratio must be improved in such a way as to take into account the temperature dependence of the spectral emissivity. After that, it, together with information about the spectral emissivity, will become necessary and sufficient conditions for minimizing/eliminating methodical errors in the method of pyrometry of the spectral ratio.

The solution of this problem is described by the author in [13].

2. In contrast to the spectral ratio pyrometry method, the emissivity correction is fundamentally necessary in the energy pyrometry method. To do this, before measuring, a correction factor is introduced into the energy pyrometer, which in this work is called the radiation coefficient. The radiation coefficients introduced into pyrometers are almost universally determined experimentally, by adjusting this coefficient to the value at which the result of temperature measurement using a pyrometer is close to the result of measurement by contact methods. Once selected in this way, the radiation coefficient is then usually transferred to all pyrometers that have to measure such an object. The measurement errors caused by such a transfer are described in [14]. And, moreover, with this approach, it is impossible to correctly take into account not only the spectral range of the pyrometer used, but also the temperature dependence of the emissivity. And this in turn leads to the appearance of additional methodical errors described in [15].

In [16], a ratio is given that allows the recognition of the spectral emissivity and spectral sensitivity characteristics of a photodiode pyrometer to correctly determine the radiation coefficient:

$$\varepsilon_{\lambda,T} = \frac{\int_{\lambda_1}^{\lambda_2} \varepsilon(\lambda,T) S(\lambda) E(\lambda,T) d\lambda}{\int_{\lambda_1}^{\lambda_2} S(\lambda) E(\lambda,T) d\lambda} \qquad (4)$$

where $\varepsilon_{\lambda,T}$ is the radiation coefficient at wavelength λ for temperature T, $\varepsilon(\lambda,T)$ is the spectral emissivity of the object; $S(\lambda)$ is the spectral characteristic of the pyrometer sensitivity; $E(\lambda, T)$ is the Planck function; λ_1 and λ_2 are the lower and upper limits of spectral sensitivity.

Since (4) represents the ratio of two definite integrals that are practically insoluble analytically, its use in practice by metrologists and technologists of enterprises is hardly possible – for this, a specialist must have a legally purchased package such as MathCad or Mathlab and be able to use it. Therefore, it is necessary to develop simple and freely distributed programs with which users with minimal computer skills could determine the radiation coefficient according to (4). One of the variants of the set of such programs is given in [17].

Further, since $\varepsilon(\lambda,T)$ and $E(\lambda, T)$ depend on the temperature of the object, the coefficient $\varepsilon_{\lambda,T}$ also depends on temperature. That is, the radiation coefficient found using (4) depends on the temperature. In this case, a vicious circle arises – in order to measure the temperature correctly with an energy pyrometer, you need to enter the correct value of the radiation coefficient into it. But to find the correct value of the radiation coefficient, you need to know the temperature of the object, which we are still only going to measure. The established practice of adjusting the radiation coefficient to the correct result, if this correct result is unknown in advance, does not solve the problem.

It follows from the above that for the accurate correction of energy pyrometers for emissivity, not only the ratio (4) is required, but also a preliminary knowledge of the temperature to be measured, because without this it is impossible to correctly select those $\varepsilon(\lambda,T)$ and $E(\lambda, T)$ that are necessary to calculate $\varepsilon_{\lambda,T}$ according to (4).

Therefore, the task can be formulated as follows: for energy pyrometers, it is necessary to develop a method of correction for emissivity, different from the one currently used, in which there is no need for prior knowledge of the temperature to be measured in order to correctly use the temperature-dependent radiation coefficient $\varepsilon_{\lambda,T}$ i.e. it is necessary to break this vicious circle when you need to know its correct value to measure temperature, and in order to calculate it correctly in accordance with (4), we need to know this temperature, which is still unknown to us. The current method of correction is not capable of breaking it without some additional information.

It is the above-mentioned method of correction, which differs from the currently used one, in combination with knowledge of temperature-dependent spectral emissivity, that will be the necessary and sufficient means to minimize/exclude methodical errors in the method of energy pyrometry.

The solution of the mentioned problem is planned by the author to be published in one of the next issues of one of the periodicals covering measuring topics. A general approach to solving this problem is formulated in [18].

The implementation of solutions to the formulated tasks will dramatically reduce the methodical errors in pyrometry to a level comparable to the level achieved by instrumental errors.

IX. Conclusion

1. The main methodological postulate specific to pyrometry is formulated – the implicitly postulated priority of radiation laws in this branch over all other laws and patterns used to determine the temperature of heated bodies. It is shown that it is the unconscious adherence to this postulate that does not allow for half a century to solve the problem of reducing/eliminating methodical errors in non-contact temperature control methods.
2. A new, alternative to the above, basic methodological postulate specific to pyrometry is formulated. He proclaims that without knowledge and use of the real (not generalized or averaged!) the temperature-spectral emissivity of a particular measured object it is impossible to exclude methodical errors in the non-contact measurement of its temperature.
3. Since to date there has not been a theory that adequately connects the temperature-spectral emissivity with the physico-chemical constants of the object's material, it is argued that it will be necessary to obtain the necessary information about the spectral emissivity experimentally. At the same time, it should be noted that at the moment there are no specialized measuring instruments for spectral emissivity on the market. Nevertheless, in a number of the author's works, the technical possibility of their creation is demonstrated, two such devices are described, one of which is protected by a patent of the Russian Federation.
4. However, knowledge of the spectral emissivity is only a necessary condition for reducing or completely eliminating large methodical errors inherent in pyrometry methods. For sufficiency, it is necessary to develop algorithms and methods for accounting for the effect on the spectral emissivity of the temperature of the measured object, which are now either insufficiently developed or completely absent.
5. References are given to the algorithms developed by the author of this article for taking into account the influence of temperature on the spectral emissivity of an object used in the methods of spectral ratio pyrometry and energy pyrometry.
6. The algorithms noted in paragraph 5 (recognition of temperature-spectral emissivity), when implemented, will reduce the methodical errors of pyrometry methods to a level comparable to the level achieved by instrumental errors.

References Références Referencias

1. *A. V. Frunze,* The development of pyrometry methodology, Scientific Review, 2014, No. 10, pp. 78-81.
2. *A. Ya. Baskakov and N. V. Tulenkov,* Methodology of scientific research: Textbook. The manual, Kiev, 2004, 216 p.
3. *D. Ya. Svet,* Objective methods of high-temperature pyrometry with a continuous radiation spectrum, Moscow, Nauka, 1968, 240 p.
4. *A. M. Belenky, M. Y. Dubinsky, M. G. Ladygichev, V. G. Lisienko,* Temperature measurement: theory, practice, experiment, Reference edition, in 3 volumes, Vol. 2, Moscow, Teplotekhnik, 2007, 736 p.
5. *A. N. Magunov,* Spectral pyrometry, Moscow, FIZMATLIT, 2012, 248 p.
6. *A. V. Frunze,* A numerical method of determining the spectral-ratio temperature, Measurement Techniques, 2010, Vol. 53, No. 6, pp. 664-667.

7. *A. V. Frunze,* Patent of the Russian Federation No. 2403539 (Russian Federation). A device for determining the spectral emissivity of heated objects. Declared on 06/23/2009.
8. *A. V. Frunze,* Development of an optoelectronic method for measuring temperature with two-spectral photodiodes based on the study on the spectral emissivity of magnetic, composite and refractory materials, abstract of the dissertation for the degree of Candidate of Technical Sciences, Russian State Technical University, K.E. Tsiolkovsky University (MATI), Moscow, 2011.
9. *A. V. Frunze,* On the need to create a primary standard of emissivity, Metrology, 2012, No. 6, pp. 22-27.
10. *A. V. Frunze,* Metrological problems of modern spectral pyrometry, Measurement Techniques, 2018, Vol. 61, No. 6, pp. 621-626.
11. *A. V. Frunze,* About one little-known feature of spectral ratio pyrometers today, Photonics, 2013, No. 3, pp. 86–94.
12. *M. L. Samoilov and A. V. Frunze,* Improving the accuracy of temperature measurements of "non–gray bodies" with a broadband pyrometer of spectral ratio, Metrology, 2010, No. 6, pp. 23–31.
13. *A. V. Frunze,* Improving the accuracy of temperature measurement by a spectral ratio pyrometer // Thermophysics and Aeromechanics, 2023, Vol. 30, No. 3. pp. 581-588.
14. *A. V. Frunze,* Metrological problems of modern energy-controlled pyrometry, Measurement Techniques, 2018, Vol. 61, No. 3, pp. 271–277.
15. *A. V. Frunze,* Methodological errors of modern pyrometers and ways to minimize them, Metrology, 2012, No. 7, pp. 25-38.
16. *D. Ya. Svet,* Optical methods for measuring true temperatures, Moscow, Nauka, 1982, 296 p.
17. *Frunze A. V., Gorbunov R. A., Simakov D. S.,* A set of low-level programs for calculating the temperature of the spectral ratio when measuring the temperature of "non-gray" bodies with two-spectral broadband pyrometers, In the collection: Current problems and prospects for the development of radio engineering and infocommunication systems "RADIOINFOCOM-2021". Collection of scientific articles of the V international scientific and practical conference, Moscow, 2021. pp. 420-426.
18. *Frunze A. V.,* An algorithm for determining the actual temperature of an object, taking into account the temperature dependence of its emissivity, In the collection: Energy-saving technologies in industry. Furnace units, ecology. Proceedings of the VII International Scientific and Practical Conference, National Research Technological University "MISIS"; Compiled by: A. M. Belenky, A. N. Bursin, N. A. Korotchenko, I. V. Korochantseva. 2014. pp. 418-424.

This page is intentionally left blank

Global Journal of Researches in Engineering: A
Mechanical and Mechanics Engineering
Volume 24 Issue 1 Version 1.0 Year 2024
Type: Double Blind Peer Reviewed International Research Journal
Publisher: Global Journals
Online ISSN: 2249-4596 & Print ISSN: 0975-5861

A Survey on Methods to Optimize Power Harvesting in Drones

By Dr. Fath Elrahman Ismaeal Ahmed, Gihad Abdelaziz Abdelghani Ibrahim, Khalil. B. Ahmed. A, Hajir Saeed & Suhail Kamil

Sudan University of Science and Technology

Abstract- This paper explores the challenges associated with limited battery capacity in drones and presents a comprehensive analysis of strategies to optimize energy harvesting and extend flight durations. Various energy generation methods, including piezoelectric and solar harvesting, are discussed, along with electrical circuit generation for wireless charging and communication-enabled energy delivery. The interdisciplinary nature of drone technology is highlighted, emphasizing the need for ongoing research in renewable energy models and innovative solutions like laser charging. The paper concludes with recommendations for further exploration and refinement of these strategies to enhance the future of UAVs.

Keywords: drones, battery capacity, energy harvesting, piezoelectric harvesting, solar-powered UAVs, wireless charging.

GJRE-A Classification: DDC Code: 629.13

ASURVEYONMETHODSTOOPTIMIZEPOWERHARVESTINGINDRONES

Strictly as per the compliance and regulations of:

Open Association of Research Society, USA

Research | Diversity | Ethics

A Survey on Methods to Optimize Power Harvesting in Drones

Dr. Fath Elrahman Ismaeal Ahmed α, Gihad Abdelaziz Abdelghani Ibrahim σ, Khalil. B. Ahmed. A ρ, Hajir Saeed Ѡ & Suhail Kamil ¥

Abstract- This paper explores the challenges associated with limited battery capacity in drones and presents a comprehensive analysis of strategies to optimize energy harvesting and extend flight durations. Various energy generation methods, including piezoelectric and solar harvesting, are discussed, along with electrical circuit generation for wireless charging and communication-enabled energy delivery. The interdisciplinary nature of drone technology is highlighted, emphasizing the need for ongoing research in renewable energy models and innovative solutions like laser charging. The paper concludes with recommendations for further exploration and refinement of these strategies to enhance the future of UAVs.

Keywords: drones, battery capacity, energy harvesting, piezoelectric harvesting, solar-powered UAVs, wireless charging.

I. Introduction

Drones have become increasingly popular for various civilian applications, including commercial, scientific, recreational, and agricultural tasks [1,2,3,4]. However, their limited on-board battery capacity has been a challenge [5,6,7]. The development in artificial intelligence and mechatronics technology have improved the capabilities of drones as aerial robots to making them cost-effective, user-friendly, safe, and environmentally friendly options [8,9,10,11,12,13]. This paper reviews studies that propose solutions to optimize energy harvesting from UAV body vibrations and explore ways to increase flight duration by improving the design and capacity of existing batteries.

II. Analysis of Power Loss during Flight

In the drone, power is lost during flight through mechanical loss (M_{PL}), magnetic loss (EMF_{PL}), iron (I_{PL}), and copper loss (C_{PL}). The total power loss (T_{PL}) is calculated by summation of this power.

$$\mathrm{T_{PL}} = \sum M_{PL} + \mathrm{EMF}_{PL} + I_{PL} + C_{PL} \tag{1}$$

The UAV energy consumption is calculated as

$$\mathrm{E_{Con}} = T_{PL} \times T \tag{2}$$

Where T is time is mints.

The total energy storage in the battery is calculated as

$$\mathrm{E_B} = V_{DC} \times C_B \times 60 \tag{3}$$

the total energy consumption percentage through the fighting is calculated as

$$C_{\%} = \frac{\mathrm{E_B} - \mathrm{E_{Con}}}{\mathrm{E_B}} \times 100\% \tag{4}$$

The features and configurations of UAVs can vary significantly based on their missions. Developing accurate and efficient energy consumption models relies on thoroughly understanding of the contributing factors. Drone operations exhibit higher sensitivity to energy considerations than traditional vehicles [14,15,16,17,18,19]. Various internal and external factors come into play, impacting energy usage. For instance, flying into headwinds has been observed to resulted in lower power consumption, attributed to increased thrust generated during the transition from hovering to forward flight [20,21,22,23,24,25]. The weight and payload of UAVs emerge as crucial factors significantly affecting energy consumption [26,27]. [28] delve into an analysis of different parameters influencing the energy consumption of UAV routing problems, examining a scenario involving a single UAV on a multiple-delivery mission. The study highlights on the relationships between UAV energy consumption and influencing parameters. Drone design, environmental conditions, drone dynamics, and delivery operations are the four main elements influencing drone energy usage, as discussed by [29,30].

III. UAV Power Harvesting Methods

The increasing demand of drones for various civilian and military applications challenges with their power consumption or battery capacity. This paper explores UAV power harvesting methods, focusing on advancements in artificial intelligence and mechatronics technology to enhance drone capabilities as aerial robots. The authors delve into solutions to optimize

Author α: Sudan University of Science and Technology, College of Engineering, Mechanical Engineering, Sudan.
Author σ: Sudan University of Science and Technology, College of Engineering, Mechanical Engineering, Sudan.
Author ρ: ALIMAM ALHADI College-Electrical Engineering, Sudan.
e-mail: kh_sm8888@hotmail.com
Author Ѡ: Sudan University of Science and Technology, College of Engineering, Mechanical Engineering, Sudan.
e-mail: Hajir2222@yahoo.com
Author ¥: SINNAR University, Faculty of Engineering, Mechanical Engineering, Sudan.

energy harvesting from UAV body vibrations and extend flight durations. The paper highlights the diverse strategies employed to make drones cost-effective, user-friendly, safe, and environmentally friendly.

Several studies have been conducted to address the limitations of drone battery capacity and enhance their overall functionality.

Mohamad Hazwan et al. introduces a real-time fault detection system for multirotor. Vibration sensors are attached to the multirotor arms to collect data, which is then analyzed by AI decision-making systems like fuzzy logic, neuro-fuzzy, and NN. The fuzzy logic method performed the best in indoor testing, while the neuro-fuzzy or NN methods may be more effective outdoors. The study suggests expanding the research to include other parameters like propeller vibration, motor condition, and battery level. Also use the accelerometer to measure vibration. using of a printed circuit board (PCB) can reduce wiring and unwanted interference [31].

Matej Karasek, Discusses the significance of stability in flying systems and introduces a new model that incorporating vibrational stabilization. This form of stability is essential important for larger flyers like hawkmoths and hummingbirds. The paper also explores the potential applications of vibrational stabilization in flapping-wing robots and MEMS sensors [32].

Kejing Chen et al, introduce the vibration modes of large-scale multi-rotor manned drones by analyzing small-scale drones through experiments and finite element analysis. It found that, accelerometers measure drone vibrations to some extent. The study also developed a second-generation large-scale drone based on the vibration characteristics of small-scale drones. Circular tubular arms were found to have strong vibrations in the z-axis direction, while elliptical arms effectively reduced vibrations in the same direction. Factors such as motor mounting position and connection between the arms and the body were identified as influences on vibrations, with longer arms causing more noticeable vibration. The study suggested that connecting structures between adjacent arms can help decrease vibration in the drone's beam structure [33].

Xunhua Dai et al, describe the optimization of the UAVs systems, by modeling various components such as the propeller, ESC, motor, and battery. Mathematical derivations estimate important parameters for each element, resulting in improved efficiency. The effectiveness of this approach is demonstrated through experiments and feedback. Optimizing the propulsion system is crucial for designing multicopters and other aircraft systems, and the theoretical analysis can also be extended to enhance the endurance of UAVs, providing opportunities for future research [34].

Abera Tullu et al, discuss the increase use of small-scale UAVs for law enforcement missions, and the need for robust autonomy in these drones. However, using multiple sensors for environmental information is often impractical due to weight and cost constraints [35].

Adam Dáugosz et al. utilized the optimal design of a drone wing made of composite materials. The goal is to improve strength and rigidity while reducing weight. The study uses a multi-objective evolutionary algorithm to optimize the wing structure. Numerical simulations and experimental tests are used to validate the design. The results show that the current design is more rigid than all the other solutions found, and the ideal Pareto solution set offers a range of diverse options for the designer to choose from. Overall, the optimization task of the drone wing design is challenging, but this study provides a promising approach to improving current designs [36].

Heung Soo Kim et al. discuss the use of piezoelectric energy harvesting from vibration sources and the limitations of using monolithic or biomorphic ceramic layers. It introduces piezoelectric total fiber composites (MFC) and three new substrate materials (copper, zinc alloy, and galvanized steel) for energy harvesting. The study includes Computational Fluid Dynamics (CFD) and finite element analysis (FEA) to analyze the performance of different substrate materials and the effect of MFC patches on the shape of an airplane wing. The results show that using MFC patches can improve the aerodynamic performance and stability of the aircraft [37].

Nikola Gavrilovic et al. introduce the feasibility of using wind energy for small UAVs, and the potential for maximizing energy extraction from wind fluctuations. The equations of motion and energy equations are used to develop control strategies that minimize energy usage during flights and maximize energy obtained from wind fluctuations. The study also explores the effects of complex and random three-dimensional wind fields on aircraft performance and power acquisition. The future focus will be on defining the design process and optimal strategies for extracting energy from storms, flight tests with wind measurement systems are necessary for complete understanding of the dynamics and energy exchanges involved [38].

Rocco Citroni et al. develop new strategies for expanding the parameters of small air vehicles (MAVs), specifically in terms of travel distance and mission duration. The first section of the paper presents a model to analyze the energy consumption of drones and proposes different scenarios for improving mission parameters. The second section discusses the design and simulation of a harvesting machine using plasmatic Nano atom technology, which shows potential for enhancing parameters. The results suggest that a hybrid system with the harvesting machine and a new rechargeable battery could indefinitely power the MAVs. [39].

Rutuja Shivgan et al. a model for drone path planning that considers energy consumption. The model focuses on drone acceleration, deceleration, hovering, and turning. The problem of finding an energy-efficient path is formulated as a traveling Salesman problem. The paper proposes a genetic algorithm to minimize energy usage by reducing the number of turns. The results demonstrate that the genetic algorithm with energy optimization significantly reduces energy consumption compared to the greedy algorithm, with more significant savings as the number of waypoints increases [40].

ALPER ERTURK et al. The study initiated a new L-shaped energy harvester design that can produce a broader range of energy. The authors propose an electromechanical model to analyze the harvester's behavior and suggest methods to avoid voltage cancellation. Additionally, the text discusses the potential use of the L-shaped harvester as a landing gear for drones, comparing it with a curved power harvester beam. The theoretical benefits of the L-shaped design are emphasized, and experiments are being conducted to confirm its performance [41].

Georgia Foutsitzi et al. The study aimed to optimize the design of a cantilever piezoelectric energy harvester (PEH) by considering multiple criteria, such as maximizing power output, minimizing system mass, and ensuring maximum bending stress constraint. Three optimization algorithms were used, and the results showed that all algorithms converged to the base Pareto optimal front after approximately ten generations. However, only the GDE3 algorithm could generate solutions with power output exceeding 284 mW/g2. Additionally, GDE3 outperformed the other algorithms regarding solution quality metrics [42].

Pedram Beigi et al. This paper explores the increasing demand for drones and how their energy consumption is crucial in determining their effectiveness. It provides an overview of research on the energy consumption of UAVs and examines the factors influencing their energy consumption during missions [43].

Alastair P et al. present static modeling approach for VTOL UAV power systems, the model accurately predicts losses and efficiency but tends to overestimate energy loss. The paper also showcases the application of the model in different power system architectures, highlighting the advantages of a hybrid system with a hydrogen fuel cell, which enables a lighter vehicle with increased payload or flight time. However, using a boost converter to a DC fixed bus reduces efficiency and flight time compared to the traditional approach [44].

Mohamed Nadir P et al. This paper examines the energy aspect of UAV propulsion systems and compares different power supply architectures and energy management strategies. It emphasizes the importance of hybrid power sources for better performance in various operating conditions. The paper also addresses the challenge of achieving unlimited endurance, and the lack of specific energy management approaches compared to electric cars. Due to limitations in weight and computational ability, real-time power optimization is limited, resulting in offline optimization based on prior knowledge of the task. The paper also discusses various power supply technologies, including switching [45].

Bowen Zhang et al. describe the different technologies used for propulsion in UAVs, such as fuel power, fuel-electric hybrid power, and electric power. This paper examines various power sources and their advantages, considering environmental concerns and the potential of electric propulsion systems. It emphasizes the importance of selecting suitable energy storage devices, distributed propulsion systems, high-energy-density motors, and superconducting motors. However, the paper also acknowledges the limitations in batteries, engines, and power management, especially for larger drones. The future focus should be developing safe and high-density energy storage technology, efficient motors and transformers, and adequate heat management technologies [46].

Jing Zhang et al. the author introduces the potential benefits of using solar-powered UAVs to increase flight time and decrease the need for human intervention in charging the drone batteries. Through augmented learning, the paper demonstrates that optimal decisions can be calculated, leading to increased communication productivity and harvested energy for UAVs, as shown in simulation results [47].

Yixin Yan et al. This paper proposes a magnetic resonance wireless charging system for lithium-battery powered drones, to address the limited battery life issue. The system comprises a transmitter inverter circuit, a coupling device, and a receiver rectifier circuit. The authors derive expressions for power reception and transmission efficiency to guide the system's design. ANSYS Maxwell analysis shows that the magnetic field is concentrated within a radius of 30 mm around the transmission coil. Experimental results demonstrate that the system can maintain stable self-induction of the coupling coil even when displaced, overcoming the low charging efficiency caused by coil misalignment during UAV landing. The system provides a constant voltage output, and the established model is accurate [48].

Zhaohui Yang et al. The paper investigates wireless communication system for energy harvesting capabilities. The system allows drones to deliver energy to users and users to harvest energy for data transfer. The problem is divided into two sub-problems: path planning and energy minimization with fixed path planning. The optimal solution is obtained through various optimization techniques. The paper also suggests that drones should stay directly overhead low-height users for efficient power and information transmission. [49].

Toan V. Quyen et al. The proposed study aims to overcome energy constraints and optimize the harvested energy for UAVs. The study focuses on using radio frequency (RF) and solar energy as sources for energy harvesting. By combining these two energy sources, the output power for the drones is increased to meet the required power parameters. With a charging system, a constant voltage of up to 23.2 V can be achieved, satisfying the standard drone battery requirements. The proposed hybrid system has been optimized, evaluated, and compared to other systems. To further improve the system performance, the charging treatment of the battery and the MPPT algorithm for the solar system should be considered. [50].

Jingjing Yao et al. propose power control in time varying IOD networks with wireless charging for data collection. The authors propose an MDP model and a deep critical actor reinforcement learning algorithm to optimize radio transmission power for each drone, aiming to reduce power consumption. Simulations demonstrate the superiority of their algorithms over existing ones, with their performance being impacted by learning rates and the number of neurons in the actor-critical components [51].

Koszewnik et al. The text enclosed using one-dimensional structures with piezo patches for energy harvesting. It focuses on optimizing the location and parameters of a piezoelectric Harvester connected to one arm of a six-rotor drone for maximum energy harvesting. Adding piezo harvesters to each arm of the drone can extend its flight duration, and further research will be done to improve the energy harvest of each arm [52].

Matthias Perez et al. the researchers conducted an analyzed of the vibrations and electrical energy generated by a quadcopter drone. They aimed to harvest energy by integrating piezoelectric elements into the drone's structure. They tested commercial and homemade transducers and found that while the energy levels obtained from the commercial transducers were suitable for sensor applications, they were insufficient to prolong the flight time. The homemade transducers showed potential, but further improvements are needed regarding adhesion and shelf life [53].

Wang, J et al. a new high-performance piezoelectric energy harvester called the three-stability runner (TGPEH). The researchers analyzed the output characteristics of TGPEH under different wind speeds and load resistance and found that it outperforms conventional power harvesters by having a lower threshold wind speed and higher output voltage. The paper also explores the transformation of potential energy into kinetic energy in the TGPEH. It discusses the increase in output voltage during the transition from oscillations inside the well to oscillations between wells. Additionally, the TGPEH exhibits a higher output power than conventional power harvesters. However, the output response of TGPEH is greatly affected by the initial conditions during the movement between potential wells [54].

Ashleigh Townsend et al. This paper introduces combustion engines, solar energy, hydrogen fuel cells, and supercapacitors. hybrid systems combining different power sources can address issues such as slow charging and poor peak power supply. Supercapacitors are commonly used in hybrid systems due to their benefits. However, more research is needed to explore the effectiveness of supercapacitors in fuel cell systems for drone applications [55].

Cuong Van Nguyen et al. propose a hybrid RF solar harvesting system to improve the flight times of drones. The system addresses the performance drop issue in autonomous systems and introduces new designs and results to solve this problem. The study also suggests enhancing efficiency and reducing bypass time by using fuzzy algorithms or PSO to control the duty cycle of the DC-DC boost transformer. This hybrid can power the drones directly and charge their batteries simultaneously. Additionally, the paper mentions the possibility of increasing the battery storage capacity as another improvement [56].

Silvia Sekander et al. The text found the development and verification of statistical models for renewable energy harvesting. It explains the significance of accurately predicting and monitoring renewable energy sources. It discusses various statistical techniques like Time Series Analysis, Regression Analysis, and machine learning algorithms used to create these models. It also highlights the challenges in validating and verifying these models, including data quality, model robustness, and the impact of external variables [57].

NABIL A. AHMED et al. a new electric power train for solar-powered UAVs. The proposed system utilizes a Zyphry UAV for AC line feed to power the fans and includes solar panels, a lithium-sulfide battery-based power management system, an inverter, and an active output filter (AOF). The AOF reduces the size and weight of the power transmission system, improves conversion efficiency, and reduces unwanted harmonics. Simulation and experimental results demonstrate the effectiveness of the proposed system, which achieves high-quality sinusoidal line voltage waveforms with low distortion. We suggest further investigation of the proposed AOF for application in large-scale photovoltaic power plants [58].

Khac Lam Pham et al. The experiment focused on converting wind energy to electric energy and found that it is a promising method for powering UAVs. Overall, the paper highlights the importance of power supply in the operation of drones and suggests potential methods for improving their efficiency [59].

Karan. Jain et al. applied the concept of staging power sources for UAVs, focusing on multiple engines. The aim is to remove energy sources that no longer save energy, reducing the vehicle's weight and thus reducing energy consumption. The article presents a model for predicting the flight time of a multistage helicopter based on power supply and consumption parameters. [60].

Mohamed Nadir Boukoberine et al. bounded the limitations of battery-powered drones regarding endurance and proposes various solutions to address this problem. These solutions include switching the laser beam in-flight for recharging, a hybrid power supply system that combines battery with fuel and solar energy cells, and supercapacitors. The paper also provides a comparative and critical study of different power supply architectures, aiming to facilitate selecting a suitable power supply system for UAVs. Additionally, the paper highlights the importance of power supply systems in drones and provides recommendations for future research [61].

Krzysztof MATEJA et al. The text discusses the need to develop a system that allows the UAV to be fully independent and suggests two ways to achieve this: determining the number of solar cells used or increasing the capacity of the batteries. It also mentions the potential of paragliding to extend flight time and the importance of creating a detailed simulation model for specific flight scenarios and conditions. Additionally, the text highlights the components of the power supply system for UAVs, such as solar cells, charge controllers, battery cells, and the building management system [62].

Wael Jaafar et al. surrounded the relationship between power, battery dynamics, and the operation of a laser-charged four-wheel drive UAV. The authors emphasize the importance of considering the battery perspective in drone-related challenges such as route planning and resource optimization. They propose reevaluating the traditional energy perspective and evaluating energy as a function of the drone's movement system. The paper also discusses techniques for prolonging drone missions, including recharging using a low-power laser source and accurately estimating power consumption. The authors use graph theory approaches to solve the path planning problem, they find that the traditional energy perspective is conservative and propose an adjustment method to evaluate energy better. Finally, the influence of factors like turbulence and distance on the charging source is studied. The authors plan to validate their results through actual tests [63].

Steven R. Anton et al. develop wing include piezoelectric layers for power generation and thin-film batteries for energy storage. The text describes the electromechanical modeling and experimental testing of the wing, as well as its ability to harvest and store electrical energy simultaneously. The potential applications of this technology in UAVs are also discussed [64].

Parvathy Rajendran et al, this paper presents a new mathematical design model for UAVs, that enhances their performance for long-duration missions. The model was verified and demonstrated a 25% decrease in power consumption compared to previous UAVs. The study also examined the differences between solar and nonsolar-powered UAVs, revealing that while they UAVs can carry more payload, they have limited endurance [65].

IV. Results and Discussion

The paper explores various strategies and technologies to overcome the limitations of drone battery capacity. It delves into energy consumption analysis during flight, power loss components, and methods to optimize energy harvesting. Notable contributions include advancements in AI-based fault detection, vibrational stabilization models, and design optimization for improved efficiency. Additionally, the integration of piezoelectric and solar energy harvesting, wireless charging systems, and hybrid power sources was discussed. The study emphasizes the importance of energy-efficient path planning, powertrain designs, and innovative solutions like the L-shaped energy harvester. Overall, it highlights various approaches to enhance drone endurance and performance across different applications.

V. Conclusions

In conclusion, the surge in drone applications across diverse industries has been accompanied by challenges, particularly in addressing limited battery capacity. Integrating artificial intelligence and mechatronics has played a pivotal role in transforming drones into cost-effective, user-friendly, safe, and environmentally friendly options. Various studies propose innovative solutions to optimize energy harvesting from UAV body vibrations and extend flight durations.

Power loss analysis during flight underscores the importance of understanding mechanical, magnetic, iron, and copper losses. Energy consumption calculations, battery storage, and the percentage of energy consumption during flight provide a comprehensive overview. Diverse UAV power harvesting methods, such as design improvements, stability considerations, vibration analysis, and propulsion system optimization, showcase the depth of research in this field.

Exploring energy generation strategies encompasses piezoelectric harvesting, wind energy utilization, solar-powered UAVs, and hybrid systems combining different power sources. Each approach presents unique benefits and challenges, highlighting the need for a nuanced understanding of power generation for sustained drone operations.

Electrical circuit generation studies delve into wireless charging systems, communication-enabled energy delivery, and optimizing harvested energy for UAVs. These advancements aim to overcome energy constraints, enhance efficiency, and provide a seamless power supply for drones.

The paper concludes by emphasizing the significance of ongoing research in developing statistical models for renewable energy harvesting, exploring new power sources like supercapacitors, and proposing innovative solutions such as laser charging and multifunctional composite power collectors. The comprehensive analysis presented in this paper underscores the interdisciplinary nature of drone technology, encouraging further exploration and refinement of these strategies for the future of UAVs.

The recommendations based on the presented research are as follows:

1. Enhance integration between artificial intelligence techniques and vibration data collection to enable real-time fault detection, improving the performance of UAVs.
2. Support research using optimized design to enhance the structural and vibrational efficiency of crucial components such as wings and engines.
3. Explore the feasibility of utilizing piezoelectric technologies for energy harvesting from multiple vibration sources to enhance the power efficiency of UAV systems.
4. Encourage further research into integrating wireless charging systems and optimizing solar energy utilization to extend the flight capabilities of UAVs.
5. Support ongoing research into efficient energy models for path planning, minimizing energy consumption during missions.
6. Promote battery technology research and performance enhancement techniques to achieve progress in increasing the capacity of UAV batteries.
7. Advocate for continued analysis of the advantages and challenges of hybrid energy systems to maximize the benefits of multiple power sources.
8. Encourage research into energy harvesting technologies from diverse environmental sources such as wind and solar to improve endurance and mission sustainability.

These recommendations aim to foster innovative technologies and improve the performance of UAVs through a comprehensive set of technical innovations and engineering concepts.

References Références Referencias

1. H.V, B.A. Jayawickrama, Empirical power consumption model for UAVs, in 2018 IEEE 88th Vehicular Technology Conference (VTC-Fall) (IEEE, 2018b).
2. C. W. Chan and T. Y. Kam, A procedure for power consumption estimation of multi-rotor unmanned aerial vehicle, J. Phys.: Conf. Ser. 1509 012015. (2020).
3. M. H. Hwang, et al., "Practical Endurance Estimation for Minimizing Energy Consumption of Multirotor Unmanned Aerial Vehicles," Energies 2018, 11, (2221).
4. M. Fathi et al. (eds.), An Overview of Drone Energy Consumption Factors and Models, Handbook of Smart Energy, Systems, https://doi.org/10.1007/978-3-030-72322-4_200-1, Springer Nature Switzerland (AG 2022).
5. H. Kim, D. Lim and K. Yee, "Development of a comprehensive analysis and optimized design framework for the multirotor UAV," 31st Congress of the International Council of the Aeronautical Sciences, Belo Horizonte, Brazil; September (2018).
6. Agatz, P. Bouman, M. Schmidt, Optimization approaches for the traveling salesman problem with drone. Transp. Sci. 52(4), (2018).
7. Cheng, Y. Adulyasak, L.-M. Rousseau, Drone routing with energy function: Formulation and exact algorithm. Transp. Res. B: Methodol, (2020).
8. Yacef, N. et al. Optimization of energy consumption for quadrotor UAV, in Proceedings of the International Micro Air Vehicle, Conference and Flight Competition (IMAV), (Toulouse, 2017).
9. Alwateer, S.W. Loke, N. Fernando, Enabling drone services: drone crowdsourcing and drone scripting. IEEE access 7, (2019).
10. Abeywickrama, et al, Comprehensive energy consumption model for unmanned aerial vehicles, based on empirical studies of battery performance. IEEE access 6, 58383–58394, (2018a).
11. S. Lee, et al. Two echelon vehicle routing problem with drones in last mile delivery. Int. J. Prod. Econ. 225, 107598 (2020).
12. C.H. Liu, et al, Energy-efficient uav control for effective and fair communication coverage: a deep reinforcement learning approach. IEEE J. Sel. Areas Commun. 36(9), 2059–2070 (2018).
13. Y. Liu. An optimization-driven dynamic vehicle routing algorithm for on-demand meal delivery using drones. Comput. Oper. Res. 111, 1–20 (2019).
14. Z. Liu, R. Sengupta, A. Kurzhanskiy, A power consumption model for multi-rotor small unmanned aircraft systems, in 2017 International Conference on Unmanned Aircraft Systems (ICUAS) (IEEE, 2017).

15. P. Moeinifard, M.S. Rajabi, M. Bitaraf, Lost vibration test data recovery using convolutional neural network: a case study, 2022. arXiv preprint arXiv: 2204.05440.
16. A. Mohebbi, S. Achiche, L. Baron, Integrated design of a vision-guided quadrotor uav: a mechatronics approach, in Proceedings of the 2015 CCToMM Symposium on Mechanisms, Machines, and Mechatronics, 2015.
17. A. Mohebbi, L. Baron, S. Achiche, L. Birglen, Trends in concurrent, multi-criteria and optimal design of mechatronic systems: a review, in Proceedings of the 2014 International Conference on Innovative Design and Manufacturing (ICIDM) (IEEE, 2014).
18. A.M. Moore, Innovative scenarios for modeling intra-city freight delivery. Transp. Res. Interdiscip. Perspect. 3, 100024 (2019).
19. K. Agrawal and P. Shrivastav, “Multi-rotors: A Revolution in Unmanned Aerial Vehicle,” International Journal of Science and Research (IJSR), vol.4, November (2015).
20. F. Bohorquez, P. Samuel, J. Sirohi, D. Pines, L. Rudd and R. Perel, “Design, Analysis and Performance of a Rotary Wing MAV,” Department of Aerospace Engineering, International Journal of Science and Research (IJSR), pp. 1-17, April 2003.
21. S. D. Prior and J. C. Bell, “Empirical Measurements of Small Unmanned Aerial Vehicle Co-Axial Rotor Systems,” ISSN 2078-5453/ Journal of Science and Innovation, vol. 1, No.1, pp. 1-18, January 2011.
22. Y. Cao, “The aerodynamics of modern helicopter rotor, BEIHANG UNIVERSITY PRESS, 2015. (In Chinese).
23. P. Andrada, M. Torrent, J. I. Perat, and B. Blanqué, “Power Losses in Outside-Spin Brushless DC Motors,” Departament d’Enginyeria Elèctrica (Universitat Politècnica de Catalunya), April 2004.
24. K. D. Patel, Jayaraman, C. Satheesh and S. K. Maurya, “Selection of BLDC Motor and Propeller for Autonomous Amphibious Unmanned Aerial Vehicle,” WSEAS Transactions on Systems and Control, vol. 10, pp. 179-185, April 2015.
25. A. Famili, A. Stavrou, H. Wang et al., Optilod: optimal beacon placement for high-accuracy indoor localization of drones (2022). arXiv preprint arXiv: 2201.10691
26. S.M. Ferrandez, T. Harbison, T. Weber, R. Sturges, R. Rich, Optimization of a truck-drone in tandem delivery network using k-means and genetic algorithm. J. Ind. Eng. Manag. (JIEM) 9(2), 374–388 (2016).
27. M.A. Figliozzi, Lifecycle modeling and assessment of unmanned aerial vehicles (drones) co2e emissions. Transp. Res. D: Transp. Environ. 57, 251–261 (2017).
28. E. Frazzoli, F. Bullo, Decentralized algorithms for vehicle routing in a stochastic time-varying environment, in 2004 43rd IEEE Conference on Decision and Control (CDC) (IEEE Cat. No. 04CH37601), vol. 4 (IEEE, 2004).
29. D.C. Gandolfo, L.R. Salinas, A. Brandão, J.M. Toibero, Stable path-following control for a quadrotor helicopter considering energy consumption. IEEE Trans. Cont. Syst. Technol. 25(4), 1423–1430 (2016).
30. Zhou, Y. Wu, H. Sun, Z. Chu, Uav-enabled mobile edge computing: offloading optimization and trajectory design, in 2018 IEEE International Conference on Communications (ICC) (IEEE, 2018).
31. Mohamad Hazwan Mohd Ghazali et al, Vibration-Based Fault Detection in Drone Using Artificial Intelligence, IEEE SENSORS JOURNAL. 2022.
32. Matěj Karásek, Good vibrations for flapping-wing flyers, Science Robotics. 2020.
33. Kejing Chen et al An investigation on the structural, International Journal of Micro Air Vehicles. 2023.
34. Xunhua Dai et al, An Analytical Design Optimization Method for Electric Propulsion Systems of Multicopter UAVs with Desired Hovering Endurance, Research Gate. 2018.
35. Abera Tullu et al, Design and Implementation of Sensor Platform for UAV-Based Target Tracking and Obstacle Avoidance, MDPI. 2022.
36. Adam Dugosz. The optimal design of UAV wing structure. Conference: COMPUTER METHODS IN MECHANICS (CMM2017): Proceedings of the 22nd International Conference on Computer Methods in Mechanics.
37. Heung Soo Kim et al, A Review of Piezoelectric Energy Harvesting Based on Vibration. December 2011International Journal of Precision Engineering and Manufacturing 12(6).
38. Nikola Gavrilovic et al, Performance Improvement of Small Unmanned Aerial Vehicles Through Gust Energy Harvesting. April 2018Journal of Aircraft 55(2):741-754.
39. Rocco Citroni et al. A Novel Shape of Bowtie Antenna Arranged in a Linear Array for Energy Harvesting in MID-IR Band. Conference: 2023 12th International Conference on Renewable Energy Research and Applications (ICRERA). August 2023.
40. Rutuja Shivgan et al. Energy-Efficient Drone Coverage Path Planning using Genetic Algorithm, on September 19,2020 at 23:14:24 UTC from IEEE Xplore.
41. ALPER ERTURK et al, Modeling of Piezoelectric Energy Harvesting from an L-shaped Beam-mass Structure with an Application to UAVs, INTELLIGENT MATERIAL SYSTEMS AND STRUCTURES. 2009.
42. Georgia Foutsitzi et al Multicriteria Approach for Design Optimization of Lightweight Piezoelectric Energy Harvesters Subjected to Stress Constraints, MDPI, 2022.

43. Pedram Beigi et al. An Overview of Drone Energy Consumption Factors and Models, on 18 Jul 2022 eess.SY.
44. Analysis and Modeling of UAV Power System Architectures, Alastair P et al. School of Electrical Engineering and Computer Science.
45. Mohamed Nadir P et al. A Critical Review on Unmanned Aerial Vehicles Power Supply and Energy Management: Solutions, Strategies, and Prospects, Elsevier Applied Energy 2019.
46. Zhang et al, Overview of Propulsion Systems for Unmanned Aerial Vehicle, Bowen MDPI, 2022.
47. Jing Zhang et al Power cognition: Enabling intelligent energy harvesting and resource allocation for solar-powered UAVs, ScienceDirect – 2020.
48. Yixin Yan et al. Design of UAV wireless power transmission system based on coupling coil structure optimization. March 2020EURASIP Journal on Wireless Communications and Networking 2020(1).
49. Zhaohui Yang et al. Energy Efficient UAV Communication with Energy Harvesting. December 2019IEEE Transactions on Vehicular Technology PP (99).
50. Toan Van Quyen et al. Optimizing Hybrid Energy Harvesting Mechanisms for UAVs. May 2020EAI Endorsed Transactions on Energy Web 7(30).
51. Jingjing Yao et al Power Control in Internet of Drones by Deep Reinforcement Learning, the U.S. National Science Foundation under Grant 2020.
52. Koszewnik et al Performance assessment of an energy harvesting system located on a copter, THE EUROPEAN PHYSICAL JOURNAL SPECIAL TOPICS. 2019.
53. Matthias Perez et al, Vibration energy harvesting on a drone quadcopter based on piezoelectric structures, Mechanics & Industry. 2022.
54. Wang, J et al, Design, modeling, and experiments of broadband tristable galloping piezoelectric energy harvester– Acta Mechanica Sinica 2020.
55. Ashleigh Townsend et al. A comprehensive review of energy sources for unmanned aerial vehicles, their shortfalls and opportunities for improvements, Heliyon, 2020.
56. Cuong Van Nguyen et al. Advanced Hybrid Energy Harvesting Systems for Unmanned Aerial Vehicles (UAVs), Advances in Science, Technology and Engineering Systems Journal, 2020.
57. Silvia Sekander et al On the Performance of Renewable Energy-Powered UAV-Assisted Wireless Communications, Silvia Sekander et al - Natural Sciences and Engineering Research Council of Canada (NSERC). 2019.
58. Nabil A. Ahmed Masafumi Miyatake. "A novel maximum power point tracking for photovoltaic applications under partially shaded insolation conditions." Electric Power Systems Research, 2008, (5): 777-784.
59. Khac Lam Pham et al The Study of Electrical Energy Power Supply System for UAVs Based on the Energy Storage Technology. Aerospace 2022, 9(9).
60. Karan Kumar Shaw et al., Design and Development of a Drone for Spraying Pesticides, Fertilizers and Disinfectants, International Journal of Engineering Research & Technology (IJERT) 2020.
61. Mohamed Nadir Boukoberine et al. Hybrid Fuel Cell Powered Drones Energy Management Strategy Improvement and Hydrogen Saving using Real Flight Test Data May 2021Energy Conversion and Management 236(Article 113987):1-11.
62. Krzysztof Mateja et al., Efficiency Decreases in a Laminated Solar Cell Developed for a UAV. MDPI. Materials 2022.
63. Wael Jaafar et al. Dynamics of Laser-Charged UAVs: A Battery Perspective. December 2020IEEE Internet of Things Journal PP(99):1-1.
64. Mohsen Safaei, R Michael Meneghini, Steven R Antonm Energy harvesting and sensing with embedded piezoelectric ceramics in knee implants, Publication date 2018/1/15 Journal IEEE/ASME Transactions on Mechatronics. Volume 23, Issue 2. IEEE.
65. Vijayanandh Raja et al. Multi-Perspective Investigations Based Design Framework of an Electric Propulsion System for Small Electric Unmanned Aerial Vehicles, MDPI Drones 7(184) March 2023.

Global Journal of Researches in Engineering: A
Mechanical and Mechanics Engineering
Volume 24 Issue 1 Version 1.0 Year 2024
Type: Double Blind Peer Reviewed International Research Journal
Publisher: Global Journals
Online ISSN: 2249-4596 & Print ISSN: 0975-5861

Calculation of Time-Varying Mesh Stiffness of Internal Gears based on Precise Tooth Profile and Dynamic Analysis of Planetary Systems with Root Cracks

By Cao Dongjiang, Qin Fengwei, Cao Lisong & Chang Hongjjie
Hebei University of Science and Technology

Abstract- The internal meshing spur gear pair is the research object, and the potential energy method is applied to calculate the time-varying meshing stiffness of the internal gear. The internal gear tooth profile is divided into two parts: involute and transition curves, and the gear tooth stiffness is calculated by numerical integration based on accurate tooth profile, which improves the calculation accuracy. Analyzed the influence of different crack size parameters on the stiffness of internal meshing gears. A coupled dynamic model of a planetary system with internal gear crack faults was established, and the influence of cracks on the dynamic response of the planetary system was studied using Zoom-FFT spectrum and cepstrum analysis methods. The simulation results show that as the crack parameter size increases, the mesh stiffness of the internal gear pair gradually weakens, and the periodic vibration impact of the planetary-internal gear pair is also more severe. Cepstrum analysis can easily capture weak fault characteristic frequency information in the system and discover their variation patterns.

Keywords: precise tooth profile, potential energy method, internal meshing gear stiffness, planetary gear dynamics, Zoom FFT analysis, cepstrum analysis, fault diagnosis.

GJRE-A Classification: *LCC: TJ184*

CALCULATIONOFTIMEVARYINGMESHSTIFFNESSOFINTERNALGEARSBASEDONPRECISETOOTHPROFILEANDDYNAMICANALYSISOFPLANETARYSYSTEMSWITHROOTCRACKS

Calculation of Time-Varying Mesh Stiffness of Internal Gears based on Precise Tooth Profile and Dynamic Analysis of Planetary Systems with Root Cracks

Cao Dongjiang α, Qin Fengwei σ, Cao Lisong ρ & Chang Hongjjie Ѡ

Abstract- The internal meshing spur gear pair is the research object, and the potential energy method is applied to calculate the time-varying meshing stiffness of the internal gear. The internal gear tooth profile is divided into two parts: involute and transition curves, and the gear tooth stiffness is calculated by numerical integration based on accurate tooth profile, which improves the calculation accuracy. Analyzed the influence of different crack size parameters on the stiffness of internal meshing gears. A coupled dynamic model of a planetary system with internal gear crack faults was established, and the influence of cracks on the dynamic response of the planetary system was studied using Zoom-FFT spectrum and cepstrum analysis methods. The simulation results show that as the crack parameter size increases, the mesh stiffness of the internal gear pair gradually weakens, and the periodic vibration impact of the planetary-internal gear pair is also more severe. Cepstrum analysis can easily capture weak fault characteristic frequency information in the system and discover their variation patterns. The research results can provide a theoretical basis for the state monitoring and fault diagnosis of gear systems with crack defects.

Keywords: precise tooth profile, potential energy method, internal meshing gear stiffness, planetary gear dynamics, Zoom FFT analysis, cepstrum analysis, fault diagnosis.

I. Introduction

Internal meshing gear transmission is widely used in power transmission equipment such as tank turrets, radar systems, and wind power gearboxes due to its compact structure and high torque to weight ratio. Planetary gear transmission is an important application of internal meshing transmission, widely used in industries, automobiles, aviation, aerospace and other fields. The gear system itself has a complex structure and is prone to faults when working in harsh environments[1], which affects the reliable operation and service life of the equipment. Therefore, monitoring and diagnosing the operating status of the gear system is of great significance[2]. Reasonable modeling and theoretical analysis of gear system dynamics are the prerequisite and foundation for effective gear fault monitoring and diagnosis, and accurate calculation of gear mesh stiffness is an essential part of analyzing system dynamics. Therefore, studying the time-varying meshing stiffness of internal meshing gears with root crack defects, analyzing the influence of root cracks on the dynamic characteristics of gear systems, is of great significance for early fault diagnosis.

Many scholars worldwide have done a lot of work in gear dynamics and time-varying meshing stiffness. Weber[3] conducted analytical calculations for gear mesh stiffness without defects. Cornell[4] and Kasuba[5] applied numerical analysis methods to calculate the gear mesh stiffness. Yang and Lin[6] used the so-called potential energy method to calculate the total meshing stiffness of gear pairs and achieved high calculation accuracy. Since then, the potential energy method has been widely accepted. Basis on Yang, Tian[7] and Wu[8] further improved the calculation model of meshing stiffness by considering the influence of load shear, However, they still did not consider the deflection of the rounded foundation. Chaari et al.[9] considered the influence of energy on various parts of the gear teeth and calculated the meshing stiffness of gears with crack faults. Wan et al.[2] considered the situation where the tooth base circle and tooth root circle do not coincide, proposed a meshing stiffness correction method, and established a tooth root crack dynamic model to study the influence of tooth root cracks on the dynamic response of gear systems. Sun[10] used a straight line segment instead of the transition curve of the tooth profile, and used the potential energy method to solve the meshing stiffness of gears with and without cracks. Zhang et al.[11] derived an analytical formula for the meshing stiffness of spur gears based on the potential energy method, and analyzed the variation of meshing stiffness with different frictional forces. Meng et al.[12] considered the gear transition curve function and used the potential energy method to calculate the stiffness changes of 10 different crack lengths. They considered the time-varying meshing stiffness and sliding friction between teeth, and analyzed the dynamic

Author α σ ρ: Qing'an Group Co., Ltd., Xi'an Shaanxi, China. e-mail: 726679818@qq.com
Author Ѡ: College of Mechanical Engineering, Hebei University of Science and Technology, Shijiazhuang, Hebei.

response of gear systems with cracks. Liu et al.[13] used the principle of generation method to calculate the tooth profile equation with the rolling angle of the cutting tool as a unified variable, and solved the time-varying meshing stiffness of the gear based on the energy method. Sun et al.[14] divided spur gears into many separate slices along the tooth width and proposed a modified calculation model for spur gear pairs with tooth profile modification based on the relationship between deformation and total stiffness of the meshing cycle. The errors of this method under different modification amounts were discussed. Cao[15] and Xu[16] considered the accurate tooth profile parameterization equation and established a tooth cantilever beam model to solve the time-varying mesh stiffness of spur gears.

However, there are still relatively few calculation and analysis models for the mesh stiffness of the internal gear pair. Hidaka et al.[17] applied the FEA method and analysis model to calculate the deformation of the internal gear ring along the mesh line based on the results of Karas[18]. Chen et al.[19] embedded the Timoshenko beam theory into the meshing stiffness model of internal meshing gear pairs and studied the influence of ring gear flexibility on internal meshing stiffness. Chen et al.[20] calculated the time-varying meshing stiffness of healthy and internal gear pairs with root cracks, and analyzed the impact of ring gear root cracks on the dynamic response of planetary systems. However, Chen et al.[19,20] did not consider the precise root transition curve when calculating the meshing stiffness of internal gears, instead, an approximation algorithm was used.

Lwicki[21-23] has conducted extensive research on the propagation path of tooth cracks and has drawn some beneficial conclusions. He pointed out that the direction of crack path propagation depends on the backup ratio, which is defined as the ratio of the thickness of the wheel rim to the tooth height, and the propagation path is often smooth and continuous. For gears with high backup ratios, tooth root cracks will propagate towards the interior of the teeth along the tooth width direction. For those teeth with lower backup ratios, cracks will pass through the rim. The initial crack angle is also a determining factor for path extension. Under small initial crack angle conditions, even with a high backup ratio, cracks will propagate through the wheel rim.

Charri et al.[24] pointed out that the dynamic response of gear systems is closely related to the time-varying meshing stiffness of gears. When specific tooth faults cause a decrease in meshing stiffness, the system will be monitored for more significant vibration impact and noise. Establishing a gear dynamics model with gear tooth faults will help analyze the changes in system dynamic characteristics, and the model can also serve as a theoretical basis for fault diagnosis. Conducting time-domain, frequency-domain, and time-frequency domain analysis on the dynamic response of gear systems is the most powerful tool for monitoring faults in rotating machinery.

The article applies the potential energy method to establish a time-varying meshing stiffness model for internal meshing gears based on precise tooth profiles. In this model, root crack defects with different size parameters are embedded, and the meshing stiffness of internal meshing gears containing root cracks is obtained. Further established a dynamic model of planetary gear system with root cracks, analyzed the impact of tooth cracks on gear dynamic characteristics, and applied widely used RMS and Kurtosis statistical indicators in vibration detection to reveal the severity of gear cracks. The dynamic response of the planetary gear system was analyzed using time-domain and FFT spectra, as well as cepstrum analysis, in order to quantitatively obtain the influence of tooth root cracks on the dynamic characteristics of gears. This is of great significance for gear condition monitoring and fault diagnosis.

II. Establishment of an Equivalent Model for Internal Gears

By applying the principle of potential energy, the internal gear tooth is simplified as a variable cross-section cantilever beam on the gear ring, and the time-varying meshing stiffness of the internal gear pair is calculated. The equivalent model is shown in Fig. 1. According to the principle of potential energy, the work exerted by an external force on the gear tooth is equal to the potential energy stored by the gear body due to deformation. The potential energy stored in the gear tooth includes four parts: bending potential energy U_b, shear deformation energy U_s, radial compression deformation energy U_a, and Hertz potential energy U_h. These four types of potential energy can be used to calculate the bending stiffness k_b, shear stiffness k_s, radial compression stiffness k_a, and Hertz stiffness k_h, respectively. The total meshing stiffness is the series form of each stiffness. From the knowledge of elasticity and material mechanics, it can be inferred that:

$$U_b = \frac{F^2}{2K_b} = \int \frac{M_f^2}{2EI_x} dx \tag{1}$$

$$U_s = \frac{F^2}{2K_s} = \int \frac{1.2F_b^2}{2GA_x} dx \tag{2}$$

$$U_a = \frac{F^2}{2k_a} = \int \frac{F_a^2}{2EA_x} dx \tag{3}$$

$$U_h = \frac{F^2}{2k_h} \tag{4}$$

Where: F represents the force acting along the meshing line at the meshing point, F_a and F_b represent the horizontal component of force F in the x-axis direction and the vertical component of force F in the y-axis direction; M_f represents the bending moment generated by force F on the beam. E is the elastic modulus, G is the shear modulus, I_x is the moment of inertia of the gear tooth section at a distance of x from the force F acting point, and A_x is the cross-sectional area of that point.

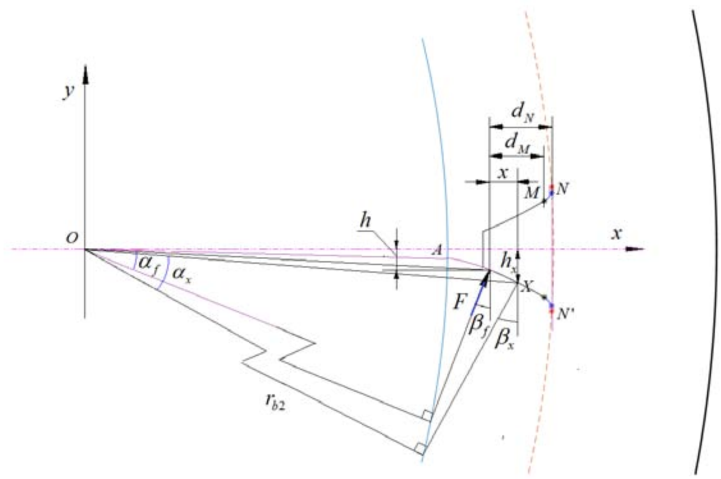

Fig. 1: Equivalent model of internal gear

III. Calculate the Meshing Stiffness of Internal Gears based on the Principle of Potential Energy

According to the cantilever beam model of the gear teeth, the internal gear tooth profile is divided into two parts: involute and transition curve. As shown in Fig. 1, point M is the tangent point of the connection between the involute and transition curve, also known as the tooth profile transition point[25], and point N is the tangent point of the connection between the transition curve and the tooth root circle. The transition curve is a curve that is enveloped by the rounded corner of the cutter tooth during the internal gear machining process. When the rounded corner of the cutter tooth is non sharp ($\rho > 0$), the transition curve is an equidistant curve of an extended epicycloid[26]. Due to the entirely different equations of tooth profile involute and transition curve, when calculating the deformation energy of internal gear tooth in this article, the cantilever beam model is divided into involute and transition curve two parts for integration. Under the action of meshing force F, the deformation energy of tooth bending, shear, and axial compression can be expressed as:

$$U_b = \frac{F^2}{2k_b} = \int_0^{d_M} \frac{\left[F_b x - F_a h\right]^2}{2EI_x} dx + \int_{d_M}^{d_N} \frac{\left[F_b x_1 - F_a h\right]^2}{2EI_{x_1}} dx_1 \tag{5}$$

$$U_s = \frac{F^2}{2K_s} = \int_0^{d_M} \frac{1.2F_b^2}{GA_x} dx + \int_{d_M}^{d_N} \frac{1.2F_b^2}{GA_{x1}} dx_1 \tag{6}$$

$$U_a = \frac{F^2}{2k_a} = \int_0^{d_M} \frac{F_a^2}{EA_x} dx + \int_{d_M}^{d_N} \frac{F_a^2}{EA_{x1}} dx_1 \tag{7}$$

For equations (5), (6), and (7), the first term represents the deformation energy generated by force F on the involute tooth profile, and the second term represents the deformation energy generated by F on the transition curve. In the formula, d_M and d_N are the x-axis distances between the meshing point F and the tooth profile transition point

M and the tooth root connection point N. $d_{MN} = d_N - d_M$, X is the point on the involute tooth profile or transition curve. *x* is the horizontal distance between point F and point X, and *h* and h_x are the distances from point F and point X on the tooth profile to the tooth symmetry line (*x*-axis), respectively. The specific values can be calculated using the following formula:

$$G = \frac{E}{2(1+v)}, \quad I_x = \frac{2}{3} h_x^{\ 3} B, \quad A_x = 2 h_x B \tag{8}$$

$$F_b = F\cos\beta_f, \; F_a = F\sin\beta_f \tag{9}$$

$$M_f = F_b x - F_a h \tag{10}$$

In the formula, *B* is the internal gear tooth width, β_f is the angle between the meshing force *F* and the *y*-axis, $\beta_f = \alpha_f + \theta'_f$, It's geometric relationship is shown in Fig. 2, where

$$\theta'_f = \theta_0 - \frac{\delta_2}{2} - inv\alpha + inv\alpha_f \tag{11}$$

Where: $\theta_0 = \pi / z_2$, z_2 is the number of teeth of the internal gear; δ_2 is the center angle of the circle corresponding to the arc tooth width S_2 of the indexing circular groove for the internal gear, $\delta_2 = S_2 / r_2$; $S_2 = m(\pi/2 + 2\xi_2 tg\alpha)$, m is the modulus of the internal gear, and ξ_2 is the displacement coefficient of internal gear; α is the pressure angle of the dividing circle; α_f is the pressure angle at point F. Similarly: $\theta'_x = \theta_0 - \frac{\delta_2}{2} - inv\alpha + inv\alpha_x$, $\theta'_M = \theta_0 - \frac{\delta_2}{2} - inv\alpha + inv\alpha_m$, α_x is the pressure angle at point X, α_m is the pressure angle at point M.

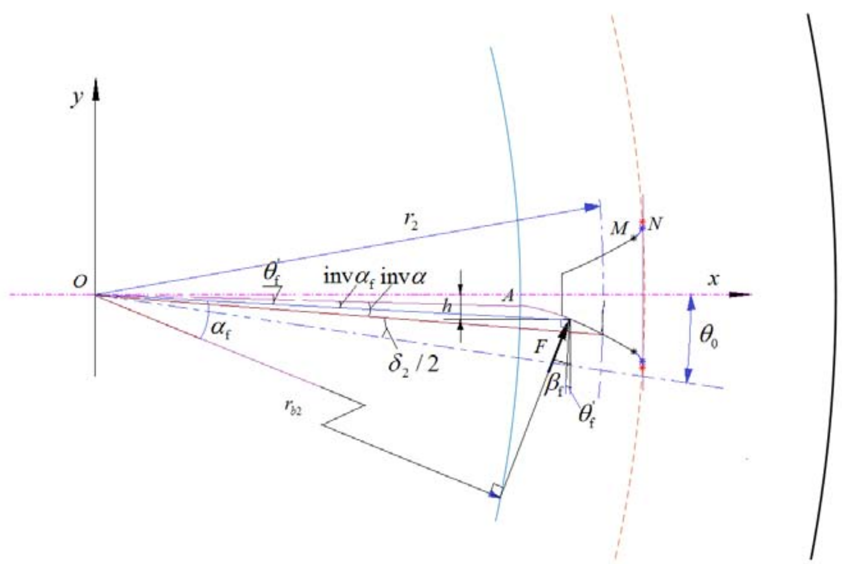

Fig. 2: Geometric relationship between meshing force angle β_f and pressure angle α_f

$$\begin{cases} h = |OF| \times \sin(\theta'_f) \\ h_x = |OX| \times \sin(\theta'_x) \end{cases} \tag{12}$$

Where: $\left|OF\right| = \dfrac{r_{b2}}{\cos\alpha_f}$ $\quad \left|OX\right| = \dfrac{r_{b2}}{\cos\alpha_x}$,

$$d_M = r_M \cos\theta_M^{'} - \left|OF\right| \cos\theta_f^{'} \tag{13}$$

Where, r_M is the vector radius of the transition point M of the internal gear tooth profile, r_{b2} represents the radius of the tooth ring base circle.

$$x = \left|OX\right| \cos\theta_x^{'} - \left|OF\right| \cos\theta_f^{'} \tag{14}$$

For the second integral in equations (5), (6), and (7), which do not include involute related parameters, the stiffness can be solved by numerical integration based on the transition curve parameter equation which can be obtained by referring to Cao et al.[27]'s reference:

$$\begin{cases} x_2 = \rho\sin(\varphi_2 - \varphi_H - \gamma) + \\ \qquad \left[\mathrm{R}_{aH} - \rho\right]\sin(\varphi_2 - \varphi_H) + a_2 \sin\varphi_2 \\ y_2 = \rho\cos(\varphi_2 - \varphi_H - \gamma) + \\ \qquad \left[\mathrm{R}_{aH} - \rho\right]\cos(\varphi_2 - \varphi_H) + a_2 \cos\varphi_2 \\ r_H{}'\sin(\gamma + \varphi_H) - \left(R_{aH} - \rho\right)\sin\gamma = 0 \end{cases} \tag{15}$$

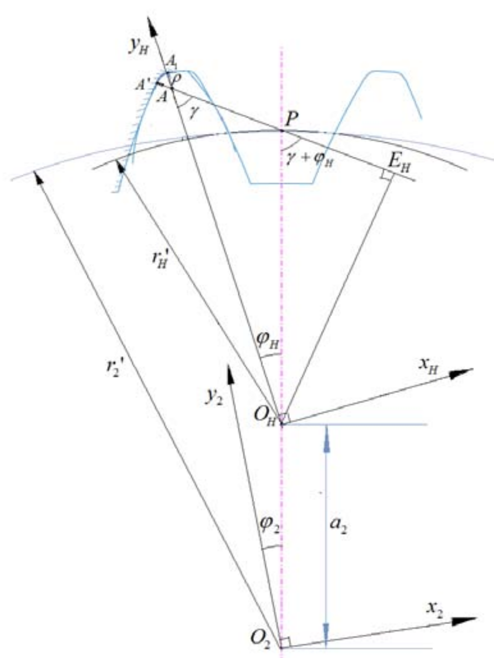

Fig. 3[27]: Transition curve of internal gear tooth profile

When $(\gamma + \varphi_H)$ taking the maximum value $(\pi/2 - \alpha'_{02})$, the tangent point M(x_{2M}, y_{2M}) connecting the tooth profile involute and the transition curve is obtained. At this time, φ_H and φ_2 take the maximum value $\varphi_{H\max}$ and $\varphi_{2\max}$, and the coordinates of point N are (x_{2N}, y_{2N}) . The relevant parameter descriptions in the formula refer to the original literature, and there are:

$$r_M = \sqrt{{x_{2M}}^2 + {y_{2M}}^2} \tag{16}$$

Where, the meaning of r_M is as described in equation (13).

For the second term in equations (5), (6), and (7), according to the transition curve equation (15), it can be obtained that: $h_{x1}=\left|x_2\right|$,

$$I_{x1}=\frac{2}{3}h_{x1}{}^3B \quad A_{x1}=2h_{x1}B \tag{17}$$

Due to the complexity of using function integration calculations, this article adopts a numerical integration method to calculate the deformation energy of the gear teeth. For the bending deformation energy at the point of force *F*, there are:

$$dU_b=\frac{\left[F_b x-F_a h\right]^2}{2EI_x}dx+\frac{\left[F_b x\ -F_a h\ \right]^2}{2EI_{x1}}dx_1 \tag{18}$$

$$U_b=\sum_{i=1}^{m}\frac{\left[F_b x_i-F_a h\right]^2}{2EI_{xi}}\Delta x_i+\sum_{j=1}^{k}\frac{\left[F_b x_i-F_a h\right]^2}{2EI_{x1j}}\Delta x_{1j} \tag{19}$$

Where, $\Delta x_i=d_M/m$, $\Delta x_{1j}=d_{MN}/k$, *m*, *k* are the number of micro segments divided by numerical integration of the involute tooth profile and transition curve, respectively. The larger the *m* and *k*, the higher the accuracy of numerical integration calculation, but the larger the computational amount. Therefore, it is necessary to choose appropriate values of *m* and *k*.

The reciprocal of the bending stiffness at the meshing force *F* can be obtained from equation (1) as:

$$\frac{1}{k_b}=\sum_{i=1}^{m}\frac{\left[x_i\cos\beta_f-h\sin\beta_f\right]^2}{EI_{xi}}\Delta x_i+\sum_{j=1}^{k}\frac{\left[x_{\ j}\cos\beta_f-h\sin\beta_f\right]^2}{EI_{x1j}}\Delta x_{1j} \tag{20}$$

Similarly, the reciprocal of the shear stiffness and compressive stiffness at the point of meshing force *F* can be obtained:

$$\frac{1}{k_s}=\sum_{i=1}^{m}\frac{1.2\left[\cos\beta_f\right]^2}{GA_{xi}}\Delta x_i+\sum_{j=1}^{k}\frac{1.2\left[\cos\beta_f\right]^2}{GA_{x1j}}\Delta x_{1j} \tag{21}$$

$$\frac{1}{k_a}=\sum_{i=1}^{m}\frac{\sin^2\beta_f}{EA_{xi}}\Delta x_i+\sum_{j=1}^{k}\frac{\sin^2\beta_f}{EA_{x1j}}\Delta x_{1j} \tag{22}$$

The range of action of meshing point F is the surface position of the involute tooth profile between the top of the internal gear tooth and the transition point M of the tooth profile, $\alpha_f\in\left[\alpha_a,\alpha_M\right]$, α_a is the pressure angle of the top of the internal gear tooth.

The stiffness of a single tooth of an internal gear can be expressed as:

$$\frac{1}{k^{\text{int}}}=\left(\frac{1}{k_b}+\frac{1}{k_s}+\frac{1}{k_a}\right) \tag{23}$$

The calculation method for the meshing stiffness of external gears can be found in many literatures. The single tooth stiffness of external gears k^{ext} in this article is based on precise tooth profiles and calculated using the Weber energy method in reference [15]. However, the calculation of external gear deformation here needs to correct an error in the original literature. When calculating single tooth deformation in the original literature, the total deformation included the calculation of contact deformation, because only the calculation of gear pair meshing deformation included the calculation of contact deformation. If each single tooth deformation calculation includes contact deformation, then two contact deformations are included in the total deformation of gear pair meshing, resulting in a smaller calculation result of gear pair meshing stiffness, So the calculation of the single tooth stiffness of the external gear here does not include the influence of contact deformation.

Based on the obtained meshing stiffness of the inner and outer teeth, derive the meshing stiffness of a single tooth pair of the inner meshing gear pair:

$$\frac{1}{k_{pair}} = \left(\frac{1}{k^{\text{int}}} + \frac{1}{k^{ext}} + \frac{1}{k_h} \right) \tag{24}$$

Where: k_h is the contact stiffness of the gear teeth. According to Hertz's contact deformation theory, assuming that the gear teeth are isotropic, the contact stiffness is only related to the parameters of the gear itself and does not change with the meshing position. And its calculation formula is:

$$k_h = \frac{\pi EB}{4(1-v^2)} \tag{25}$$

Where, v is the Poisson's ratio.

For meshing gears with contact ratio $\varepsilon_a = 1 \sim 2$, when two pairs of gears mesh simultaneously, the total effective meshing stiffness K_d is:

$$K_d = k_{pair1} + k_{pair2} \tag{26}$$

IV. Stiffness Analysis of Internal Meshing Gears with Root Cracks

a) Modeling and Analysis of Gear Cracks

Internal gear root cracks are usually caused by stress concentration caused by insufficient rim thickness in the design, improper processing, material defects and harsh working conditions etc. The internal gear tooth crack propagation model is shown in Fig. 4. According to Lewicki[21,22], crack propagation depends on the backup ratio, which is defined as the ratio of the thickness of the wheel rim to the height of the tooth. For gears with high backup ratios, the analysis predicts that crack propagation will follow the direction of tooth thickness (as shown by crack line 1 in Fig. 4), while for gears with low backup ratios, crack propagation will propagate towards the ring gear along the direction of crack line 2 in Fig. 4. Initial crack angle α_c also explains the direction of crack propagation. α_c is defined as the intersection angle between the crack and the centerline of the gear, for low α_c. even in high backup ratios, cracks will propagate through the ring gear, as shown α_{c2} in Fig. 4. Lewicki [28] pointed out that the crack propagation path is often smooth, continuous, and quite straight with only slight bending.

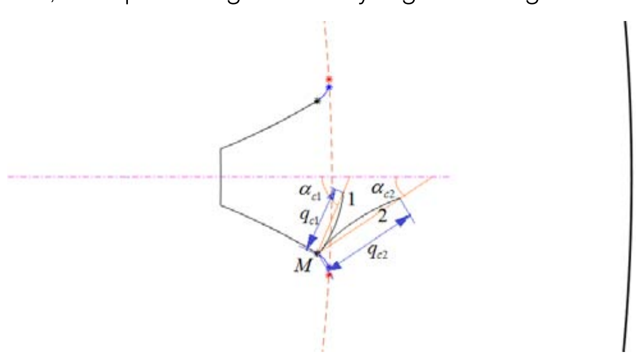

Fig. 4: Influence of backup ratio on the propagation direction of gear cracks

The presence of root cracks will reduce the effective tooth thickness, thereby reducing the stiffness of the gear tooth. In condition monitoring and fault diagnosis, it is necessary to detect gear faults as early as possible. Therefore, this article studies the root cracks of internal meshing gears in the initial stage, and the gear cracks do not extend to the centerline of the teeth. Assuming that the root crack is a straight line as shown in Fig. 5, located at the intersection point M of the involute and the transition curve, with a depth of q_c and an inclination angle α_c, When the crack occurs, the radial compression stiffness calculation of the gear teeth is still the same as that of a normal gear.

The area inertia moment I_x and cross-sectional area A_x in the formula for calculating the bending stiffness and shear stiffness of the gear tooth will change. The formula is as follows:

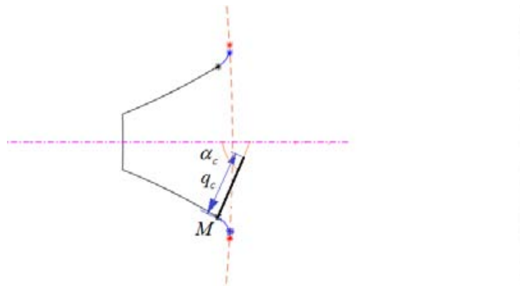

Fig. 5: Schematic diagram of gear crack model

$$I_x = \begin{cases} \frac{1}{12}\left(h_{qc}+h_x\right)^3 B & h_x > h_{qc} \\ \frac{1}{12}\left(2h_x\right)^3 B & h_x \le h_{qc} \end{cases} \tag{27}$$

$$A_x = \begin{cases} \left(h_{qc}+h_x\right)B & h_x > h_{qc} \\ 2h_x\mathrm{B} & h_x \le h_{qc} \end{cases} \tag{28}$$

In the formula, h_{qc} is the distance from the crack endpoint to the centerline of the gear tooth. The prerequisite for applying the formula is: $x \le d_M + q_c \cos\alpha_c$. When $x > d_M + q_c \cos\alpha_c$, I_x and A_x will still be calculated according to equation (17).

In reference[29], the propagation pattern of gear tooth cracks along the tooth width and tooth thickness directions was studied. As shown in Fig. 6[29], the crack depth q_c is also uneven along the tooth width direction, which can be expressed as a function of the tooth width position x, i.e. $q=q(x)$. When calculating the stiffness of the gear tooth, the gear tooth is cut into many thin slices along the tooth width direction. For each slice, the crack depth is considered a constant, and the stiffness of each slice can be calculated using formulas (20) to (22). In this article, the crack depth is set to be distributed in a parabolic shape along the tooth width, and the crack inclination angle α_c is a constant. The solid line curve in Fig. 6 represents the situation where the crack does not penetrate the tooth width, while the dashed line curve represents the situation where the crack penetrates the entire tooth width. Cracks can be defined as Crack (q_c, B_c/B, q_2, α_c), and finally, by integrating and calculating the stiffness of all these sliced teeth, the stiffness of the entire faulty gear tooth can be obtained.

For the solid crack curve in Fig. 6, the crack depth equation is:

$$\begin{cases} q(x) = q_c\sqrt{\dfrac{x+B_c-B}{B_c}} & x\in\left[B-B_c, B\right] \\ q(x)=0 & x\in\left[0, B-B_c\right] \end{cases} \tag{29}$$

For the dashed crack curve in Fig. 6, the crack depth equation is:

$$q(x) = \sqrt{\frac{{q_c}^2+{q_2}^2}{B}x - q_2^2} \tag{30}$$

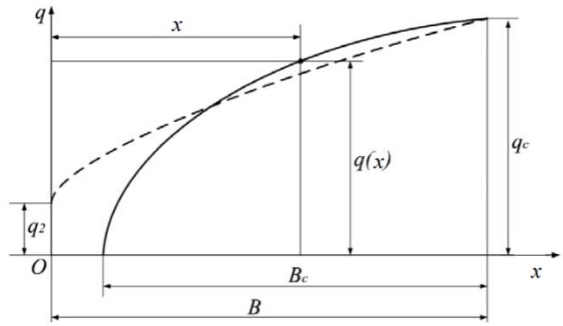

Fig. 6[29]*:* Distribution model of gear cracks along the tooth width direction

b) The Influence of Tooth Root Cracks on the Stiffness of Internal Meshing Gears

Based on the above gear crack analysis model, calculate and study the influence of gear tooth crack size on gear mesh stiffness. The main parameters of the internal gear pair in the text are shown in Table 1. In order to simulate the propagation of internal gear cracks, the crack size Crack (q_c, B_c/B, q_2, α_c), is given in Table 2. Crack A in Table 2 is a healthy gear without any cracks; B and C represent smaller crack sizes, where the cracks do not penetrate the entire tooth width; Cases D, E, and F represent more extensive crack situations, where the cracks extend further longitudinally along the entire tooth width.

Table 1: Gear Parameters Table

Parameter Name	Pinion	Ring gear
Number of teeth	z_1=17	z_2=52
Pressure angle α(°)	25	25
Module (mm)	3	3
Displacement coefficient	x_1=0.296	x_2=-0.16
Contact ratio ε_a	1.2112	
Tooth width b(mm)	24	24
Input speed of driving wheel (rpm)	1000	
Young's modulus E (N/mm^2)	2.07e5	2.07e5
Poisson's ratio	0.3	0.3

Table 2: Internal gear tooth crack size (Note: Crack parameters q_c and q_2, Unit: mm)

Crack	A	B	C
C(q_c,B_c/B,q_2, α_c)	(0,0,0,0)	(1,0.7,0,80°)	(1.2,0.8,0,80°)
Crack	D	E	F
C(q_c,B_c/B,q_2, α_c)	(1.5,1,1.5,80°)	(2,1,1.5,80°)	(3,1,2,80°)

Fig. 7 shows the single tooth stiffness of the external gear in the gear pair, with the external gear being a healthy gear. Fig. 8 and Fig. 9 show the single tooth stiffness and single tooth pair meshing stiffness curves of internal gears with different crack sizes. The comprehensive meshing stiffness reflecting the alternating meshing process of single and double teeth pair is shown in Fig. 10. From the figures, it can be observed that whether it is the stiffness of a single tooth or the meshing stiffness of a pair of teeth, the stiffness curve decreases compared to healthy teeth when tooth cracks are introduced, and the decrease is faster with the extension of the cracks. Large cracks in D, E, and F will weaken the stiffness of the teeth more significantly. Here, the contact position of the gear pair moves along the tooth profile from the top of the ring gear to the root position; The maximum stiffness reduction of cracked teeth occurs at the top of the teeth where the cracked gear begins to mesh. This is because compared to the position closer to the root circle on the inner tooth profile, the tooth flexibility at the tooth tip circle is greater.

Global Journal of Research in Engineering (A) XXIV Issue I Version I Year 2024

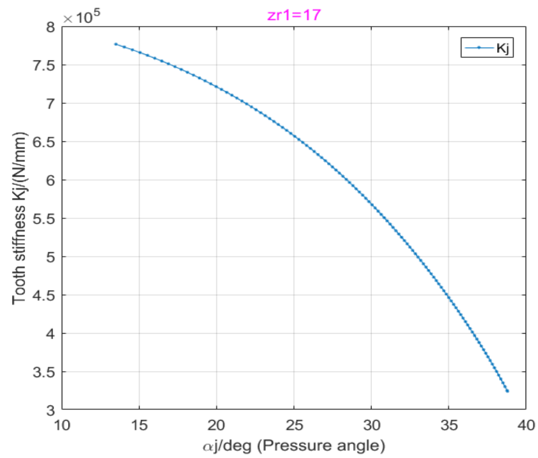

Fig. 7: Single tooth meshing stiffness curve of external gear

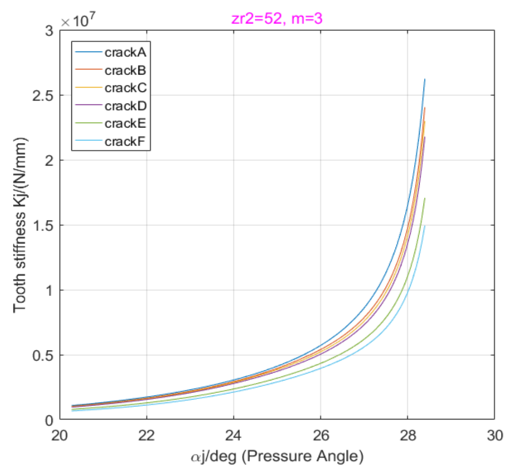

Fig. 8: Single tooth stiffness curve of internal gears with cracks of different sizes

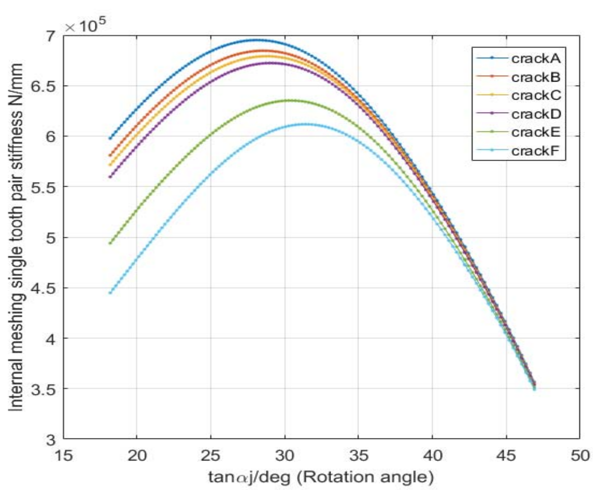

Fig. 9: Single pair teeth meshing stiffness of cracked faulty gears

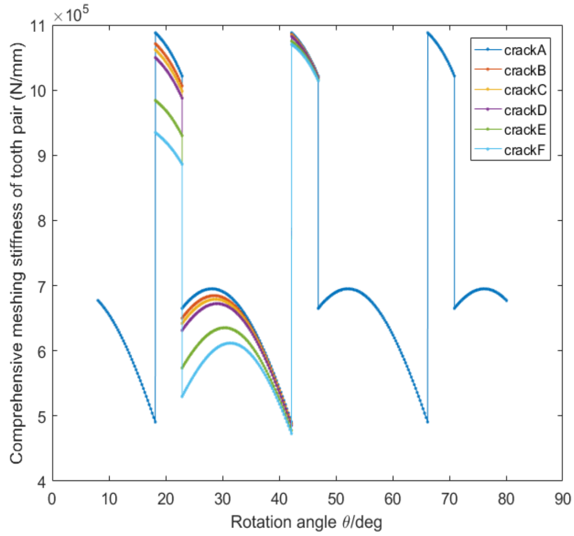

Fig. 10: Comprehensive meshing stiffness of internal meshing gears with crack faults

V. Dynamic Analysis of Planetary Gear System with Crack Faults

a) *Dynamics Equation of Planetary Gear System*

Based on the meshing stiffness of the internal meshing gear pair with root cracks calculated earlier, establish a 2K planetary gear system dynamics model. Calculate the system dynamic response caused by the decrease in meshing stiffness of the gear ring with crack defects through the model. The model was established using the centralized mass parameter method, also known as the analytical model, initially developed by Lin and Parker[30].

The main components of a planetary system include the sun gear (s), ring gear (r), planetary carrier (c), and N planetary gears (p), each of which is considered a rigid body. The coordinates of each component are shown in Fig. 11, and each component has three degrees of freedom: two translations and one rotation. The translation coordinates of the sun gear, ring gear, and planetary carrier are x_j, y_j, (j=s,r,c), and the translation coordinates of the planetary gear are ζ_n, η_n (1,2,...N), which are the radial and tangential deflection coordinates of the nth planetary gear measured relative to the rotation coordinate system $(O, \vec{i}, \vec{j}, \vec{k})$ fixed on the planetary carrier at the origin O. The basic coordinate system $(O, \vec{i}, \vec{j}, \vec{k})$ rotates at a constant planetary carrier angular velocity ω_c, x_j (j=s,r,c) pointing towards the equilibrium position of planetary gear 1. The coordinates of the rotational degrees of freedom of the component are: $u_j = r_j\theta_j, (j = c, r, s, 1, \ldots N)$, where θ_j is the rotational deflection displacement, r_j is the radius of the gear base circle or the radius of the planetary gear center distribution circle. Ψ_n is the circumferential position angle of the planetary gear relative to the rotational base vector $\vec{i}$, which is a fixed angle, where ψ_1=0.

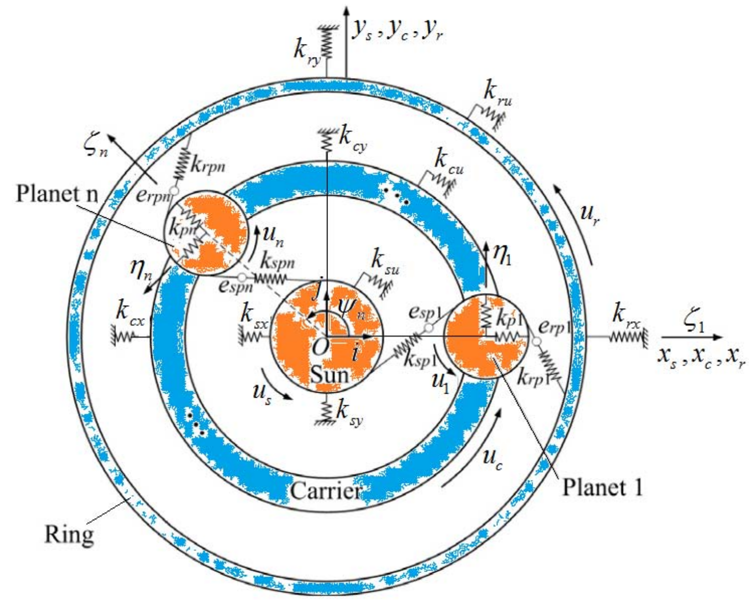

Fig. 11: Planetary gear system dynamics model

The stiffness of each supporting bearing in the planetary system is modeled by linear springs, and the damping is introduced in parallel with the gear meshing stiffness and bearing support stiffness. δ_{sn}, $e_{sp}(t)$, δ_{rn}, $e_{rp}(t)$ represent the meshing displacement and transmission error models on the meshing lines of the sun-planetary gear group and the planet- ring gear group, respectively, and have:

$$\begin{cases}\delta_{rn}=\zeta_n\sin\alpha_r-\eta_n\cos\alpha_r-x_r\sin\psi_{rn}+y_r\cos\psi_{rn}+u_r-u_n+e_{rn}(t)\\ \delta_{sn}=y_s\cos\psi_{sn}-x_s\sin\psi_{sn}-\eta_n\cos\alpha_s-\zeta_n\sin\alpha_s+u_s+u_n+e_{sn}(t)\\ e_{sn}(t)=\sum\limits_{m=1}^{\infty}\overline{E}_{sm}\sin(2\pi m f_{esn}t+\xi_{sn})\\ e_{rn}(t)=\sum\limits_{m=1}^{\infty}\overline{E}_{rm}\sin(2\pi m f_{ern}t+\xi_{rn})\end{cases} \tag{31}$$

Where: $\psi_{sn}=\psi_n-\alpha_s$, $\psi_{rn}=\psi_n+\alpha_r$. α_s,α_r are the working pressure angle of the sun-planet gear pair and planet-ring gearpair. $\overline{E}_{sm}$, $\overline{E}_{rm}$, f_{esn}, f_{ern}, ξ_{sn}, ξ_{rn}, are the tooth profile error modulus, meshing frequency, and meshing phase of the sun-planetary gear pair and the planetary-ring gear pair[31], respectively.

Establish a motion control equation system for planetary gear systems with 3N+9 degrees of freedom, and assemble the equation system to obtain the matrix equation of the system:

$$M\ddot{q}+(\omega_c G+C)\dot{q}+(K_b+K_m-\omega_c{}^2K_\Omega)q=T+F(t) \tag{32}$$

Where, $q=[x_c,y_c,u_c,x_r,y_r,u_r,x_s,y_s,u_s,\zeta_1,\eta_1,u_1,...,\zeta_N,\eta_N,u_N]$, $q/\dot{q}/\ddot{q}$ are the displacement, velocity, and acceleration of the degree of freedom vector, M is the mass matrix, G is the gyroscopic matrix, K_b is the bearing stiffness matrix, K_Ω is the centripetal stiffness matrix, and $K_m(t)$ is the time-varying meshing stiffness matrix. T is the external torque, which is set as a constant here, and $F(t)$ is the excitation force caused by transmission error. The damping matrix C is calculated from the formula $C=U^{-T}diag(2\rho_i\omega_i)U^{-1}$, where ρ_i is the modal damping ratio, and the natural frequency ω_i and orthogonal normalized modal matrix U are derived from a time invariant system that simplifies time-varying mesh stiffness to average values[32].

The configuration parameters of the planetary gear system analyzed in this article are shown in Table 3.

Table 3: Planetary gear system configuration parameters

Gear mesh parameters	Sun gear	Planet gear(mesh with ring gear)	Ring gear	
Number of teeth	$z_s=20$	$z_p=15$	$z_r=52$	
Module (mm)	3	3	3	
Teeth width (mm)	24	24	24	
Pressure angle (deg)	28.22	21.33	21.33	
Cutting tool tip radius (mm)	1.04	1.04	0.735	
Base circle dia. (mm)	27.189	20.391	70.692	
Outer dia. (mm)	——	——	95.91	
		System parameters		
	Sun gear	Planet gear	Ring gear	carrier
Mass (kg)	1.52	0.3	3.23	0.513
I/r^2 (kg)	0.926	0.183	1.4485	1.413
Bearing stiffness (N/m)	$k_{cb}=k_{pb}=k_{sb}=k_{rb}=10^8$			
Torsional stiffness (N/m)	$k_{su}=0$;	$k_{pu}=0$	$k_{ru}=10^9$	$k_{cu}=0$
Input speed (rpm)/power (W)	500/3000	——	——	——

b) Dynamic Simulation of Planetary Gear System with Tooth Cracks

i. RMS and Kurtosis Indicator Statistics

The dynamic response of cracked gear tooth was simulated using a planetary dynamics model, and Fig. 12 shows the dynamic meshing displacement curve between planetary gear 1 and the ring gear. Fig. 12A shows the dynamic response curve of a healthy gear. When the root crack of the ring gear is in the early stage, it is difficult to observe the pulse waveform it produces, as shown in Figures 12B and C. However, as the crack size expands, two evident pulse vibrations appear in Fig. 12E and Fig. 12F, with the interval between the two adjacent pulses precisely equal to the timeit takes for the planetary gear to mesh with the crack ring gear for one cycle (T=0.43s).

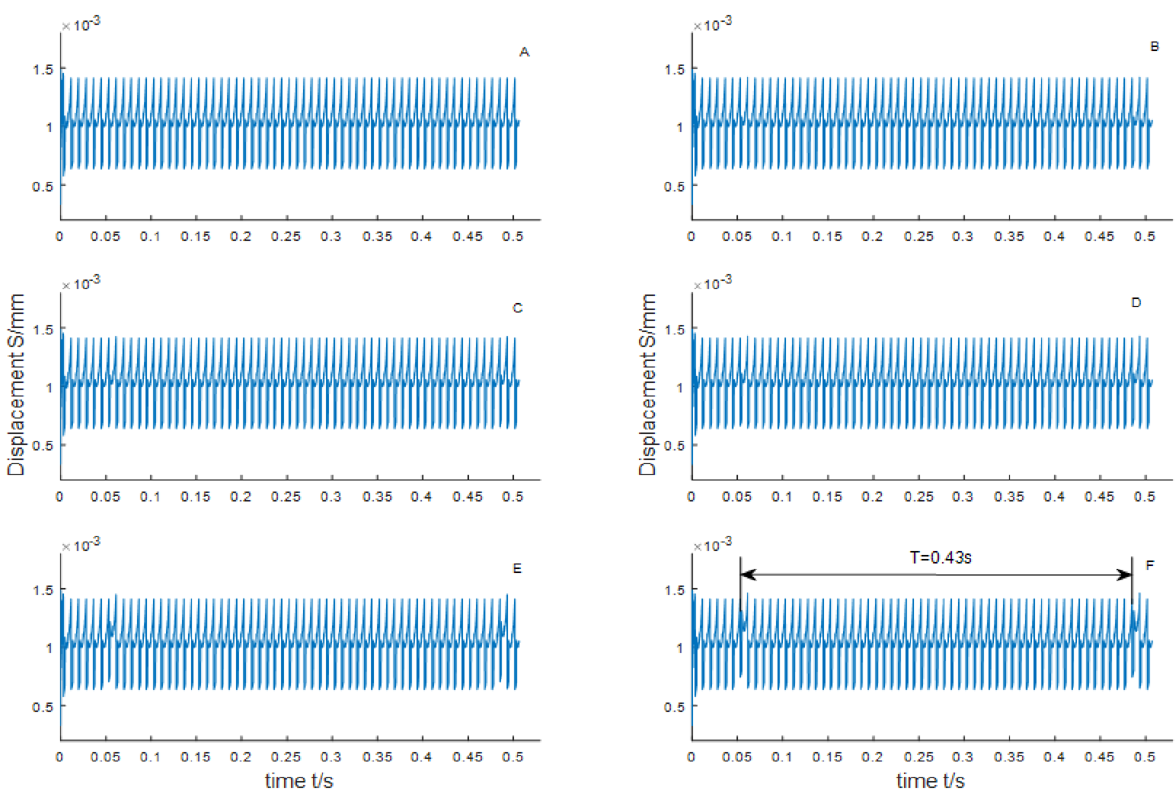

Fig. 12: Shows the dynamic meshing displacement between the planetary gear and the ring gearwith root cracks, (A, B, C, D, E, and F correspond to the crack sizes of six groups of gear teeth in Table 2, respectively)

The statistical characteristics of vibration signal measurement are widely used in mechanical fault detection. Wu et al.[8] investigated the performance of some statistical indicators when cracks with different sizes and depths appeared in meshing gears. The results show that using RMS and Kurtosis indicators to detect the severity of crack propagation has good performance. This article applies RMS and Kurtosis indicators to analyze the dynamic characteristics exhibited by six sets of meshing displacement data and evaluates the severity of tooth root cracks.

RMS is the root mean square value of the vibration signal (describing the energy of the vibration signal), and its calculation formula is:

$$RMS = \sqrt{\frac{1}{N}\sum_{n=1}^{N} x(n)^2} \tag{33}$$

Kurtosis describes the impact characteristics reflected in vibration signals, and its calculation formula is:

$$Kurtosis = \frac{\frac{1}{N}\sum_{n=1}^{n=N}\left(|x(n)| - \bar{x}\right)^4}{\left(\frac{1}{N}\sum_{n=1}^{n=N} x(n)^2\right)^2} \tag{34}$$

In the formula: $x(n)$—is the numerical value of the collected data; N—is the length of the collected data; $\bar{x} = \frac{1}{N}\sum_{n=1}^{N} x(n)$ is the average value of the signal.

Fig. 13 shows the trend of calculated RMS and Kurtosis indices varying with crack propagation, with crack indices 1~6 corresponding to six root crack sizes A, B, C, D, E, and F. From the graph results, it can be seen that for the data in groups A, B, C, and D as shown in Fig. 13, the displacement fluctuations caused by cracks are not significant, and the RMS and Kurtosis indicators are also relatively flat. Correspondingly, the impact fluctuations of the data in groups E and F in Fig. 13 are more prominent, and the statistical indicators also show a clear change trend. RMS shows an upward trend, while Kurtosis indicators show a downward trend. This pattern is similar to the simulation results of L. Cui et al.[33].

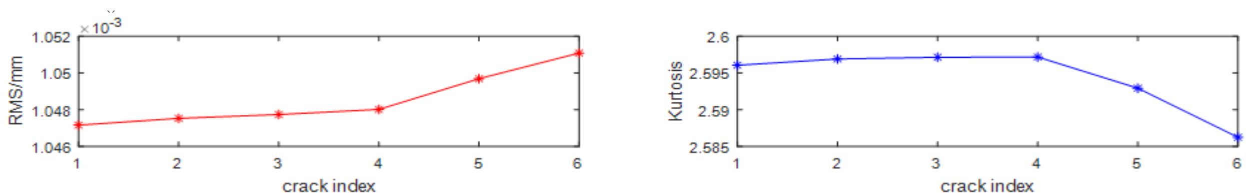

Fig. 13: RMS and Kurtosis indices vary with crack propagation

ii. *Spectrum Analysis*

1) *FFT spectrum and Zoom FFT analysis*

From the dynamic response of planetary-ring gear group meshing in Fig. 12, it can be seen that when a root crack is generated in the ring gear, a pulse vibration will occur. However, when the crack size is small, it is difficult to detect its pulse characteristics in the time domain coordinates. As the crack size expands, obvious pulse vibration will be discovered. In addition to analyzing the characteristics of vibration signals in the time domain, observing their dynamic characteristics in the frequency domain is also an effective way to demonstrate the influence of tooth root cracks.

In order to better analyze the vibration response, calculate the various characteristic frequencies of the planetary system according to equation (35):

$$\begin{cases} f_s = \dfrac{n_s}{60}, \\ f_c = \dfrac{z_s}{z_s + z_r} f_s \\ f_p = \dfrac{(f_s - f_c) z_s}{z_p} \\ f_{mesh} = f_c z_r \end{cases} \tag{35}$$

The calculated frequency data of the planetary system are shown in Table 4, where the frequency of crack faults is the planetary carrier rotation frequency f_c=1/T=2.315Hz.

Table 4: Characteristic frequencies of planetary gear systems

Sun gear rotation frequency f_s	Planetary carrier rotation frequency f_c	Planetary gear rotation frequency f_p	Planetary-ring gear meshing frequency f_{mesh}
8.333Hz	2.315Hz	8.025 Hz	120.37 Hz

According to the resolution ratio formula $\Delta f = f_s / N$, under the condition of a specific sampling frequency f_s, increasing the number of FFT sampling points N can reduce the resolution Δf. Therefore, here, the vibration signal time history in Fig. 12 is extended (increased by N) to be greater than two meshing periods (9.3s). Taking the crack response curve in Fig. 12B as an example of frequency spectrum analysis, the results are shown in Fig. 14. The time-domain data in Fig. 14 is formed by eliminating trend terms or normalizing the original data. In its spectrum, the prominent frequency amplitude is the amplitude of the meshing frequency f_{mesh}=120.8Hz and its doubling spectrum. There are also many sidebands around the meshing fundamental frequency and its harmonics, as shown in Fig. 15(a). Fig. 15(b) shows an enlarged image of the low-frequency part of the spectrum, but due to its low resolution (0.73Hz), it is not possible to clearly display the f_c and its harmonic lines.

In order to extract accurate spectral information, Zoom FFT analysis is performed on the frequency band of the 0-500Hz component to accurately determine the fault frequency and meshing frequency sideband information. The meshing frequency f_{mesh} is accurate to 120.4Hz. The enlarged images of the fault low-frequency band f_c and meshing frequency f_{mesh} sideband information are shown in Figures 16 to 21 (flaw1 to flaw6 correspond to the crack groups A to F in Table 2, respectively). It can be seen from the figure that due to the interference of spectral clutter, the peak characteristics of the planetary carrier rotation frequency (fault frequency band f_c) cannot be accurately displayed when healthy teeth (flaw1) and minior-sized cracks (flaw2) are present. As the crack size increases, the peak amplitude of the fault frequency and its harmonics gradually becomes apparent and increases. Chen et al.[20] argue that the fundamental frequency of gear meshing and its harmonics are difficult to be affected by cracks. For those sidebands, it can be seen from the Zoomed spectrum that there are no fault frequencies around the meshing frequency, and their sidebands amplitudes (121.9Hz and 123Hz) do not change with the increase of crack size. For simplicity, only in Fig. 16b and Fig. 21b the meshing frequency f_{mesh} and its side frequency information are displayed.

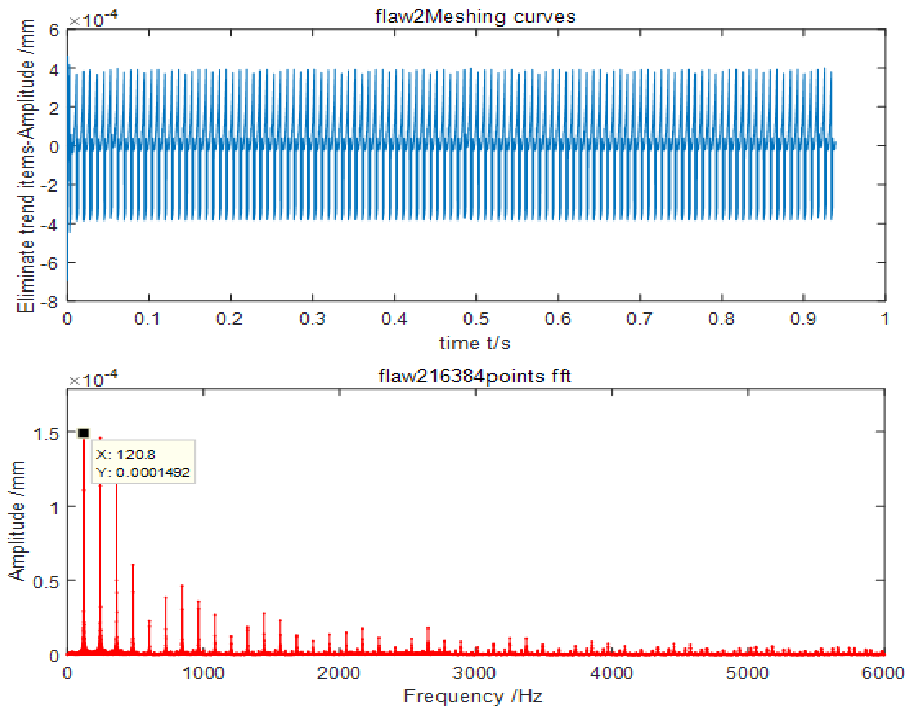

Fig. 14: Frequency domain analysis of meshing curve with B-group size (flaw2) crack

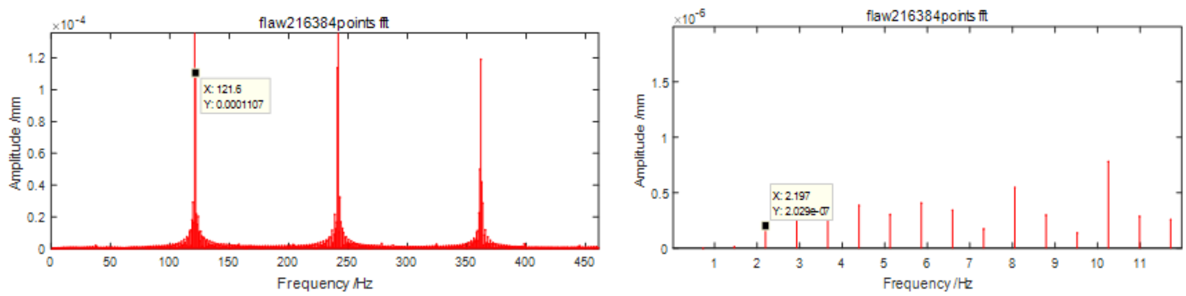

(a) Planetary-ring gear meshing frequency f_{mesh} and its side frequency

(b) Enlarged image of low-frequency part of flaw2 crack response

Fig. 15: Enlarged frequency domain analysis of flaw2 crack meshing

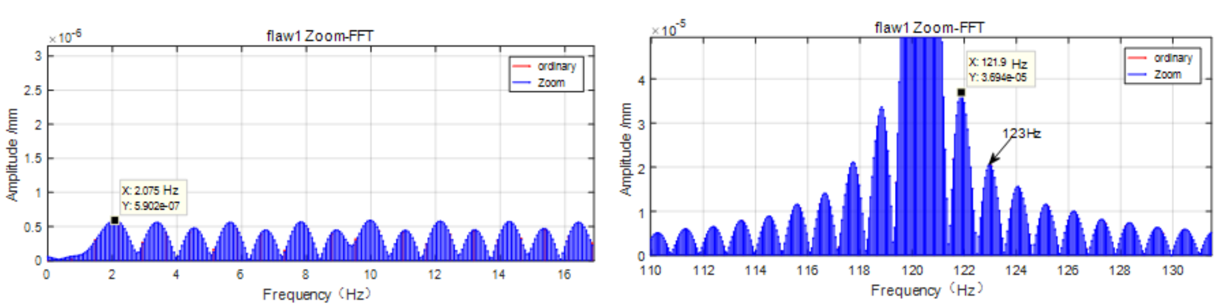

(a) Enlarged low-frequency part of flaw1 crack response

(b) Planetary-ring gear meshing frequency f_{mesh} and its side frequency

Fig. 16: Flaw1 Crack response spectrum refinement and enlargement

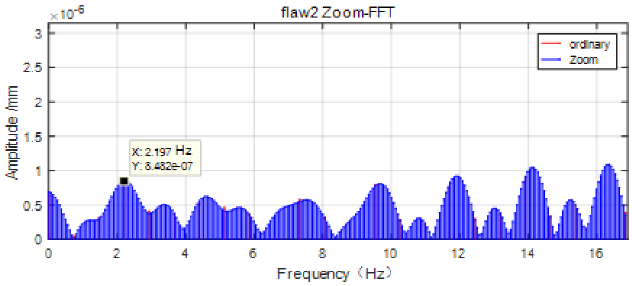

Fig. 17: Enlarged low-frequency part of flaw2 crack response

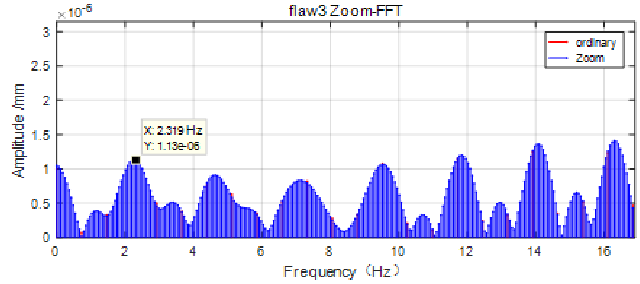

Fig. 18: Enlarged low-frequency part of flaw3 crack response

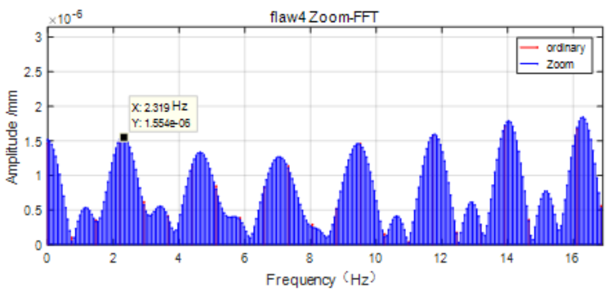

Fig. 19: Enlarged low-frequency part of flaw4 crack response

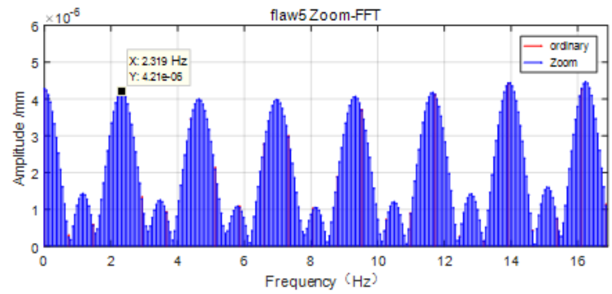

Fig. 20: Enlarged low-frequency part of flaw5 crack response

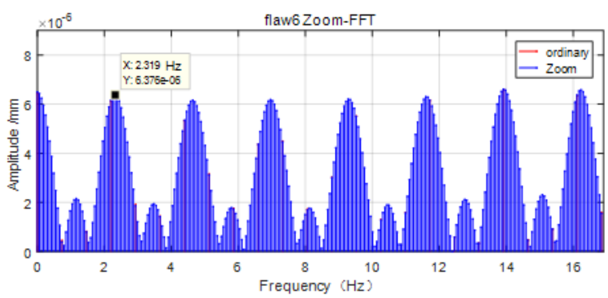

(a) Enlarged image of the low-frequency part of flaw6 crack response

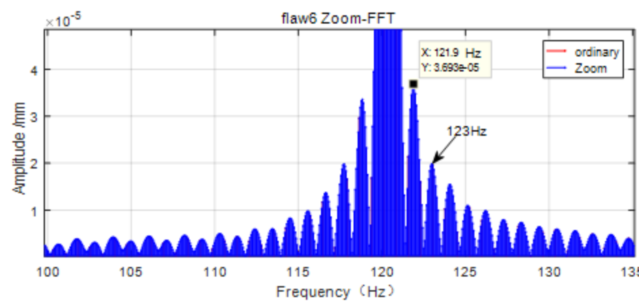

(b) Planetary-ring gear meshing frequency f_{mesh} and its side frequency

Fig. 21: Flaw6 crack response spectrum refinement and enlargement

2) *Cepstrum Analysis*

Cepstrum analysis, also known as secondary spectrum analysis, is equivalent to performing logarithmic weighting on the signal spectrum, resulting in higher weighting of low amplitude frequency components, which is more conducive to extracting and analyzing periodic components in the signal spectrum[34]. Cepstrum can simplify the family of sideband spectral lines on the original spectrum into a single discrete spectral line, and its spectral line height reflects the size of the periodic component of the power spectrum[35].

In the FFT spectrum analysis mentioned above, due to the interference of spectral clutter, it isn't easy to detect the information of feature frequency f_c in the spectrum of healthy tooth and tooth with minior root cracks (flaw2). Therefore, further application of cepstrum analysis and identification of fault frequency f_c information is needed. The simulation results are shown in Fig. 22 to Fig. 27. Unlike the FFT spectrogram, the cepstral spectrogram is based on the time t as the x-axis, where the reciprocal $1/t$ of the t coordinate scale represents the frequency value at that coordinate. The frequency component identified at $t=0.00833$ is $f=1/0.00833=120$Hz, which is the meshing frequency f_{mesh}. The identified $t=0.4321$ corresponds to $f=1/0.4321=2.314$Hz, which is the component information of the frequency f_c. The information of the characteristic frequency f_c was identified through cepstral analysis. As the size of the root crack expands, the amplitude of the fault frequency f_c also increases accordingly. The amplitude data of f_c in the cepstral spectrum was extracted and plotted in Fig. 28. The trend of the cepstral amplitude response of f_c with crack propagation can be intuitively seen, which is consistent with the performance trend of the RMS index mentioned above. This further verifies the consistency of the essential characteristics of time-domain and frequency-domain signal analysis.

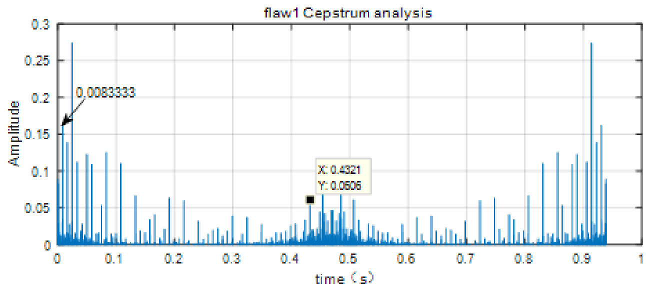

Fig. 22: Flaw1 crack response cepstrum analysis

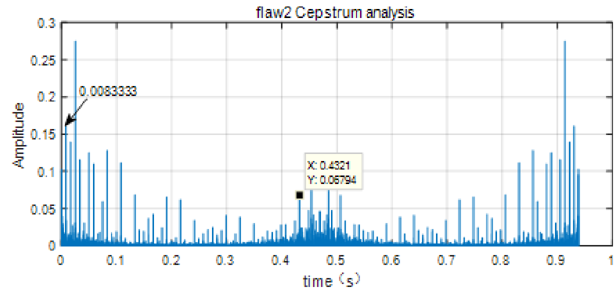

Fig. 23: Flaw2 crack response cepstrum analysis

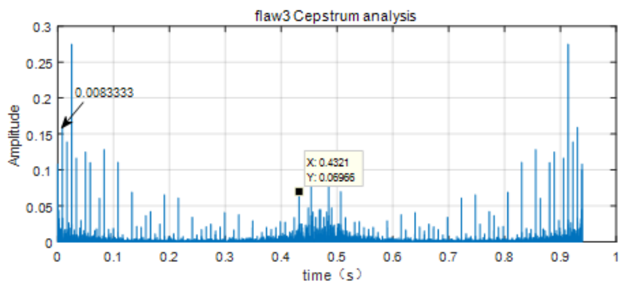

Fig. 24: Flaw3 crack response cepstrum analysis

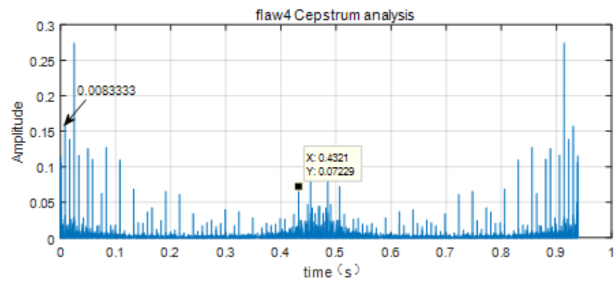

Fig. 25: Flaw4 crack response cepstrum analysis

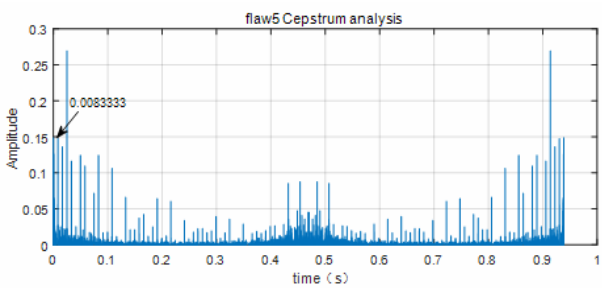

Fig. 26: Flaw5 crack response cepstrum analysis

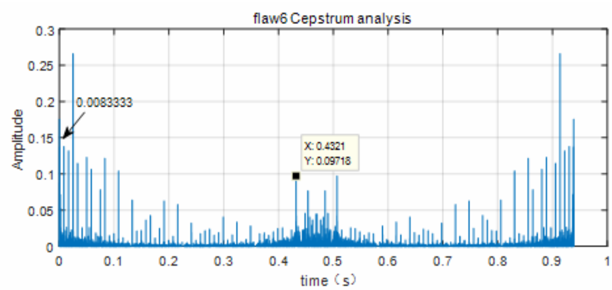

Fig. 27: Flaw6 crack response cepstrum analysis

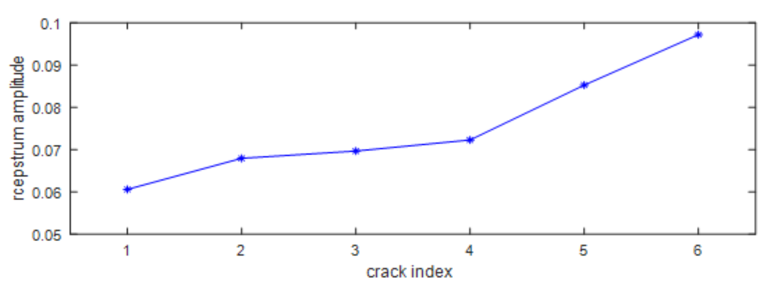

Fig. 28: f_c recpstrum amplitude variation with crack propagation

VI. Conclusion

Based on the principle of potential energy, the time-varying meshing stiffness of internal gears was derived, and the influence of root cracks on the meshing stiffness of internal gears was studied. Based on the meshing stiffness model of internal gear pairs with root cracks, a planetary gear system dynamics model is established to study the influence of cracks on the dynamic response of planetary gear sets. Using vibration statistical indicators to evaluate the severity of tooth root cracks, and applying FFT spectrum, ZoomFFT analysis and cepstrum analysis to extract and analyze the dynamic response characteristics of cracks.

(1) The internal gear cantilever beam model is divided into two parts: involute and transition curves for numerical integration. The transition curve part is calculated using ideal parameterized equations, which can accurately calculate the tooth deformation energy and improve the accuracy of stiffness calculation.
(2) Gear cracks can weaken and reduce the meshing stiffness, further causing impact vibration of the planetary gear set. As the crack size expands, the impact vibration caused by the fluctuation of meshing stiffness will become more severe.
(3) In the vibration spectrum of planetary gear systems, there will be relatively mixed spectra. In the initial stage of crack occurrence, the application of FFT spectrum and its refined analysis cannot observe these weak vibration components. Cepstrum analysis can easily extract the amplitude information of the characteristic frequency f_c, and as the crack size increases, its amplitude also shows a significant growth trend. The analysis results are consistent with the trend judgment of crack propagation using RMS indicators.

References Références Referencias

1. Li Runfang, Wang Jianjun. Systematic dynamics of gear, vibration, shock, noise [M]. Beijing: Science Press, 1997.
2. Wan Zhiguo, Zi YanYang, Cao Hongrui, et al. Time-varying mesh stiffness algorithm correction and tooth crack dynamic modeling[J]. Journal of Mechanical Engineering, 2013, 49(11):153-160.
3. Weber C. The deformation of loaded gears and the effect on their load carrying capacity, Sponsored research (Germany). British Dept. of Sci. and Ind. Res. Report No.3:1949.
4. Cornell RW. Compliance and stress sensitivity of spur gear teeth. ASME J. Mesh Des. 1981;103:447-59.
5. Kasuba R, Evans JW. An extended model for determining dynamic loads in spur gearing. J. Mech Des, Trans Am Soc Mech Eng 1981;103(2):398–409.
6. Yang DCH, Lin JY. Hertzian damping, tooth friction and bending elasticity in gear impact dynamics. Journal of Mechanisms, Transmissions, and Automation in Design. 1987;109(2):189-96.
7. Tian X H. Dynamic simulation for system response of gearbox including localized gear faults [D]. Edmonton: University of Alberta, 2004:19-49.
8. Wu Siyan, Zuo Mingjian, Parey A. Simulation of spurgear dynamics and estimation of fault growth[J]. Journal of Sound and Vibration, 2008, 317(3): 608-624.
9. Charri F, Fakhfakh T, Haddar M. Analytical modeling of spur gear tooth crack and influence on gear mesh stiffness [J]. European Journal of Mechanics/A Solids, 2008, 28(3):461-468.
10. Sun Yalin. Research on fault vibration characteristics of gear train tooth cracks based on lumped parameter model[D]. Guangzhou: South China University of Technology, 2019:8-26.
11. Zhang Tao, He Zeyin, Yin Shirong, et al. Calculation of meshing stiffness of spur gear pair considering time-varying friction and analysis of its influencing factors[J]. Journal of Mechanical Transmission, 2019, 43(9): 54-59.
12. Meng Zong, Shi Guixia, Wang Fulin, et al. Analysis of vibration characteristics of cracked faulty gears based on time-varying mesh stiffness[J]. Journal of Mechanical Engineering, 2020, 56(17):108-115.
13. Liu Yang, Cui Xi, Wang Jiexin. Calculation and analysis of meshing stiffness of spur gears considering wear[J]. Journal of Mechanical Transmission, 2021, 45(1): 65-70.
14. Sun Z, Chen S, Hu Z, et al. Improved mesh stiffness calculation model of comprehensive modification gears considering actual manufacturing[J]. Mechanism and Machine Theory, 2022, 167:104470.
15. Cao Dongjiang, Shang Peng, Zhao Yang. Calculation and analysis of modified gear Time-varying Meshing Stiffness based on matlab [J]. Journal of Mechanical Transmission. 2022, V46(5):100-107.
16. Xu Kejun, Jiao Wei, Qin Haiqin. Research on the Time-varying Meshing Stiffness algorithm of spur gears based on an improved potential energy method. Journal of Mechanical Transmission. 2023, V47(2):1-7.
17. Hidaka T, Terauchi Y, Nohara M, et al. Dynamic behavior of planetary gear – 3rd report: displacement of ring gear in direction of line of action. BullJSME 1977;20(150):1663–72.
18. Karas F. nElastiche Formanderung und Lasterverteilung heim Doppleleingriff geroder Stirnradzahne. V.D.I. Forschh. vol. 406; 1941.
19. Chen Zaigang, Shao Yimin. Mesh stiffness of an internal spur gear pair with ring gearrim deformation. Mechanism and Machine Theory. 69(2013) 1-12.
20. Chen Zaigang, Shao Yimin. Dynamic simulation of planetary gear with tooth root crack in ring gear. Engineering Failure Analysis. 31 (2013) 8-18.
21. Lewicki DG, Ballarini R. Effect of rim thickness on gear crack propagation path. NASA technical memorandum 107229. Army research laboratory. Technical report ARL-TR-1110; 1996.
22. Lewicki DG, Ballarini R. Gear crack propagation investigations. NASA technical memorandum 107147. Army research laboratory. Technical report ARL-TR-957; 1996.

23. Lewicki DG, Spievak LE, Wawrzynek PA. Consideration of moving tooth load in gear crack propagation predictions. NASA/TM-2000-210227; 2000.
24. Chaari F. Baccar W. Abbes Ms. et al. Effect of spalling or tooth breakage on gear mesh stiffness and dynamic response of a one-stage spur gear transmission. Eur J Mech A-Solids 2008;27:691-705.
25. Meng Lingru, Sha Yuzhang, Ding Shiwei. On interference in machining internal gear pair [J]. Journal of Shenyang Institute of Technology 1998, V17 (2), 96-99.
26. Zhang Lintong. Determination of addendum arc of internal gear sharper cutter [j]. Tool Engineering, 1991, v25 (11): 7-9.
27. Cao Dongjiang, Shang peng, Cui Hongtao et al. Parametric design of internal gear based on accurate tooth profile modeling[J]. Journal of Mechanical Transmission, 2023,47(9): 66-73.
28. Lewicki DG, Gear crack propagation path studies guidelines for ultra-safe design. NASA/TM-2001-211073. ARL-TR-2468; 2001.
29. Chen Z, Shao Y. Dynamic simulation of spur gear with tooth root crack propagating along tooth width and crack depth. Eng Fail Anal2011;18(8):2149–64.
30. J. Lin, R.G. Parker, Analytical characterization of the unique properties of planetary gear free vibration, Journal of Vibration and Acoustics. 121 (3) (1999) 316–321.
31. Chaari Fakher, Fakhfakh Tahar, Hbaieb Riadh, et al. Influence of manufacturing errors on the dynamical behavior of planetary gear. Int J Adv ManufTechnol 2006;27:738–46.
32. V.K. Ambarisha, R.G. Parker. Nonlinear dynamics of planetary gears using analytical and finite element models. Journal of Sound and Vibration 302 (2007):577–595.
33. L. Cui et al. Research on the meshing stiffness and vibration response of cracked gears based on the universal equation of gear profile. Mechanism and Machine Theory 94 (2015) 80–95.
34. Wang Ji, Hu Xiao. Application of MATLAB in vibration signal processing [M]. China Water Resources and Hydropower Press, Intellectual Property Press, January 2006, 137-138.
35. Zhong Binglin, Huang Ren. Mechanical fault diagnosis (Third edition) [M]. Machinery Industry Press, July 2013.

Global Journal of Researches in Engineering: A
Mechanical and Mechanics Engineering
Volume 24 Issue 1 Version 1.0 Year 2024
Type: Double Blind Peer Reviewed International Research Journal
Publisher: Global Journals
Online ISSN: 2249-4596 & Print ISSN: 0975-5861

Studies of the Mechanism of Adhesion of Polymer Coatings on the Oxidized Surface of Aluminum and Magnesium Alloys

By Makarychev Yu. B., Kuzenkov Yu. A., Chugunov D. O. & Grafov O. Yu.

Abstract- The adhesion of the polymer paint Lakroten E-244 was investigated on oxidized aluminum A5154 and magnesium MA-20 alloys. It is shown that the adhesion of the polymer coating on the chemically oxidized surface of the aluminum alloy is significantly greater than on the anodic film of the magnesium alloy. Using photoelectron XPS spectroscopy and SEM analysis, the chemical composition and morphology of the alloys have been investigated. The dependence of these factors on the adhesion force of the polymer coating to the oxidized surface of aluminum and magnesium alloys has been established. Methods of modification of conversion coatings with ethylen glycol, which significantly improve the adhesion of polymer layers, have been proposed. The chemical composition and morphology of these coatings have been investigated. An explanation of the mechanism of improvement of adhesion properties of modified coatings on aluminum and magnesium alloys is given. The mechanism of improving the adhesive properties of modified coatings on aluminum and magnesium alloys is explained.

Keywords: *adhesion strength, x-ray photoelectron spectroscopy, conversion coatings, paints.*

GJRE-A Classification: *LCC: TP1180, QD549*

STUDIESOFTHEMECHANISMOFADHESIONOFPOLYMERCOATINGSONTHEOXIDIZEDSURFACEOFALUMINUMANDMAGNESIUMALLOYS

Studies of the Mechanism of Adhesion of Polymer Coatings on the Oxidized Surface of Aluminum and Magnesium Alloys

Makarychev Yu. B. [α], Kuzenkov Yu. A. [σ], Chugunov D. O. [ρ] & Grafov O. Yu. [ω]

Abstract- The adhesion of the polymer paint Lakroten E-244 was investigated on oxidized aluminum A5154 and magnesium MA-20 alloys. It is shown that the adhesion of the polymer coating on the chemically oxidized surface of the aluminum alloy is significantly greater than on the anodic film of the magnesium alloy. Using photoelectron XPS spectroscopy and SEM analysis, the chemical composition and morphology of the alloys have been investigated. The dependence of these factors on the adhesion force of the polymer coating to the oxidized surface of aluminum and magnesium alloys has been established. Methods of modification of conversion coatings with ethylen glycol, which significantly improve the adhesion of polymer layers, have been proposed. The chemical composition and morphology of these coatings have been investigated. An explanation of the mechanism of improvement of adhesion properties of modified coatings on aluminum and magnesium alloys is given. The mechanism of improving the adhesive properties of modified coatings on aluminum and magnesium alloys is explained.

Keywords: adhesion strength, x-ray photoelectron spectroscopy, conversion coatings, paints.

I. Introduction

Aluminum and magnesium alloys are widely used as structural materials in the aerospace, electronics and automotive industries due to their low density and high strength. The disadvantage of these alloys is their low corrosion resistance in aqueous electrolytes, which limits their use without special preparation. To protect aluminum and magnesium alloys from corrosion, paints and varnishes are commonly used, which are applied to conversion coatings. To improve the adhesion of aluminum and magnesium alloys to paints, alkaline treatment is often recommended to increase the concentration of -Me-OH atomic groups on their surface. To enhance the adhesive activity of aluminum and magnesium alloys to paints, alkaline treatment is often recommended in order to increase the concentration of Me-OH groups of atoms on their surface. At the same time, an increase in the adhesive force is associated with the chemical interaction of surface metal hydroxides with paintwork components. Most coatings in their composition contain monomers with the general formula R-OH and R-COOH, where R is aliphatic or cyclic hydrocarbons. In this case, the chemical interaction of the paint with metal occurs as a result of the condensation reaction, which can be represented in the form of equations:

$$\text{Me-OH+ R-OH =Me-OR+H2O} \quad (1)$$

$$\text{Me-OH +R-COOH =MeOCOR +H2O} \quad (2)$$

Thus, for the paint to form chemical bonds with the conversion coating, chemically active hydroxyl groups of atoms must be present in its composition. Most studies on the modification of conversion coatings are aimed at changing their structure rather than their chemical composition, based on the assumption that the main factor that increases adhesion is the mechanical bonding of the paint to the pore walls. However, the rapid development of technologies based on the use of organosilane primers indicates the significant role of chemical interaction in the formation of strong bonds of coating materials with the surface of metals. Conversion coatings on aluminum and magnesium alloys consist mainly of metal oxides and hydroxides. Only metal hydroxides participate in the formation of chemical bonds by the mechanism of hydrolytic condensation, so the adhesion strength should depend on the MeO/MeOH ratio in the conversion coating. In this work, the chemical compositions of anodized layers on aluminum A5154 and magnesium MA-20 alloys will be investigated by XPS methods in order to determine the influence of the chemical composition of conversion coatings on the adhesion force to paints. The coatings impregnation was carried out with acrylic paint based on Lakroten E-244 dispersion. The copolymer of this dispersion is acrylic acid which can interact with metal hydroxides by reaction (2).

II. Material and Methods

The work used samples of aluminum and magnesium alloys, the composition of which is shown in Table 1.

Author α σ ρ Ѡ: A.N. Frumkin Institute of Physical Chemistry and Electrochemistry, Russian Academy of Sciences, Leninsky pr. 31, Moscow, Russian. e-mail: makarychev-1949@mail.ru

Table 1: Compositions of aluminum alloy A 5154 and magnesium alloy MA-20

	Mass fraction of elements, %							
Alloy grade	Fe	Cu	Mn	Mg	Cr	Zn	Ce	Al
A5154	0.25	0.4	0.1	0.1	3.1	15	0.2	93.8
MA20	0.05	0.03	0.04	97.94	1.5	0.12	0.02	0.2

The following substances were used to compose inhibitory compositions:

- Ethylene glycol (EG), HO-CH_2-CH_2-OH (Chem.Russia);
- Vinyltrimethoxysilane (VS) (WitcoCo);

Compositions of oxidation electrolytes of aluminum alloy A 5154 and magnesium alloy MA-20 is shown in Table 2.

Table 2: Compositions of oxidation electrolytes of aluminum alloy A 5154 and magnesium alloy MA-20

Sample	Conversion Coating	Modified Conversion Coating
A5154	35g/l NaH_2PO_4,10gl $AlNO_3$, 5 г/л NaOH	35g/l NaH_2PO_4,10gl $AlNO_3$, 5 г/л NaOH,50 г/л EG
MA20	55g/l NaOH, 35g/l Na_2HPO_4, 10g/l $Al(NO_3)_3$	55g/l NaOH, 35g/l Na_2HPO_4 10g/l $Al(NO_3)_3$,50 г/л EG

a) Adhesion Measurement

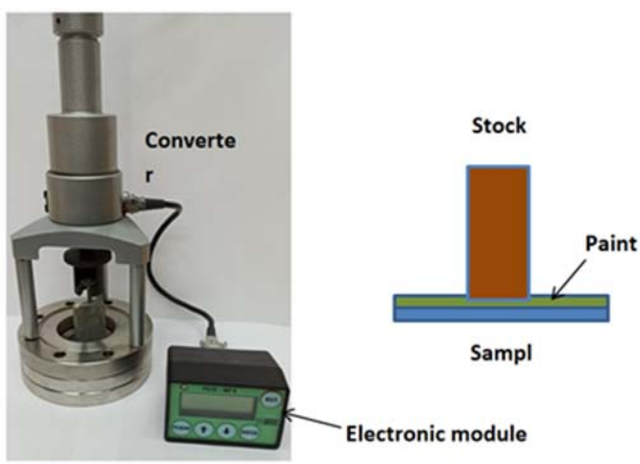

Fig. 1: Electronic adhesion meter PSO-MG4g

The coating adhesion test during separation was carried out using an electronic adhesion meter PSP-MP4 (Russia), shown in Fig. 1. Samples with conversion coating were placed in a fixed holder. Super glue was applied to the surface of an aluminum rod with a diameter of 10 mm and then brought into contact with the test samples. After curing the glue, the joint was stretched at a constant speed of 5 mm/min. For each test, five repeating samples with the specified mean value were used.

b) X-ray Photoelectron Spectroscopy (XPS) Study

X-ray photoelectronic spectra (XPS) were recorded using the Omicron+ X-ray photoelectron spectrometer (FRG). The pressure in the analyzer chamber did not exceed 10-8 Torr. The radiation of an X-ray Al-anode (radiation energy 1486.6 eV, power 200 W) was used as a source. The transmission energy of the analyzer is set to 20 eV. The binding energy of the electrons was calibrated according to the XPS peak of C1s electrons, the binding energy of which was assumed to be 285.0 eV and which is due to the settled layers of diffusion oil vapor. Photoionization cross sections of the corresponding electron shells taken from [19] were used for quantitative evaluation. The integral peak intensities were obtained after subtracting the background using the Shirley method [20] and by fitting the observed peaks with Gauss curves with the contribution of the Lorentz component. To obtain information about the thicknesses of the layers formed on the surface, the MultiQuant program was used [21], the photoionization sections of the corresponding electron shells given by Schofield [22] were selected. To calculate the thicknesses of the layers, the values of electron free path lengths (or average attenuation coefficients) calculated by the method proposed by Kampson and Sih were used [23].

c) SEM of the Study

SEM images were obtained by a JSM-6400 scanning microscope with an electron-beam intensity of 20 keV, unless otherwise written. Analysis of the elements was performed with SEM equipped with energy-dispersive X-ray analysis (EDX) with a WinEDS EUMEX analyzer (Germany). The thickness of the polymer siloxane coatings was determined using the ZAF correction algorithm for Ka-ratios samples with a known coating thickness.

d) EIS Study

An electrochemical complex consisting of a potentiostat with a frequency analyzer (FRA) is used to measure the impedance. The measurements were carried out in a three-electrode electrochemical cell with a corrosion potential using the Solartron electrochemical complex with a change in the frequency of alternating current from 60,000 to 0.1 Hz (ΔE = 10 Mv).. The impedance data was analyzed using ZView® electrochemical impedance software (version Scribner Associates, Inc., USA).

III. Experimental

The adhesion of coating materials to metal surfaces depends mainly on the chemical composition of the surface, the thickness and porosity of the adhesion layer. The thickness and porosity of conversion coatings for aluminum and magnesium alloys differ to a lesser extent than the chemical composition. Anodic coatings on magnesium alloy AZ91D contain mainly MgO, Al_2O_3 and $MgAl_2O_4$ [24,25]. The adhesion of the paint to such a surface should depend on the thickness and porosity of the conversion coating, since the chemical interaction is minimized. The addition of reagents to anodizing electrolytes that are susceptible to hydrolysis increases the hydroxide ion content of the conversion coating and thus, according to equation (1.2), the adhesion of the coating to the alloy surface. Since the adhesive strength of the coating depends on the chemical composition of the substrate, XPS studies of conversion coatings were carried out.

a) XPS and SEM Investigation of the Chemical Composition of the Conversion Coating on the MA-20 Alloy

The elemental composition of the conversion coating obtained by anodizing the MA-20 alloy in an alkaline solution is shown in Table 3.

Table 3: The elemental composition of the conversion coating on the MA-20 alloy

Sample	Mg,% at	Al,% at	C,% at	O,% at	Thickness, mkm
MA-20	30.3	8.4	19.2	42.1	23.0±5.0

From the results of the chemical analysis given in Table 2, it can be seen that the composition of the conversion coating includes significant amounts of aluminum compounds that fall into the coating from the substrate or electrolyte during oxidation. Figure 2 shows the XPS spectra of Mg2p and Al2p in the conversion coating. After decomposition of the spectra into components, it is seen that the conversion coating consists mainly of magnesium and aluminum oxides. A study of the adhesion of acrylic paint on anodised magnesium alloy surfaces showed extremely low adhesion strength. To increase the adhesive strength of aluminium and magnesium alloys, it is often recommended to hydroxylate the surface by treatment in alkaline solutions. It is possible to increase the concentration of adhesively active R–OH radicals in the conversion coating by adding polyfunctional alcohols to the anodizing electrolytes.

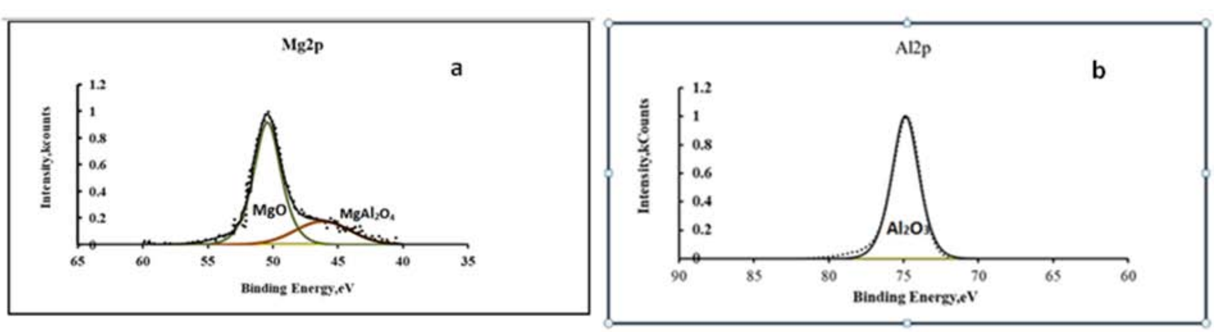

Fig. 2: X-ray spectra of Mg2p (a) and C1s (b) in the conversion coating

In the articles [26,27], studies were carried out on the anodizing of magnesium alloys in aqueous solutions of ethylene glycol and glycerin. The authors of these works found that the conversion coatings obtained in these solutions are formed at sufficiently high speeds, have a porous structure, have high hardness and wear resistance. However, studies of the chemical composition and adhesive strength were not carried out in these works. Morphology and chemical composition of the magnesium layers obtained with ethylene glycol additives in anodizing solutions were studied. Figure 4 shows SEM images of the surface of the anodized alloy before and after modification with ethylene glycol.

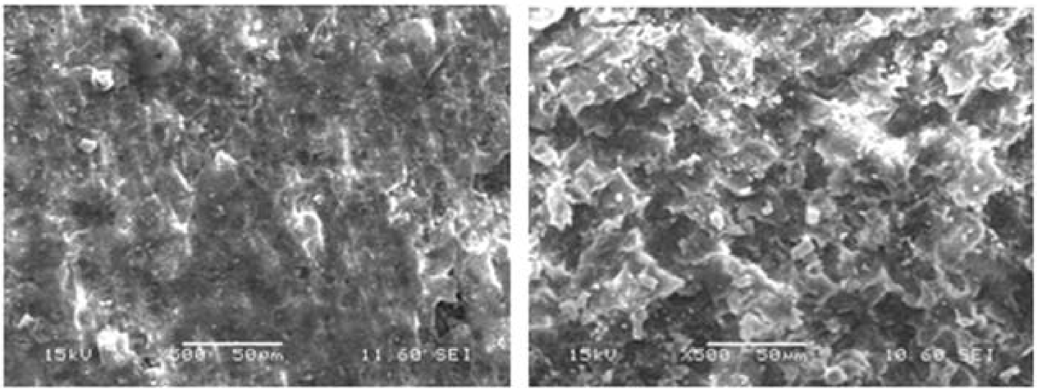

Fig. 3: SEM images of the surface of the anodized alloy before and after modification with ethylene glycol

The addition of ethylene glycol to the electrolyte leads to an increase in the roughness and thickness of the coating. The increase in roughness is apparently due to the formation of magnesium glycolate macromolecules [29] linked together by a bridging bond. Table 4 shows the chemical composition of the modified composite coating.

Table 4: Elemental composition of the modified composite coating

Sample	Mg, % ат.	Al, % ат.	C, % ат.	O, % ат.	Thickness, mkm
MA-20	22,3	2.4	43.2	32,1	32.4.0±5.0

The results of chemical analysis show that the composite coating contains a significant amount of carbon. According to [29], magnesium hydroxide molecules interact with ethylene glycol to form magnesium ethylene glycolate by reaction (3). Magnesium glycolates can interact with each other to form macromolecules by reaction (4).

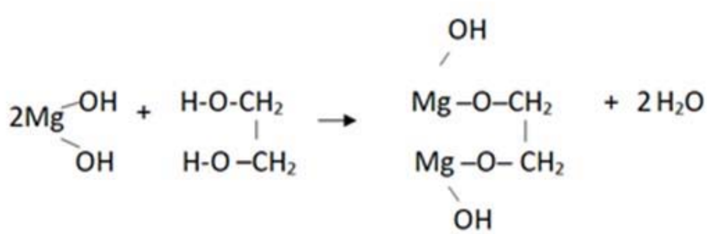

(3)

$$n[HO\text{-}MgO(CH_2)OMg\text{-}OH] \rightarrow [\text{-}O\text{-}Mg\text{-}O(CH_2)OMgO\text{-}]n + nH_2O \qquad (4)$$

Macromolecules, together with magnesium oxides, are embedded in the structure of globules that make up conversion coating [29,30]. Polyglycolates contain in their composition adhesive active groups – OH, through which interaction with paints and individual globules with each other is carried out. On the XPS spectra of Mg2, magnesium ethylene glycolates can be observed by the appearance of a peak with E_b= 53.5 eV (Fig. 5), and on the spectra of C1s with E_b = 288.2 eV (Fig. 6).

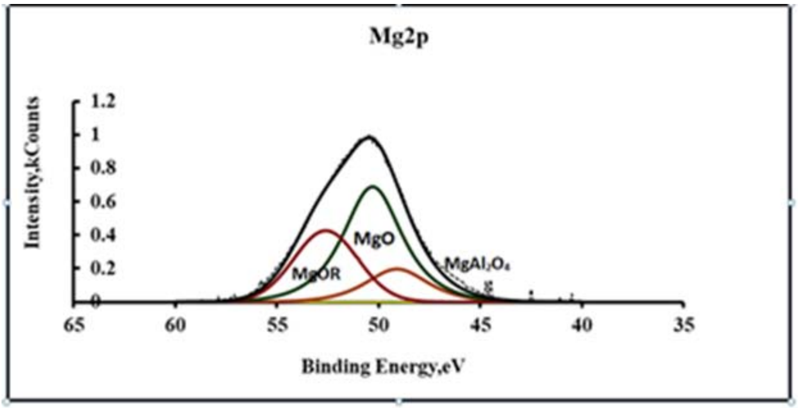

Fig. 4: XPS spectra of Mg2p in a modified inversion coating

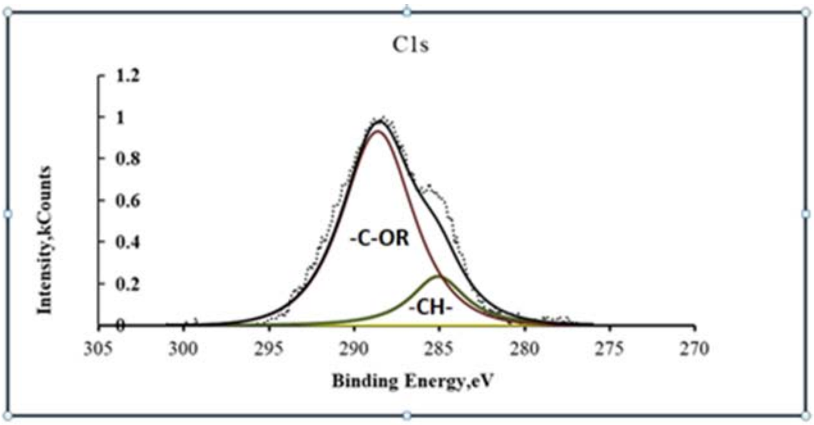

Fig. 5: XPS spectra of C1S carbon in a modified conversion coating

The amounts of ethylene glycolates and magnesium hydroxides in the original and modified conversion coating are shown in Table 5.

Table 5: Chemical composition and tensile strength of the initial and modified MA-20 alloy

Type of coating	MgO, % ат.	Mg glycolate% ат.	$MgAlO_4$ % ат.	Adhesion strength KPa
1. Initial coating	84,6	-	15.4	300±50
2. Modified	57.2	36.2	18.6	1180±50

The inclusion of magnesium glycolates in the conversion coating should change the concentration of chemically active groups -OH. Figure 6 shows the XPS spectra of O1s oxygen in the modified conversion coating.

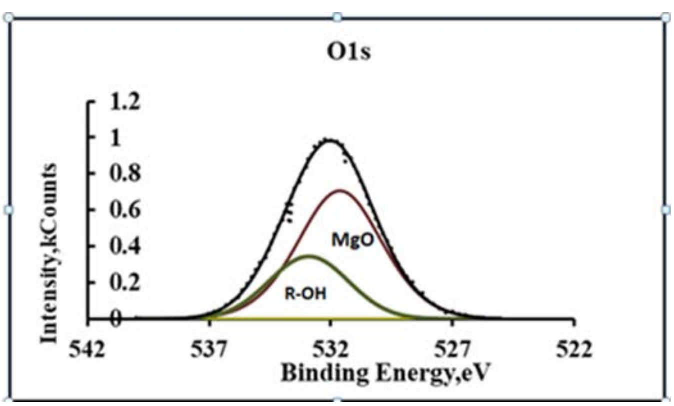

Fig. 6: XPS-spectra of O1s oxygen in the modified conversion coating

Quantitative calculations have shown that the ratio of [O]/[OH] concentrations in the conversion coating changes towards an increase in hydroxide ions mainly due to magnesium ethylene glycolate. An increase in the adhesive strength of the modified conversion coating may be due to an increase in roughness or due to the formation of chemical bonds with the paint. With the help of vapor-gas deposition of vinyltrimethoxysilane (VS) [31], its roughness was reduced on the surface of the modified conversion coating. The coating thickness was 150-200 nm. To assess the roughness of the conversion coating, EIS studies were conducted.

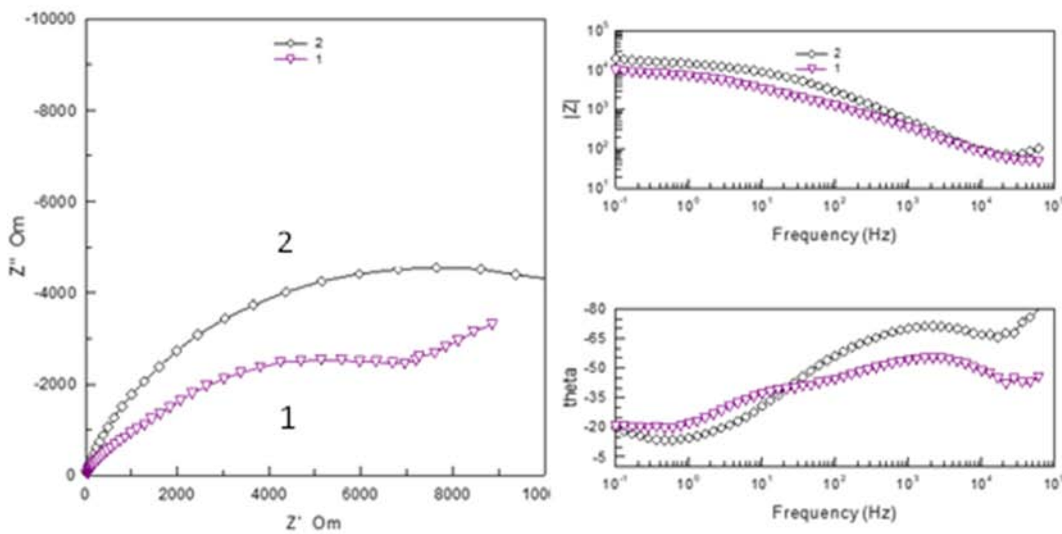

Fig. 7: Nyquist and Bode plots for modified conversion coating (plot 1) and after VS impregnation (plot 2)

In plot 1 (Fig. 7), there is a rectilinear section with an angle of 45° in the high frequency region. This form of the Nyquist graph is characteristic of mass transfer in porous systems. After impregnation, the Nyquist graph has the form of a hemisphere, characteristic of a smoothed surface. The Bode graphs for the initial conversion coverage show the presence of two well-defined time constants. In the high frequency range the time constant can be explained by the barrier properties of coatings. In the low-frequency region, 10-50 Hz is attributed to corrosion processes at the boundary of the coating and metal. After the vapor-gas modification of the conversion coverage, the through pores are filled with polymer and a wide area of change in the phase angle of the barrier coating remains. Silane coating practically does not change $|Z|$, which indicates partial filling of the pores and a slight change in the structure of the coating. The decrease in the roughness and pore volume of the conversion coverage should have reduced the adhesive force at the same time, it increased after steam-gas treatment by ~ 20-30%, which indicates the predominant influence of chemical interaction over mechanical. Impregnation of the coatings with vinylsilane increases the number of functional groups involved in the formation of chemical bonds in connection with which it can be used to enhance the adhesion of the coating with paint. Table 6 shows the adhesion strength of Lakroten E-244 to oxidized alloys MA-20 and A5154.with paint.

Table 6: Adhesive strength of Lakroten E-244 to oxidized alloys MA-20 and A5154

Conversion coverage on MA-20	Adhesion strength, KPa
1. Initial	300±50
2. Modified with ethylene glycol	1180±50
3. Modified with ethylene glycol+VS	1350±100
Conversion coverage on A 5154	
4. Initial	1600±100
5. Conversion coverage on A 5154	1850±100

From the data given in Table 6, it can be seen that the adhesion of Lakroten E-244 on the modified chemically oxidized alloy A5154 is maximum. To clarify the influence of the morphology and chemical composition of the aluminum alloy on the adhesion of the paint, XPS and SEM studies were conducted.

b) XPS and SEM Study of the Chemical Composition of the Conversion Coating on Aluminum Alloy A5154

The conversion coating on chemically oxidized alloy A5154 consists mainly of $Al(OH)_4$, which is obtained by the equation:

$$Al_2O_3 + 2OH^- + 3H_2O \rightarrow 2\,Al(OH)_4 \qquad (5)$$

This explains the high adhesion of coatings to these alloys. Chemical oxidation is used along with electrochemical, but is inferior to the latter in terms of performance characteristics, primarily mechanical strength and wear resistance. Modification of a chemically oxidized conversion coating with ethylene glycol can increase its mechanical properties due to additional chemical bonds between individual amorphous $Al(OH)_4$ globules of which conversion coating consists [32]. Along with high adhesive activity, such coatings could significantly expand their application areas.

The conversion coating on alloy A 5154 was modified with ethylene glycol by adding it to oxidation solutions. Figure 8 shows a SEM images of the surface of the conversion coating on the original and modified alloy.

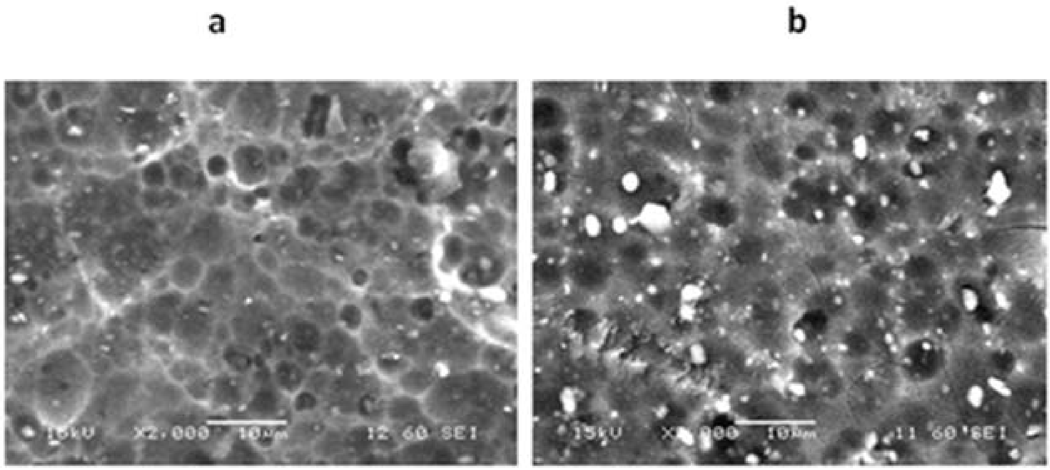

Fig. 8: SEM images of the surface of the conversion coating on the original (a) and modified (b) alloy

It can be seen that the structure of conversion coating A5154 is fine-grained with vertical pores of 5-10 microns in size, in contrast to magnesium MA-20. On the modified alloy the structure is also granular but the number and diameter of the pores are larger. Inclusions of white colour according to X-ray microanalysis data are microphases of magnesium glycolate. The chemical composition of the alloys is given in Table 7.

Table 7: Chemical composition of the initial and modified conversion coating on alloy A5154

Conversion coating on alloy A5154	Mg, % ат.	Al, % ат.	C, % ат.	O, % ат.	Thickness, mKm
Initial	2,3	14.4	25.1	58.2	3.2
Modified	1.8	11.6	42.8	43.8	2.8

Comparing the chemical analysis data of the original and modified coating, it is clear that the latter contains a significant amount of carbon belonging to magnesium and aluminum glycolates. Aluminum glycolates can be detected by the appearance of a peak on the Al 2p spectra with an energy of 71.4 eV and a peak with an energy of 288.2 eV on the C1s spectra (Fig. 9).

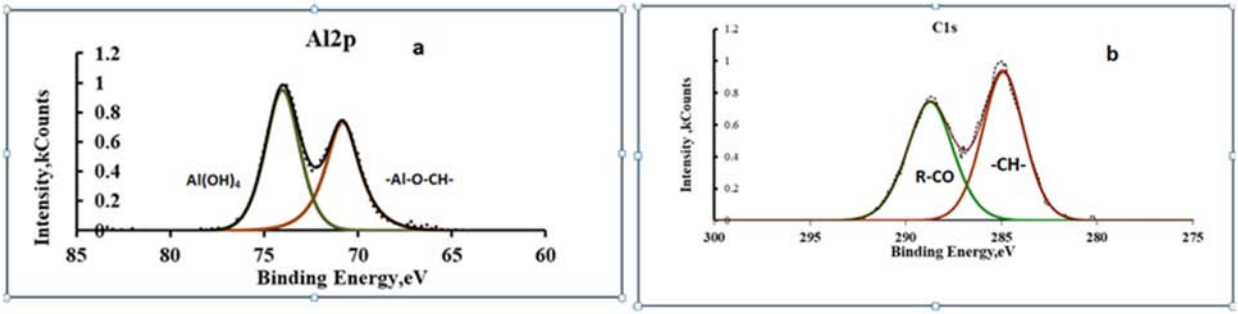

Fig. 9: XPS spectra of Al 2p(a) and C1s (b) for a modified conversion coating on alloy A 5154

A symmetrical doublet on the Al2p spectrum indicates the existence of two types of chemical compounds of aluminum distributed in the conversion coating as separate phases. One of these phases is $Al(OH)_4$, the other is aluminum glycolate. Quantitative calculations of the XPS spectra belonging to aluminum hycolates have shown that two aluminum atoms account for approximately the same number of carbon atoms. This ratio corresponds to the reaction of the formation of aluminum glycolate according to equation (6).

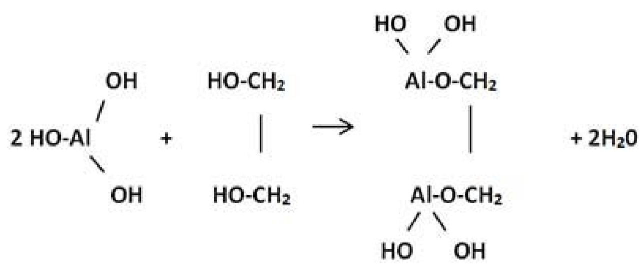

(6)

Aluminum glycolate molecules can interact with each other to form macromolecules and individual phases in the conversion coating. A significant amount of aluminum glycolate in the coating indicates a high chemical activity of ethylene glycol to aluminum hydroxides. The inclusion of aluminum glycolate in the composition of the conversion coating changes its structure and possibly mechanical properties in the direction of increasing strength due to the formation of new chemical bond. The adhesive strength of the modified conversion coating is slightly higher than the initial one due to mechanical adhesion, since the concentration of chemically active –OH groups varies slightly.

IV. Results and Discussion

Published studies of paint adhesion to aluminium and magnesium alloys are random and adhesion strength is mainly attributed to mechanical adhesion in the pore volume. At the same time, our studies have shown that the adhesion strength of paint to the surface of these alloys can vary by an order of magnitude. In this work, the surface of the alloys was subjected to chemical and anodic oxidation. Conversion coatings on aluminium alloy A5154 were obtained by chemical oxidation in alkaline solutions. Oxide coatings on magnesium alloys Ma-20 were obtained by anodising in alkaline solutions. From the point of view of the theory of mechanical adhesion of paints with the alloy surface, conversion coatings on Ma-20 alloy are more preferable because they have a more developed structure on the surface and inside the oxide layer. However, studies have shown that the adhesion force on aluminium alloys is 5-6 times greater than on magnesium alloys. It has been suggested that this is due to the chemical composition of the conversion layers. On aluminium alloys they consist of aluminium hydroxides $Al(OH)_4$ and on magnesium alloys of oxides. According to equations (1,2) the formation of strong chemical bonds with paints is possible only on aluminium alloy. Modification of the conversion coating with ethylene glycol leads to an increase in its concentration of -OH groups capable of chemical interaction with paintwork materials, as a result of which the adhesive force increases. It is possible to increase the concentration of hydroxides in the coating by introducing compounds that form -R-OH groups of atoms as a result of hydrolysis, such as organosilanes, into the anodising electrolyte. Modification of aluminium alloys with ethylene glycol does not lead to a significant increase in adhesion strength because the conversion coating consists of aluminium hydroxides. However, there is an increase in the number and size of pores, which increases the adhesive strength.

V. Conclusions

Studies of the adhesion of the acrylic paint Lakroten E-244 to aluminum A5154 and magnesium Ma-20 alloys have been carried out. Significant differences in the adhesive activity of these alloys to polymer coatings were found. With the help of XPS and SEM, studies of the chemical composition and morphology of alloys were carried out. It is shown that the adhesion of coatings to the surface of alloys depends mainly on the ratio of MeO/MeO in the conversion coating. Modification of the conversion coating on a magnesium alloy with ethylene glycol significantly increases the adhesive strength of the alloy to paints. The chemical composition of magnesium ethylene glycolate macromolecules and their amount in the conversion coating were determined with the help of XPS studies. The addition of ethylene glycol increases the thickness of the conversion coating and its strength due to the formation of additional chemical bonds of magnesium ethylene glycol macromelecules with inside and on the border of globules. Studies of the chemical composition, morphology and adhesive activity of conversion coatings on the surface of aluminum alloys modified with ethylene glycol have been carried out. It is shown that the increase in the adhesive activity of modified aluminum alloys is mainly due to an increase in the number and size of pores. The chemical composition and quantity have been established macromolecules of aluminum ethylene glycolate in the conversion coating of aluminum alloy. Modification of the ethylene glycol conversion coating on magnesium and aluminum alloys changes their structure and chemical composition, which contributes to a significant increase in their adhesive activity.

References Références Referencias

1. S. A. Kulinicha, b and A. S. Akhtara, On Conversion Coating Treatments to Replace Chromating for Al Alloys: Recent Developments and Possible Future Directions, Russian Journal of NonFerrous Metals, 2012, Vol. 53, No. 2, pp. 176–203. © Allerton Press, Inc., 2012.
2. J.-P. Dasquet a, U, D. Caillardb, Investigation of the anodic oxide layer on 1050 and 2024T3 aluminium alloys by electron microscopy and electrochemical impedance spectroscopy Thin Solid Films 371 2000 183-190.
3. Yoganandan, J. N. Balaraju*, Synergistic effect of V and Mn oxyanions for the corrosion protection of anodized aerospace aluminum alloy, Surface Engineering Division, CSIR National Aerospace Laboratories, Post Bag No. 1779 Bangalore 560017, Karnataka, India a.
4. Golru SS, Attar M, Ramezanzadeh B (2015) Effects of surface treatment of aluminium alloy 1050 on the adhesion and anticorrosion properties of the epoxy coating. Appl Surf Sci 345:360–36.
5. Zhu W, Li W, Mu S, Fu N, Liao Z (2017) Comparative study on Ti/Zr/V and chromate conversion treated aluminum alloys: anticorrosion performance and epoxy coating adhesion properties. Appl Surf Sci 405:157–168.
6. Li Y, Zhang P, Bai P, Wu L, Liu B, Zhao Z (2018) Microstructure and properties of Ti/TiBCN coating on 7075 aluminum alloy by laser cladding. Surf Coat Technol 334:142–149.
7. Sabouri M, Khoei SM (2018) Plasma electrolytic oxidation in the presence of multiwall carbon nanotubes on aluminum substrate: morphological and corrosion studies. Surf Coat Technol 334:543–555.
8. Meis N, van der Ven L, van Benthem R (2014) Extreme wet adhesion of a novel epoxy-amine coating on aluminum alloy 2024-T3. Prog Org Coat 77(1):176–183.
9. Fabiola Pinedac, Carola Martínezb,d, Mamié Sancyb, Marcela UrzuaeMarcos Floresf, María V. Encinasg, Maritza A. Páeza. Improving the interaction between aluminum surfaces and polymer coating, Surface and Coatings Technology. Volume 358, 25 January 2019, Pages 435-442.
10. Ruiyue Zhanga, Shu Cai a,∗, Guohua Xub,∗∗, Huan Zhaoa, Yan Li a, Xuexin Wanga, Kai Huanga, Mengguo Rena, Xiaodong Wub. Crack self-healing of phytic acid conversion coating on AZ31magnesium alloy by heat treatment and the corrosion resistance. Applied Surface Science,V3,2014 p.831-836.
11. R. F Zhang, J. Bu, C. Lin, G. Song, Recent progress in corrosion protection of magnesium alloys by organic coatings, Prog. Org. Coat. 73 (2012) 129–141.
12. R. F. Zhang, S. F. Zhang a b, N. Yang b, L.J. Yao b, F.X. He b, Y.P. Zhou b, X. Xu b, L. Chang b, S.J. Bai b Journal of Alloys and Compounds Influence of 8-hydroxyquinoline on properties of anodic coatings obtained by micro arc oxidation on AZ91 magnesium alloys. Volume 539, 25 October 2012, Pages 249-255.
13. Srinivasan PB, Liang J, Blawert C, Störmer M, Dietzel W. Characterization of calcium containing plasma electrolytic oxidation coatings on AM50 magnesium alloy. Appl Surf Sci 2010; 256:4017–22.
14. Ximei Wang, Liqun Zhu, Weiping Li, Huicong Liu, Yihong Li, Effects of half-wave and full-wave power source on the anodic oxidation process on AZ91D

magnesium alloy, Volume 255, Issue 11, 15 March 2009, Pages 5721-5728.

15. R. F. Zhang a b, Yu Zuo a, Guochao Nie, The enhanced properties of anodic films on AZ91D magnesium alloy by addition of oxide nanoparticles, Journal of Alloys and Compounds, Volume 834, 5 September 2020, 1550.
16. Gen Zhang a, Aitao Tang a b, Liang Wu a b, Zeyu Zhang a, Hongxin Liao a, Ying Long a, Lingjie Li c, Andrej Atrens d, Fusheng Pan a b, In-situ grown super- or hydrophobic Mg-Al layered double hydroxides films on the anodized magnesium alloy to improve corrosion properties, Surface and Coatings Technology Volume 366, 25 May 2019, Pages 238-247.
17. Jothi a, Akeem Yusuf Adesina b, A. Madhan Kumar b, Mohammad Mizanur Rahman b, J.S. Nirmal Ram, Enhancing the biodegradability and surface protective performance of AZ31 Mg alloy using polypyrrole/gelatin composite coatings with anodized Mg surface, Surface and Coatings Technology Volume 381, 15 January 2020, 125139.
18. Y. R. Ding, X. W. Guo, Y. F. Jiang, et al., Effects of triethanolamine on the performances of the anodicing film of AZ31B magnesium alloy, Mater. Sci. Forum, 488e489 (2005) 657e660.
19. D. A. Shirley, High-resolution X-ray photoemission spectrum of the valence bands of gold, Phys. Rev. B 5 (1972) 4709–4713.
20. M. Mohai, XPS MultiQuant: multimodel XPS quantification software, Surf. Interface Anal. 36 (2004) 828–832. DOI
21. R. A. Waldo, An Iteration Procedure to Calculate Film Compositions and Thicknesses in Electron-Probe Microanalysis, San Francisco Press, San-Francisco, 1988.
22. Cumpson P. J., Seah M. P. Elastic Scattering Correction in AES and XPS. II. Estimating Attenuation Lengths and Conditions Required for their Valid Use on Overlayer/Substrate Experiments. // Surf. Interface Anal., 1997, V. 25, № 6, P. 430-446.
23. Pei Zhang a, b, Yu Zuo a, *, Guochao Nie c The enhanced properties of anodic films on AZ91D magnesium alloby addition of oxide nanoparticles Journal of Alloys and Compounds 834 (2020) 155041.
24. H. Y. Hsiao, W. T. Tsai, Characterization of anodic films formed on AZ91D magnesium alloy, Surf. Coating. Technol. 190 (2005) 299e308.
25. Hiroki Habazaki a b, Fumitaka Kataoka a, Khurram Shahzad a, Etsushi Tsuji a b, Yoshitaka Aoki a b, Shinji Nagata c, Peter Skeldon d, George E. Thompson d, Growth of barrier-type anodic films on magnesium in ethylene glycol electrolytes containing fluoride and water, Electrochimica Acta, Volume 179, 10 October 2015, Pages 402-413.
26. A. Němcová a, O. Galal a, P. Skeldon a, I. Kuběna b, M. Šmíd c, E. Briand d, I. Vickridge d, J-J. Ganem d, H. Habazaki, Film growth and alloy enrichment during anodizing AZ31 magnesium alloy in fluoride/glycerol electrolytes of a range of water contents, Electrochimica Acta Volume 219, 20 November 2016, Pages 28-37.
27. Makarychev Yu. B., Kuzenkov Yu. A., Chugunov D. O., Grafov O. Yu., Aliev A. D., Vapor-phase deposition of polymer siloxane coatings on aluminum and magnesium alloys Prog. Org. Coat. Volume 183, October 2023, 107755.
28. Santamaria M, DiQuarto F, Zanna S, Marcus P. Initial surface film on magnesium metal: a characterization by X-ray photoelectron spectroscopy (XPS) and photocurrent spectroscopy (PCS). Electrochimica 2007;53(3):1315–25.
29. Zhou W, Shan D, Han E, Ke W. Structure and formation mechanism ophosphate conversion coating on die-cast AZ91D magnesium alloy. Corros Sci. 2008;50:329–37.
30. Makarychev Yu B., Luchkin A. Yu, Grafov O. Yu, Andreev N. N, Vapor-phase deposition of polymer siloxane coatings on the surface of copper and low-carbon steel. International Journal of Corrosion and Scale Inhibition, V 11, № 3, с. 980-1000 DOI.
31. Synergistic effect of V and Mn oxyanions for the corrosion protection of anodized aerospace aluminum alloy G. Yoganandan, J. N. Balaraju*, Surface Engineering Division, CSIR National Aerospace Laboratories, Post Bag No. 1779 Bangalore 560017, Karnataka, India.

Global Journals Guidelines Handbook 2024

www.GlobalJournals.org

Memberships

FELLOWS/ASSOCIATES OF ENGINEERING RESEARCH COUNCIL

FERC/AERC MEMBERSHIPS

Introduction

FERC/AERC is the most prestigious membership of Global Journals accredited by Open Association of Research Society, U.S.A (OARS). The credentials of Fellow and Associate designations signify that the researcher has gained the knowledge of the fundamental and high-level concepts, and is a subject matter expert, proficient in an expertise course covering the professional code of conduct, and follows recognized standards of practice. The credentials are designated only to the researchers, scientists, and professionals that have been selected by a rigorous process by our Editorial Board and Management Board.

> Associates of FERC/AERC are scientists and researchers from around the world are working on projects/researches that have huge potentials. Members support Global Journals' mission to advance technology for humanity and the profession.

FERC

FELLOW OF ENGINEERING RESEARCH COUNCIL

FELLOW OF ENGINEERING RESEARCH COUNCIL is the most prestigious membership of Global Journals. It is an award and membership granted to individuals that the Open Association of Research Society judges to have made a 'substantial contribution to the improvement of computer science, technology, and electronics engineering.

> The primary objective is to recognize the leaders in research and scientific fields of the current era with a global perspective and to create a channel between them and other researchers for better exposure and knowledge sharing. Members are most eminent scientists, engineers, and technologists from all across the world. Fellows are elected for life through a peer review process on the basis of excellence in the respective domain. There is no limit on the number of new nominations made in any year. Each year, the Open Association of Research Society elect up to 12 new Fellow Members.

Benefit

To the Institution

Get letter of appreciation

Global Journals sends a letter of appreciation of author to the Dean or CEO of the University or Company of which author is a part, signed by editor in chief or chief author.

Exclusive Network

Get access to a closed network

A FERC member gets access to a closed network of Tier 1 researchers and scientists with direct communication channel through our website. Fellows can reach out to other members or researchers directly. They should also be open to reaching out by other.

Career Credibility Exclusive Reputation

Certificate

Certificate, LoR and Laser-Momento

Fellows receive a printed copy of a certificate signed by our Chief Author that may be used for academic purposes and a personal recommendation letter to the dean of member's university.

Career Credibility Exclusive Reputation

Designation

Get honored title of membership

Fellows can use the honored title of membership. The “FERC” is an honored title which is accorded to a person’s name viz. Dr. John E. Hall, Ph.D., FERC or William Walldroff, M.S., FERC.

Career Credibility Exclusive Reputation

Recognition on the Platform

Better visibility and citation

All the Fellow members of FERC get a badge of "Leading Member of Global Journals" on the Research Community that distinguishes them from others. Additionally, the profile is also partially maintained by our team for better visibility and citation. All fellows get a dedicated page on the website with their biography.

Career Credibility Reputation

Future Work

Get discounts on the future publications

Fellows receive discounts on the future publications with Global Journals up to 60%. Through our recommendation programs, members also receive discounts on publications made with OARS affiliated organizations.

Career Financial

GJ Account

Unlimited forward of Emails

Fellows get secure and fast GJ work emails with unlimited storage of emails that they may use them as their primary email. For example, john [AT] globaljournals [DOT] org.

Career Credibility Reputation

Premium Tools

Access to all the premium tools

To take future researches to the zenith, fellows receive access to all the premium tools that Global Journals have to offer along with the partnership with some of the best marketing leading tools out there.

Financial

Conferences & Events

Organize seminar/conference

Fellows are authorized to organize symposium/seminar/conference on behalf of Global Journal Incorporation (USA). They can also participate in the same organized by another institution as representative of Global Journal. In both the cases, it is mandatory for him to discuss with us and obtain our consent. Additionally, they get free research conferences (and others) alerts.

Career Credibility Financial

Early Invitations

Early invitations to all the symposiums, seminars, conferences

All fellows receive the early invitations to all the symposiums, seminars, conferences and webinars hosted by Global Journals in their subject.

Exclusive

Publishing Articles & Books

Earn 60% of sales proceeds

Fellows can publish articles (limited) without any fees. Also, they can earn up to 70% of sales proceeds from the sale of reference/review books/literature/publishing of research paper. The FERC member can decide its price and we can help in making the right decision.

Exclusive Financial

Reviewers

Get a remuneration of 15% of author fees

Fellow members are eligible to join as a paid peer reviewer at Global Journals Incorporation (USA) and can get a remuneration of 15% of author fees, taken from the author of a respective paper.

Financial

Access to Editorial Board

Become a member of the Editorial Board

Fellows may join as a member of the Editorial Board of Global Journals Incorporation (USA) after successful completion of three years as Fellow and as Peer Reviewer. Additionally, Fellows get a chance to nominate other members for Editorial Board.

Career Credibility Exclusive Reputation

And Much More

Get access to scientific museums and observatories across the globe

All members get access to 5 selected scientific museums and observatories across the globe. All researches published with Global Journals will be kept under deep archival facilities across regions for future protections and disaster recovery. They get 10 GB free secure cloud access for storing research files.

ASSOCIATE OF ENGINEERING RESEARCH COUNCIL

ASSOCIATE OF ENGINEERING RESEARCH COUNCIL is the membership of Global Journals awarded to individuals that the Open Association of Research Society judges to have made a 'substantial contribution to the improvement of computer science, technology, and electronics engineering.

> The primary objective is to recognize the leaders in research and scientific fields of the current era with a global perspective and to create a channel between them and other researchers for better exposure and knowledge sharing. Members are most eminent scientists, engineers, and technologists from all across the world. Associate membership can later be promoted to Fellow Membership. Associates are elected for life through a peer review process on the basis of excellence in the respective domain. There is no limit on the number of new nominations made in any year. Each year, the Open Association of Research Society elect up to 12 new Associate Members.

Benefit

To the Institution

Get letter of appreciation

Global Journals sends a letter of appreciation of author to the Dean or CEO of the University or Company of which author is a part, signed by editor in chief or chief author.

Exclusive Network

Get access to a closed network

A AERC member gets access to a closed network of Tier 1 researchers and scientists with direct communication channel through our website. Associates can reach out to other members or researchers directly. They should also be open to reaching out by other.

Career | Credibility | Exclusive | Reputation

Certificate

Certificate, LoR and Laser-Momento

Associates receive a printed copy of a certificate signed by our Chief Author that may be used for academic purposes and a personal recommendation letter to the dean of member's university.

Career | Credibility | Exclusive | Reputation

Designation

Get honored title of membership

Associates can use the honored title of membership. The “AERC” is an honored title which is accorded to a person’s name viz. Dr. John E. Hall, Ph.D., AERC or William Walldroff, M.S., AERC.

Career | Credibility | Exclusive | Reputation

Recognition on the Platform

Better visibility and citation

All the Associate members of AERC get a badge of "Leading Member of Global Journals" on the Research Community that distinguishes them from others. Additionally, the profile is also partially maintained by our team for better visibility and citation. All associates get a dedicated page on the website with their biography.

Career | Credibility | Reputation

Future Work

Get discounts on the future publications

Associates receive discounts on the future publications with Global Journals up to 60%. Through our recommendation programs, members also receive discounts on publications made with OARS affiliated organizations.

Career Financial

GJ Account

Unlimited forward of Emails

Associates get secure and fast GJ work emails with unlimited storage of emails that they may use them as their primary email. For example, john [AT] globaljournals [DOT] org..

Career Credibility Reputation

Premium Tools

Access to all the premium tools

To take future researches to the zenith, associates receive access to all the premium tools that Global Journals have to offer along with the partnership with some of the best marketing leading tools out there.

Financial

Conferences & Events

Organize seminar/conference

Associates are authorized to organize symposium/seminar/conference on behalf of Global Journal Incorporation (USA). They can also participate in the same organized by another institution as representative of Global Journal. In both the cases, it is mandatory for him to discuss with us and obtain our consent. Additionally, they get free research conferences (and others) alerts.

Career Credibility Financial

Early Invitations

Early invitations to all the symposiums, seminars, conferences

All associates receive the early invitations to all the symposiums, seminars, conferences and webinars hosted by Global Journals in their subject.

Exclusive

Publishing Articles & Books

Earn 30-40% of sales proceeds

Associates can publish articles (limited) without any fees. Also, they can earn up to 30-40% of sales proceeds from the sale of reference/review books/literature/publishing of research paper.

Exclusive Financial

Reviewers

Get a remuneration of 15% of author fees

Associate members are eligible to join as a paid peer reviewer at Global Journals Incorporation (USA) and can get a remuneration of 15% of author fees, taken from the author of a respective paper.

Financial

And Much More

Get access to scientific museums and observatories across the globe

All members get access to 2 selected scientific museums and observatories across the globe. All researches published with Global Journals will be kept under deep archival facilities across regions for future protections and disaster recovery. They get 5 GB free secure cloud access for storing research files.

Associate	Fellow	Research Group	Basic
$4800 **lifetime designation**	$6800 **lifetime designation**	$12500.00 **organizational**	APC **per article**
Certificate, LoR and Momento **2** discounted publishing/year **Gradation** of Research **10** research contacts/day **1 GB** Cloud Storage **GJ** Community Access	**Certificate,** LoR and Momento **Unlimited** discounted publishing/year **Gradation** of Research **Unlimited** research contacts/day **5 GB** Cloud Storage **Online Presense** Assistance **GJ** Community Access	**Certificates,** LoRs and Momentos **Unlimited** free publishing/year **Gradation** of Research **Unlimited** research contacts/day **Unlimited** Cloud Storage **Online Presense** Assistance **GJ** Community Access	**GJ** Community Access

We accept the manuscript submissions in any standard (generic) format.

We typeset manuscripts using advanced typesetting tools like Adobe In Design, CorelDraw, TeXnicCenter, and TeXStudio. We usually recommend authors submit their research using any standard format they are comfortable with, and let Global Journals do the rest.

Alternatively, you can download our basic template from https://globaljournals.org/Template.zip

Authors should submit their complete paper/article, including text illustrations, graphics, conclusions, artwork, and tables. Authors who are not able to submit manuscript using the form above can email the manuscript department at submit@globaljournals.org or get in touch with chiefeditor@globaljournals.org if they wish to send the abstract before submission.

Before and during Submission

Authors must ensure the information provided during the submission of a paper is authentic. Please go through the following checklist before submitting:

1. Authors must go through the complete author guideline and understand and *agree to Global Journals' ethics and code of conduct,* along with author responsibilities.
2. Authors must accept the privacy policy, terms, and conditions of Global Journals.
3. Ensure corresponding author’s email address and postal address are accurate and reachable.
4. Manuscript to be submitted must include keywords, an abstract, a paper title, co-author(s') names and details (email address, name, phone number, and institution), figures and illustrations in vector format including appropriate captions, tables, including titles and footnotes, a conclusion, results, acknowledgments and references.
5. Authors should submit paper in a ZIP archive if any supplementary files are required along with the paper.
6. Proper permissions must be acquired for the use of any copyrighted material.
7. Manuscript submitted *must not have been submitted or published elsewhere* and all authors must be aware of the submission.

Declaration of Conflicts of Interest

It is required for authors to declare all financial, institutional, and personal relationships with other individuals and organizations that could influence (bias) their research.

Policy on Plagiarism

Plagiarism is not acceptable in Global Journals submissions at all.

Plagiarized content will not be considered for publication. We reserve the right to inform authors’ institutions about plagiarism detected either before or after publication. If plagiarism is identified, we will follow COPE guidelines:

Authors are solely responsible for all the plagiarism that is found. The author must not fabricate, falsify or plagiarize existing research data. The following, if copied, will be considered plagiarism:

- Words (language)
- Ideas
- Findings
- Writings
- Diagrams
- Graphs
- Illustrations
- Lectures

- Printed material
- Graphic representations
- Computer programs
- Electronic material
- Any other original work

Authorship Policies

Global Journals follows the definition of authorship set up by the Open Association of Research Society, USA. According to its guidelines, authorship criteria must be based on:

1. Substantial contributions to the conception and acquisition of data, analysis, and interpretation of findings.
2. Drafting the paper and revising it critically regarding important academic content.
3. Final approval of the version of the paper to be published.

Changes in Authorship

The corresponding author should mention the name and complete details of all co-authors during submission and in manuscript. We support addition, rearrangement, manipulation, and deletions in authors list till the early view publication of the journal. We expect that corresponding author will notify all co-authors of submission. We follow COPE guidelines for changes in authorship.

Copyright

During submission of the manuscript, the author is confirming an exclusive license agreement with Global Journals which gives Global Journals the authority to reproduce, reuse, and republish authors' research. We also believe in flexible copyright terms where copyright may remain with authors/employers/institutions as well. Contact your editor after acceptance to choose your copyright policy. You may follow this form for copyright transfers.

Appealing Decisions

Unless specified in the notification, the Editorial Board's decision on publication of the paper is final and cannot be appealed before making the major change in the manuscript.

Acknowledgments

Contributors to the research other than authors credited should be mentioned in Acknowledgments. The source of funding for the research can be included. Suppliers of resources may be mentioned along with their addresses.

Declaration of funding sources

Global Journals is in partnership with various universities, laboratories, and other institutions worldwide in the research domain. Authors are requested to disclose their source of funding during every stage of their research, such as making analysis, performing laboratory operations, computing data, and using institutional resources, from writing an article to its submission. This will also help authors to get reimbursements by requesting an open access publication letter from Global Journals and submitting to the respective funding source.

Preparing your Manuscript

Authors can submit papers and articles in an acceptable file format: MS Word (doc, docx), LaTeX (.tex, .zip or .rar including all of your files), Adobe PDF (.pdf), rich text format (.rtf), simple text document (.txt), Open Document Text (.odt), and Apple Pages (.pages). Our professional layout editors will format the entire paper according to our official guidelines. This is one of the highlights of publishing with Global Journals—authors should not be concerned about the formatting of their paper. Global Journals accepts articles and manuscripts in every major language, be it Spanish, Chinese, Japanese, Portuguese, Russian, French, German, Dutch, Italian, Greek, or any other national language, but the title, subtitle, and abstract should be in English. This will facilitate indexing and the pre-peer review process.

The following is the official style and template developed for publication of a research paper. Authors are not required to follow this style during the submission of the paper. It is just for reference purposes.

Manuscript Style Instruction (Optional)

- Microsoft Word Document Setting Instructions.
- Font type of all text should be Swis721 Lt BT.
- Page size: 8.27" x 11'", left margin: 0.65, right margin: 0.65, bottom margin: 0.75.
- Paper title should be in one column of font size 24.
- Author name in font size of 11 in one column.
- Abstract: font size 9 with the word "Abstract" in bold italics.
- Main text: font size 10 with two justified columns.
- Two columns with equal column width of 3.38 and spacing of 0.2.
- First character must be three lines drop-capped.
- The paragraph before spacing of 1 pt and after of 0 pt.
- Line spacing of 1 pt.
- Large images must be in one column.
- The names of first main headings (Heading 1) must be in Roman font, capital letters, and font size of 10.
- The names of second main headings (Heading 2) must not include numbers and must be in italics with a font size of 10.

Structure and Format of Manuscript

The recommended size of an original research paper is under 15,000 words and review papers under 7,000 words. Research articles should be less than 10,000 words. Research papers are usually longer than review papers. Review papers are reports of significant research (typically less than 7,000 words, including tables, figures, and references)

A research paper must include:

a) A title which should be relevant to the theme of the paper.
b) A summary, known as an abstract (less than 150 words), containing the major results and conclusions.
c) Up to 10 keywords that precisely identify the paper's subject, purpose, and focus.
d) An introduction, giving fundamental background objectives.
e) Resources and techniques with sufficient complete experimental details (wherever possible by reference) to permit repetition, sources of information must be given, and numerical methods must be specified by reference.
f) Results which should be presented concisely by well-designed tables and figures.
g) Suitable statistical data should also be given.
h) All data must have been gathered with attention to numerical detail in the planning stage.

Design has been recognized to be essential to experiments for a considerable time, and the editor has decided that any paper that appears not to have adequate numerical treatments of the data will be returned unrefereed.

i) Discussion should cover implications and consequences and not just recapitulate the results; conclusions should also be summarized.
j) There should be brief acknowledgments.
k) There ought to be references in the conventional format. Global Journals recommends APA format.

Authors should carefully consider the preparation of papers to ensure that they communicate effectively. Papers are much more likely to be accepted if they are carefully designed and laid out, contain few or no errors, are summarizing, and follow instructions. They will also be published with much fewer delays than those that require much technical and editorial correction.

The Editorial Board reserves the right to make literary corrections and suggestions to improve brevity.

Format Structure

It is necessary that authors take care in submitting a manuscript that is written in simple language and adheres to published guidelines.

All manuscripts submitted to Global Journals should include:

Title

The title page must carry an informative title that reflects the content, a running title (less than 45 characters together with spaces), names of the authors and co-authors, and the place(s) where the work was carried out.

Author details

The full postal address of any related author(s) must be specified.

Abstract

The abstract is the foundation of the research paper. It should be clear and concise and must contain the objective of the paper and inferences drawn. It is advised to not include big mathematical equations or complicated jargon.

Many researchers searching for information online will use search engines such as Google, Yahoo or others. By optimizing your paper for search engines, you will amplify the chance of someone finding it. In turn, this will make it more likely to be viewed and cited in further works. Global Journals has compiled these guidelines to facilitate you to maximize the web-friendliness of the most public part of your paper.

Keywords

A major lynchpin of research work for the writing of research papers is the keyword search, which one will employ to find both library and internet resources. Up to eleven keywords or very brief phrases have to be given to help data retrieval, mining, and indexing.

One must be persistent and creative in using keywords. An effective keyword search requires a strategy: planning of a list of possible keywords and phrases to try.

Choice of the main keywords is the first tool of writing a research paper. Research paper writing is an art. Keyword search should be as strategic as possible.

One should start brainstorming lists of potential keywords before even beginning searching. Think about the most important concepts related to research work. Ask, “What words would a source have to include to be truly valuable in a research paper?” Then consider synonyms for the important words.

It may take the discovery of only one important paper to steer in the right keyword direction because, in most databases, the keywords under which a research paper is abstracted are listed with the paper.

Numerical Methods

Numerical methods used should be transparent and, where appropriate, supported by references.

Abbreviations

Authors must list all the abbreviations used in the paper at the end of the paper or in a separate table before using them.

Formulas and equations

Authors are advised to submit any mathematical equation using either MathJax, KaTeX, or LaTeX, or in a very high-quality image.

Tables, Figures, and Figure Legends

Tables: Tables should be cautiously designed, uncrowned, and include only essential data. Each must have an Arabic number, e.g., Table 4, a self-explanatory caption, and be on a separate sheet. Authors must submit tables in an editable format and not as images. References to these tables (if any) must be mentioned accurately.

Figures

Figures are supposed to be submitted as separate files. Always include a citation in the text for each figure using Arabic numbers, e.g., Fig. 4. Artwork must be submitted online in vector electronic form or by emailing it.

Preparation of Eletronic Figures for Publication

Although low-quality images are sufficient for review purposes, print publication requires high-quality images to prevent the final product being blurred or fuzzy. Submit (possibly by e-mail) EPS (line art) or TIFF (halftone/ photographs) files only. MS PowerPoint and Word Graphics are unsuitable for printed pictures. Avoid using pixel-oriented software. Scans (TIFF only) should have a resolution of at least 350 dpi (halftone) or 700 to 1100 dpi (line drawings). Please give the data for figures in black and white or submit a Color Work Agreement form. EPS files must be saved with fonts embedded (and with a TIFF preview, if possible).

For scanned images, the scanning resolution at final image size ought to be as follows to ensure good reproduction: line art: >650 dpi; halftones (including gel photographs): >350 dpi; figures containing both halftone and line images: >650 dpi.

Color charges: Authors are advised to pay the full cost for the reproduction of their color artwork. Hence, please note that if there is color artwork in your manuscript when it is accepted for publication, we would require you to complete and return a Color Work Agreement form before your paper can be published. Also, you can email your editor to remove the color fee after acceptance of the paper.

Tips for Writing a Good Quality Engineering Research Paper

Techniques for writing a good quality engineering research paper:

1. Choosing the topic: In most cases, the topic is selected by the interests of the author, but it can also be suggested by the guides. You can have several topics, and then judge which you are most comfortable with. This may be done by asking several questions of yourself, like "Will I be able to carry out a search in this area? Will I find all necessary resources to accomplish the search? Will I be able to find all information in this field area?" If the answer to this type of question is "yes," then you ought to choose that topic. In most cases, you may have to conduct surveys and visit several places. Also, you might have to do a lot of work to find all the rises and falls of the various data on that subject. Sometimes, detailed information plays a vital role, instead of short information. Evaluators are human: The first thing to remember is that evaluators are also human beings. They are not only meant for rejecting a paper. They are here to evaluate your paper. So present your best aspect.

2. Think like evaluators: If you are in confusion or getting demotivated because your paper may not be accepted by the evaluators, then think, and try to evaluate your paper like an evaluator. Try to understand what an evaluator wants in your research paper, and you will automatically have your answer. Make blueprints of paper: The outline is the plan or framework that will help you to arrange your thoughts. It will make your paper logical. But remember that all points of your outline must be related to the topic you have chosen.

3. Ask your guides: If you are having any difficulty with your research, then do not hesitate to share your difficulty with your guide (if you have one). They will surely help you out and resolve your doubts. If you can't clarify what exactly you require for your work, then ask your supervisor to help you with an alternative. He or she might also provide you with a list of essential readings.

4. Use of computer is recommended: As you are doing research in the field of research engineering then this point is quite obvious. Use right software: Always use good quality software packages. If you are not capable of judging good software, then you can lose the quality of your paper unknowingly. There are various programs available to help you which you can get through the internet.

5. Use the internet for help: An excellent start for your paper is using Google. It is a wondrous search engine, where you can have your doubts resolved. You may also read some answers for the frequent question of how to write your research paper or find a model research paper. You can download books from the internet. If you have all the required books, place importance on reading, selecting, and analyzing the specified information. Then sketch out your research paper. Use big pictures: You may use encyclopedias like Wikipedia to get pictures with the best resolution. At Global Journals, you should strictly follow here.

6. Bookmarks are useful: When you read any book or magazine, you generally use bookmarks, right? It is a good habit which helps to not lose your continuity. You should always use bookmarks while searching on the internet also, which will make your search easier.

7. Revise what you wrote: When you write anything, always read it, summarize it, and then finalize it.

8. Make every effort: Make every effort to mention what you are going to write in your paper. That means always have a good start. Try to mention everything in the introduction—what is the need for a particular research paper. Polish your work with good writing skills and always give an evaluator what he wants. Make backups: When you are going to do any important thing like making a research paper, you should always have backup copies of it either on your computer or on paper. This protects you from losing any portion of your important data.

9. Produce good diagrams of your own: Always try to include good charts or diagrams in your paper to improve quality. Using several unnecessary diagrams will degrade the quality of your paper by creating a hodgepodge. So always try to include diagrams which were made by you to improve the readability of your paper. Use of direct quotes: When you do research relevant to literature, history, or current affairs, then use of quotes becomes essential, but if the study is relevant to science, use of quotes is not preferable.

10. Use proper verb tense: Use proper verb tenses in your paper. Use past tense to present those events that have happened. Use present tense to indicate events that are going on. Use future tense to indicate events that will happen in the future. Use of wrong tenses will confuse the evaluator. Avoid sentences that are incomplete.

11. Pick a good study spot: Always try to pick a spot for your research which is quiet. Not every spot is good for studying.

12. Know what you know: Always try to know what you know by making objectives, otherwise you will be confused and unable to achieve your target.

13. Use good grammar: Always use good grammar and words that will have a positive impact on the evaluator; use of good vocabulary does not mean using tough words which the evaluator has to find in a dictionary. Do not fragment sentences. Eliminate one-word sentences. Do not ever use a big word when a smaller one would suffice.

Verbs have to be in agreement with their subjects. In a research paper, do not start sentences with conjunctions or finish them with prepositions. When writing formally, it is advisable to never split an infinitive because someone will (wrongly) complain. Avoid clichés like a disease. Always shun irritating alliteration. Use language which is simple and straightforward. Put together a neat summary.

14. Arrangement of information: Each section of the main body should start with an opening sentence, and there should be a changeover at the end of the section. Give only valid and powerful arguments for your topic. You may also maintain your arguments with records.

15. Never start at the last minute: Always allow enough time for research work. Leaving everything to the last minute will degrade your paper and spoil your work.

16. Multitasking in research is not good: Doing several things at the same time is a bad habit in the case of research activity. Research is an area where everything has a particular time slot. Divide your research work into parts, and do a particular part in a particular time slot.

17. Never copy others' work: Never copy others' work and give it your name because if the evaluator has seen it anywhere, you will be in trouble. Take proper rest and food: No matter how many hours you spend on your research activity, if you are not taking care of your health, then all your efforts will have been in vain. For quality research, take proper rest and food.

18. Go to seminars: Attend seminars if the topic is relevant to your research area. Utilize all your resources.

19. Refresh your mind after intervals: Try to give your mind a rest by listening to soft music or sleeping in intervals. This will also improve your memory. Acquire colleagues: Always try to acquire colleagues. No matter how sharp you are, if you acquire colleagues, they can give you ideas which will be helpful to your research.

20. Think technically: Always think technically. If anything happens, search for its reasons, benefits, and demerits. Think and then print: When you go to print your paper, check that tables are not split, headings are not detached from their descriptions, and page sequence is maintained.

21. Adding unnecessary information: Do not add unnecessary information like "I have used MS Excel to draw graphs." Irrelevant and inappropriate material is superfluous. Foreign terminology and phrases are not apropos. One should never take a broad view. Analogy is like feathers on a snake. Use words properly, regardless of how others use them. Remove quotations. Puns are for kids, not grunt readers. Never oversimplify: When adding material to your research paper, never go for oversimplification; this will definitely irritate the evaluator. Be specific. Never use rhythmic redundancies. Contractions shouldn't be used in a research paper. Comparisons are as terrible as clichés. Give up ampersands, abbreviations, and so on. Remove commas that are not necessary. Parenthetical words should be between brackets or commas. Understatement is always the best way to put forward earth-shaking thoughts. Give a detailed literary review.

22. Report concluded results: Use concluded results. From raw data, filter the results, and then conclude your studies based on measurements and observations taken. An appropriate number of decimal places should be used. Parenthetical remarks are prohibited here. Proofread carefully at the final stage. At the end, give an outline to your arguments. Spot perspectives of further study of the subject. Justify your conclusion at the bottom sufficiently, which will probably include examples.

23. Upon conclusion: Once you have concluded your research, the next most important step is to present your findings. Presentation is extremely important as it is the definite medium though which your research is going to be in print for the rest of the crowd. Care should be taken to categorize your thoughts well and present them in a logical and neat manner. A good quality research paper format is essential because it serves to highlight your research paper and bring to light all necessary aspects of your research.

Informal Guidelines of Research Paper Writing

Key points to remember:

- Submit all work in its final form.
- Write your paper in the form which is presented in the guidelines using the template.
- Please note the criteria peer reviewers will use for grading the final paper.

Final points:

One purpose of organizing a research paper is to let people interpret your efforts selectively. The journal requires the following sections, submitted in the order listed, with each section starting on a new page:

The introduction: This will be compiled from reference matter and reflect the design processes or outline of basis that directed you to make a study. As you carry out the process of study, the method and process section will be constructed like that. The results segment will show related statistics in nearly sequential order and direct reviewers to similar intellectual paths throughout the data that you gathered to carry out your study.

The discussion section:

This will provide understanding of the data and projections as to the implications of the results. The use of good quality references throughout the paper will give the effort trustworthiness by representing an alertness to prior workings.

Writing a research paper is not an easy job, no matter how trouble-free the actual research or concept. Practice, excellent preparation, and controlled record-keeping are the only means to make straightforward progression.

General style:

Specific editorial column necessities for compliance of a manuscript will always take over from directions in these general guidelines.

To make a paper clear: Adhere to recommended page limits.

Mistakes to avoid:

- Insertion of a title at the foot of a page with subsequent text on the next page.
- Separating a table, chart, or figure—confine each to a single page.
- Submitting a manuscript with pages out of sequence.
- In every section of your document, use standard writing style, including articles ("a" and "the").
- Keep paying attention to the topic of the paper.

- Use paragraphs to split each significant point (excluding the abstract).
- Align the primary line of each section.
- Present your points in sound order.
- Use present tense to report well-accepted matters.
- Use past tense to describe specific results.
- Do not use familiar wording; don't address the reviewer directly. Don't use slang or superlatives.
- Avoid use of extra pictures—include only those figures essential to presenting results.

Title page:

Choose a revealing title. It should be short and include the name(s) and address(es) of all authors. It should not have acronyms or abbreviations or exceed two printed lines.

Abstract: This summary should be two hundred words or less. It should clearly and briefly explain the key findings reported in the manuscript and must have precise statistics. It should not have acronyms or abbreviations. It should be logical in itself. Do not cite references at this point.

An abstract is a brief, distinct paragraph summary of finished work or work in development. In a minute or less, a reviewer can be taught the foundation behind the study, common approaches to the problem, relevant results, and significant conclusions or new questions.

Write your summary when your paper is completed because how can you write the summary of anything which is not yet written? Wealth of terminology is very essential in abstract. Use comprehensive sentences, and do not sacrifice readability for brevity; you can maintain it succinctly by phrasing sentences so that they provide more than a lone rationale. The author can at this moment go straight to shortening the outcome. Sum up the study with the subsequent elements in any summary. Try to limit the initial two items to no more than one line each.

Reason for writing the article—theory, overall issue, purpose.

- Fundamental goal.
- To-the-point depiction of the research.
- Consequences, including definite statistics—if the consequences are quantitative in nature, account for this; results of any numerical analysis should be reported. Significant conclusions or questions that emerge from the research.

Approach:

- o Single section and succinct.
- o An outline of the job done is always written in past tense.
- o Concentrate on shortening results—limit background information to a verdict or two.
- o Exact spelling, clarity of sentences and phrases, and appropriate reporting of quantities (proper units, important statistics) are just as significant in an abstract as they are anywhere else.

Introduction:

The introduction should "introduce" the manuscript. The reviewer should be presented with sufficient background information to be capable of comprehending and calculating the purpose of your study without having to refer to other works. The basis for the study should be offered. Give the most important references, but avoid making a comprehensive appraisal of the topic. Describe the problem visibly. If the problem is not acknowledged in a logical, reasonable way, the reviewer will give no attention to your results. Speak in common terms about techniques used to explain the problem, if needed, but do not present any particulars about the protocols here.

The following approach can create a valuable beginning:

- o Explain the value (significance) of the study.
- o Defend the model—why did you employ this particular system or method? What is its compensation? Remark upon its appropriateness from an abstract point of view as well as pointing out sensible reasons for using it.
- o Present a justification. State your particular theory(-ies) or aim(s), and describe the logic that led you to choose them.
- o Briefly explain the study's tentative purpose and how it meets the declared objectives.

Approach:

Use past tense except for when referring to recognized facts. After all, the manuscript will be submitted after the entire job is done. Sort out your thoughts; manufacture one key point for every section. If you make the four points listed above, you will need at least four paragraphs. Present surrounding information only when it is necessary to support a situation. The reviewer does not desire to read everything you know about a topic. Shape the theory specifically—do not take a broad view.

As always, give awareness to spelling, simplicity, and correctness of sentences and phrases.

Procedures (methods and materials):

This part is supposed to be the easiest to carve if you have good skills. A soundly written procedures segment allows a capable scientist to replicate your results. Present precise information about your supplies. The suppliers and clarity of reagents can be helpful bits of information. Present methods in sequential order, but linked methodologies can be grouped as a segment. Be concise when relating the protocols. Attempt to give the least amount of information that would permit another capable scientist to replicate your outcome, but be cautious that vital information is integrated. The use of subheadings is suggested and ought to be synchronized with the results section.

When a technique is used that has been well-described in another section, mention the specific item describing the way, but draw the basic principle while stating the situation. The purpose is to show all particular resources and broad procedures so that another person may use some or all of the methods in one more study or referee the scientific value of your work. It is not to be a step-by-step report of the whole thing you did, nor is a methods section a set of orders.

Materials:

Materials may be reported in part of a section or else they may be recognized along with your measures.

Methods:

- Report the method and not the particulars of each process that engaged the same methodology.
- Describe the method entirely.
- To be succinct, present methods under headings dedicated to specific dealings or groups of measures.
- Simplify—detail how procedures were completed, not how they were performed on a particular day.
- If well-known procedures were used, account for the procedure by name, possibly with a reference, and that's all.

Approach:

It is embarrassing to use vigorous voice when documenting methods without using first person, which would focus the reviewer's interest on the researcher rather than the job. As a result, when writing up the methods, most authors use third person passive voice.

Use standard style in this and every other part of the paper—avoid familiar lists, and use full sentences.

What to keep away from:

- Resources and methods are not a set of information.
- Skip all descriptive information and surroundings—save it for the argument.
- Leave out information that is immaterial to a third party.

Results:

The principle of a results segment is to present and demonstrate your conclusion. Create this part as entirely objective details of the outcome, and save all understanding for the discussion.

The page length of this segment is set by the sum and types of data to be reported. Use statistics and tables, if suitable, to present consequences most efficiently.

You must clearly differentiate material which would usually be incorporated in a study editorial from any unprocessed data or additional appendix matter that would not be available. In fact, such matters should not be submitted at all except if requested by the instructor.

Content:

- Sum up your conclusions in text and demonstrate them, if suitable, with figures and tables.
- In the manuscript, explain each of your consequences, and point the reader to remarks that are most appropriate.
- Present a background, such as by describing the question that was addressed by creation of an exacting study.
- Explain results of control experiments and give remarks that are not accessible in a prescribed figure or table, if appropriate.
- Examine your data, then prepare the analyzed (transformed) data in the form of a figure (graph), table, or manuscript.

What to stay away from:

- Do not discuss or infer your outcome, report surrounding information, or try to explain anything.
- Do not include raw data or intermediate calculations in a research manuscript.
- Do not present similar data more than once.
- A manuscript should complement any figures or tables, not duplicate information.
- Never confuse figures with tables—there is a difference.

Approach:

As always, use past tense when you submit your results, and put the whole thing in a reasonable order.

Put figures and tables, appropriately numbered, in order at the end of the report.

If you desire, you may place your figures and tables properly within the text of your results section.

Figures and tables:

If you put figures and tables at the end of some details, make certain that they are visibly distinguished from any attached appendix materials, such as raw facts. Whatever the position, each table must be titled, numbered one after the other, and include a heading. All figures and tables must be divided from the text.

Discussion:

The discussion is expected to be the trickiest segment to write. A lot of papers submitted to the journal are discarded based on problems with the discussion. There is no rule for how long an argument should be.

Position your understanding of the outcome visibly to lead the reviewer through your conclusions, and then finish the paper with a summing up of the implications of the study. The purpose here is to offer an understanding of your results and support all of your conclusions, using facts from your research and generally accepted information, if suitable. The implication of results should be fully described.

Infer your data in the conversation in suitable depth. This means that when you clarify an observable fact, you must explain mechanisms that may account for the observation. If your results vary from your prospect, make clear why that may have happened. If your results agree, then explain the theory that the proof supported. It is never suitable to just state that the data approved the prospect, and let it drop at that. Make a decision as to whether each premise is supported or discarded or if you cannot make a conclusion with assurance. Do not just dismiss a study or part of a study as "uncertain."

Research papers are not acknowledged if the work is imperfect. Draw what conclusions you can based upon the results that you have, and take care of the study as a finished work.

- You may propose future guidelines, such as how an experiment might be personalized to accomplish a new idea.
- Give details of all of your remarks as much as possible, focusing on mechanisms.
- Make a decision as to whether the tentative design sufficiently addressed the theory and whether or not it was correctly restricted. Try to present substitute explanations if they are sensible alternatives.
- One piece of research will not counter an overall question, so maintain the large picture in mind. Where do you go next? The best studies unlock new avenues of study. What questions remain?
- Recommendations for detailed papers will offer supplementary suggestions.

Approach:

When you refer to information, differentiate data generated by your own studies from other available information. Present work done by specific persons (including you) in past tense.

Describe generally acknowledged facts and main beliefs in present tense.

The Administration Rules

Administration Rules to Be Strictly Followed before Submitting Your Research Paper to Global Journals Inc.

Please read the following rules and regulations carefully before submitting your research paper to Global Journals Inc. to avoid rejection.

Segment draft and final research paper: You have to strictly follow the template of a research paper, failing which your paper may get rejected. You are expected to write each part of the paper wholly on your own. The peer reviewers need to identify your own perspective of the concepts in your own terms. Please do not extract straight from any other source, and do not rephrase someone else's analysis. Do not allow anyone else to proofread your manuscript.

Written material: You may discuss this with your guides and key sources. Do not copy anyone else's paper, even if this is only imitation, otherwise it will be rejected on the grounds of plagiarism, which is illegal. Various methods to avoid plagiarism are strictly applied by us to every paper, and, if found guilty, you may be blacklisted, which could affect your career adversely. To guard yourself and others from possible illegal use, please do not permit anyone to use or even read your paper and file.

Criterion for Grading a Research Paper (Compilation) by Global Journals

Please note that following table is only a Grading of "Paper Compilation" and not on "Performed/Stated Research" whose grading solely depends on Individual Assigned Peer Reviewer and Editorial Board Member. These can be available only on request and after decision of Paper. This report will be the property of Global Journals.

Topics	Grades		
	A-B	**C-D**	**E-F**
Abstract	Clear and concise with appropriate content, Correct format. 200 words or below	Unclear summary and no specific data, Incorrect form Above 200 words	No specific data with ambiguous information Above 250 words
Introduction	Containing all background details with clear goal and appropriate details, flow specification, no grammar and spelling mistake, well organized sentence and paragraph, reference cited	Unclear and confusing data, appropriate format, grammar and spelling errors with unorganized matter	Out of place depth and content, hazy format
Methods and Procedures	Clear and to the point with well arranged paragraph, precision and accuracy of facts and figures, well organized subheads	Difficult to comprehend with embarrassed text, too much explanation but completed	Incorrect and unorganized structure with hazy meaning
Result	Well organized, Clear and specific, Correct units with precision, correct data, well structuring of paragraph, no grammar and spelling mistake	Complete and embarrassed text, difficult to comprehend	Irregular format with wrong facts and figures
Discussion	Well organized, meaningful specification, sound conclusion, logical and concise explanation, highly structured paragraph reference cited	Wordy, unclear conclusion, spurious	Conclusion is not cited, unorganized, difficult to comprehend
References	Complete and correct format, well organized	Beside the point, Incomplete	Wrong format and structuring

INDEX

save our planet

Global Journal of Researches in Engineering

Visit us on the Web at www.GlobalJournals.org | www.EngineeringResearch.org
or email us at helpdesk@globaljournals.org

ISSN 9755861